Universidade de Aveiro Departamento de Química
2012

Matilde Pereira Neves Melo

Neuroproteção mediada pela adição de DJ-1 recombinante

The role of exogenous DJ-1 in neuroprotection

Universidade de Aveiro Departamento de Química
2012

Matilde Pereira Neves Melo

Neuroproteção mediada pela adição de DJ-1 recombinante

The role of exogenous DJ-1 in neuroprotection

Dissertação apresentada à Universidade de Aveiro para cumprimento dos requisitos necessários à obtenção do grau de Mestre em Biotecnologia, realizada sob a orientação científica do Dr. Bruno Manadas, Investigador Auxiliar do Centro de Neurociências e Biologia Celular da Universidade de Coimbra e do Dr. Rui Vitorino, Investigador Auxiliar do Departamento de Química da Universidade de Aveiro.

o júri

Presidente

Prof. Dr. Jorge Manuel Alexandre Saraiva
Investigador Auxiliar do Departamento de Química da Universidade de Aveiro

Prof. Dr. Isaura Isabel Gonçalves Simões
Investigador Auxiliar do Centro de Neurociências e Biologia Celular da Universidade de Coimbra

Prof. Dr. Bruno José Fernandes Oliveira Manadas
Investigador Auxiliar do Centro de Neurociências e Biologia Celular da Universidade de Coimbra

Prof. Dr. Rui Miguel Pinheiro Vitorino
Investigador Auxiliar do Departamento de Química da Universidade de Aveiro

agradecimentos

Em primeiro lugar, gostaria de agradecer ao Doutor Bruno Manadas e ao Doutor Mário Grãos pela oportunidade que me deram de integrar este projeto e pela forma como me receberam. Obrigada por todas por todas as horas despendidas comigo e com o meu trabalho. Obrigada por todos os conhecimentos, conselhos e críticas; por toda a compreensão e pela motivação que sempre me transmitiram.

Em segundo lugar, um agradecimento sincero ao Dr. Rui Vitorino pela sua disponibilidade e pela compreensão sempre demonstrada.

Gostaria ainda de agradecer ao Doutor Pedro Castanheira por todos os conhecimentos que me transmitiu e por todas as horas que passou a ensinar-me e a acompanhar o meu trabalho na Unidade de Biotecnologia Molecular do Biocant.

Um agradecimento também a todos os meus colegas do Biocant pelo carinho com que me receberam e ajudaram sempre.

Em particular, da Unidade de Proteómica e Metabolómica, gostaria de agradecer em especial à Sandra Anjo que foi orientadora, professora, amiga e conselheira (literalmente, o meu Anjo-da-guarda!). Sem a sua ajuda não teria conseguido... Quero agradecer-lhe por todos os conhecimentos práticos e teóricos que me transmitiu e por todas as horas que disponibilizou para me ouvir e ajudar. Gostaria também de agradecer à Cátia Santa que, em qualquer que fosse a tarefa, esteve sempre disposta a ajudar. Às duas gostava de agradecer pelas gargalhadas e pela companhia durante as longas horas de trabalho. À Vera pelos conselhos, pela amizade e pelos conhecimentos que me transmitiu, à Alexandra Gonçalves, ao José Carvalho e à Margarida Coelho pela amizade e pela boa disposição.

Da Unidade de Biologia Celular gostaria de agradecer especialmente ao Sandro Pereira por todos os conhecimentos que me transmitiu, por toda a ajuda com a análise estatística e pelas gargalhadas que me "roubou". À Tânia Lourenço pela companhia a horas menos "normais" e pela amizade. Às ex-colegas, Cristiana Leite e Tatiana Silva, obrigada também pela amizade e simpatia.

Da Unidade de Biotecnologia Molecular, gostaria de agradecer ao Rui Cruz que esteve sempre disponível para me ajudar e esclarecer todas as dúvidas, bem como, à Ana Sofia Lourenço, à Ana Rita Leal, ao Pedro Curto e à Liliana Antunes (ex-colega).

Gostaria de agradecer também a todos os meus amigos e familiares que sempre me apoiaram e que me foram fazendo sair da rotina para a seguir voltar com as baterias recarregadas. Em especial aos "Ms. Pepper & The Love Band" por toda a compreensão, por toda a amizade e pelos momentos únicos que temos vivido e me fazem esquecer as tristezas e recuperar o fôlego.

Por último, mas não menos importantes, gostaria de agradecer aos meus pais, porque sem eles eu não seria quem sou hoje e nunca teria chegado até aqui! Obrigada pelo vosso amor e pelo infinito apoio e confiança. Obrigada ao Bernardo por ter estado (e por estar) sempre ao meu lado, por me ter dado a confiança e a força que precisei, por me ouvir sempre (mesmo que muitas vezes não perceba o que digo), pela paciência, pela compreensão, pela tolerância e por me ter ajudado em tudo o que podia durante a escrita da dissertação.

Obrigada!

palavras-chave DJ-1; neuroprotecção; internalização; interactoma extracelular; doença Parkinson.

resumo

A Doença de Parkinson (DP) é a segunda doença neurodegenerativa progressiva mais comum e afeta profundamente o movimento. A DP é patologicamente caracterizada pela degeneração dos neurónios dopaminérgicos na *substantia nigra pars compacta* que leva a um decréscimo de dopamina no estriado. Apesar de pouco conhecida, a etiologia da DP parece envolver fatores genéticos e ambientais, correspondendo 10% dos casos a formas monogénicas da doença.

Mutações na proteína DJ-1 têm sido relacionadas com a patogénese da doença e o interesse no estudo desta proteína tem vindo a crescer ao longo dos anos. Vários estudos mostram um envolvimento direto e indireto da DJ-1 nos mecanismos de neuroprotecção contra o stress oxidativo. Esta proteína foi encontrada em muitos tipos de células, incluindo neurónios e células da glia, com uma distribuição generalizada pelos diferentes compartimentos sub-celulares. Para além disso, a DJ-1 é secretada pelos astrócitos, mas o mecanismo pelo qual esta conferirá neuroproteção aos neurónios adjacentes é ainda desconhecido. Algumas das hipóteses que permanecem em aberto são: a internalização da DJ-1 oriunda dos astrócitos pelos neurónios para exercer os seus mecanismos de neuroprotecção no espaço intracelular; e a ativação de recetores membranares e de vias de sinalização celular.

Este estudo pretende revelar algumas pistas sobre os mecanismos de neuroprotecção da DJ-1, usando uma proteína recombinante adicionada exogenamente a células SH-SY5Y. A proteína dimérica produzida revelou um efeito neuroprotetor em células SH-SY5Y sob condições de stress oxidativo. A adição desta proteína, em condições normais ou sob stress oxidativo, levou ainda à ativação das vias de sinalização Akt e ERK1/2.

Neste estudo não se observou a internalização da DJ-1 em células SH-SY5Y nem a sua interação com nenhuma proteína membranar, permanecendo por explicar o mecanismo neuroprotetor que a DJ-1 secretada pelos astrócitos exerce nos neurónios.

De forma a identificar possíveis interactores extracelulares, isto é, proteínas com as quais a DJ-1 interaja no espaço extracelular, foi feito um ensaio de 'pull-down' seguido de uma análise por cromatografia líquida acoplada a espectrometria de massa. Este primeiro ensaio permitiu a identificação de algumas proteínas interessantes, incluindo proteínas de adesão, proteínas envolvidas em processos celulares, como a orientação axonal, migração e proliferação celular, metabolismo dos carbohidratos, processos sinápticos e regulação positiva ou negativa de vias de sinalização celular.

Os hipotéticos interactores deverão ser validados em estudos futuros, mas poderão ser uma ferramenta importante na compreensão dos mecanismos moleculares envolvidos na DP.

keywords DJ-1; neuroprotection; internalization; extracellular interactome; Parkinson's disease.

abstract

Parkinson's disease (PD) is the second most common progressive neurodegenerative disorder and profoundly affects movement. PD is pathologically characterized by the degeneration of the dopaminergic neurons in the *substantia nigra pars compacta* leading to loss of dopamine in the striatum. The etiology of PD is not well understood but seems to involve both genetic and environmental factors, and 10% of the cases correspond to monogenic forms of the disease.

Mutations in DJ-1 protein have been linked to the pathogenesis of PD, with a growing interest in the study of this protein over the last years. Several studies have shown a direct and indirect involvement of this protein in neuroprotection mechanisms against oxidative stress insults. DJ-1 was found in different cell types, including neurons and glial cells, with a widespread sub-cellular distribution. Furthermore, DJ-1 has also been shown to be secreted by astrocytes, but its neuroprotective role underlying this process is still not understood. Some hyposthesis of DJ-1 neuroprotective mechanisms include triggering neuronal internalization of the protein and receptor-mediated activation of signalling pathways.

This study intended to give some clues about these mechanisms possibly involved in neuroprotection by using a recombinant DJ-1 exogenously added to SH-SY5Y cells.

The dimeric produced protein had a neuroprotective effect in cultured SH-SY5Y cells under oxidative stress conditions. Moreover, although preliminary results, the exogenously addition of this protein, under normal or oxidative stress conditions, activated the Akt and the ERK1/2 signaling pathways in the same cell line.

On the other hand, there was no evidence for a DJ-1 uptake by the neuroblastoma cells, as there was also no evidence for any interaction of DJ-1 with membrane proteins, so DJ-1 must be exerting its neuroprotective effect outside of cells, probably not needing to be internalized by neurons after its secretion from astrocytes.

In order to find some possible extracellular DJ-1 interactors a pull-down assay followed by LC-MS/MS analysis was performed. This preliminary approach allowed the identification of some interesting proteins, including cell adhesion proteins, proteins involved in cellular processes, such as, axon guidance, cell migration and proliferation, carbohydrate metabolism, synaptic process and positive or negative regulation of signalling pathways.

The identified putative DJ-1 interactors must be validated, but can be an usefull tool to understand the molecular mechanisms that lead to PD.

TABLE OF CONTENTS

LIST OF ABBREVIATIONS

A	**ACN**	acetonitrile
	AD	autosomal dominant
	Akt	protein kinase B
	ANOVA	ANalysis Of Variance
	AP2	adaptor protein complex 2
	APs	assembly proteins
	AR	autosomal recessive
	ATP	adenosine triphosphate
B	**BCA**	bicinchoninic acid
	BRI2	integral membrane protein 2B
C	**C106**	cysteine-106
	CADs	cationic amphiphilic drugs
	CCVs	clathrin-coated vesicles
	CME	clathrin-mediated endocytosis
	CNS	central nervous system
	CO_2	carbon dioxide
	ConA	concanavalin A
D	**DA**	dopamine
	DAT	dopamine transporter
	DMEM	Dulbecco's modified eagle medium
	dNTP's	deoxyribonucleotide triphosphates
	DPBS	Dulbecco's phosphate buffered saline
	DTSSP	3,3´-dithiobis(sulfosuccinimidylpropionate)
	DTT	dithiothreitol
E	***E. coli***	*Escherichia coli*
	ECF	enhanced chemifluorescence
	EDTA	ethylenediamine tetraacetic acid
	EIF4G1	eukaryotic translation initiation factor 4G1
	EMARS	enzyme-mediated activation of radical sources
	EOPD	early-onset PD
	ER	endoplasmic reticulum
	ERK1/2	extracellular signal-regulated protein kinases 1 and 2
F	**FA**	formic acid

	FB1	fumonisin B1
	FBS	fetal bovine serum
	FDR	false discovery rate
G	**GAPDH**	glyceraldehyde 3-phosphate dehydrogenase
	GCS	glucosylceramide synthase
	GST	glutatione S-transferase
	GWAS	genome-wide association studies
H	**H_2O_2**	hydrogen peroxide
	HPLC	high-performance liquid chromatography
I	**IDA**	information dependent acquisition
	IPTG	isopropyl β-D-1-thiogalactopyranoside
J	**JOPD**	juvenile-onset PD
L	**LB**	Lewy bodies
	LB medium	Luria-Bertani agar médium
	LC-MS/MS	liquid chromatography coupled to tandem mass spectrometry
	LD	levodopa
	LRRK2	leucine-rich repeat kinase 2
K	**K_2HPO_4**	dipotassium phosphate
M	**MAPK**	mitogen activated protein kinases
	MDC	monodansylcadaverine
	$MPDP^+$	1-methyl-4-phenyl-2,3-dihydropyridinium ion
	MPP+	1-methyl-4-phenylpyridinium
	MPTP	1-methyl-4-phenyl-1,2,3,6-tetrahydropyridine
	MS	mass spectrometry
	MS/MS	tandem mass spectrometry
	mtDNA	mitochondrial DNA
	MβCD	methyl-β-cyclodextrin
N	**NaCl**	sodium chloride
	$NaH_2PO_4 \cdot H_2O$	sodium phosphate monobasic monohydrate
	Nrf2	nuclear factor erythroid 2-related factor
O	**o.n.**	over-night
P	**p-Akt**	phosphorylated form of Akt

	PBS	phosphate buffered saline
	PBS-T	PBS with Tween 20
	PCR	polymerase chain reactions
	PD	Parkinson's disease
	Pen-Strep	penicilin-streptomycin solution
	p-ERK1/2	phosphorylated form of ERK1/2
	PI3K	phosphatidylinositol 3-kinases
	PINK1	PTEN-induced putative kinase 1
	PVDF	polyvinylidene fluoride
	p	p-value
R	**RIPA buffer**	radioimmunoprecipitation assay buffer
	ROS	reactive oxygen species
	RT	room temperature
S	**S.E.M**	standard error of the mean
	SDS	sodium dodecyl sulfate
	SDS-PAGE	sodium dodecyl sulfate polyacrylamide gel electrophoresis
	SEC	size exclusion chromatography
	SNpc	*substantia nigra pars compacta*
T	**TH**	tyrosine hydroxylase
	Tris	tris(hydroxymethyl)aminomethane phosphate
	Tris-HCl	Tris-Hydrochloride
U	**UPS**	ubiquitin proteasomal system
V	**v/v**	volume/volume
	VPS35	vacuolar protein sorting 35
W	**w/v**	weight/volume
	WT	wild-type
X	**X-Gal**	5-bromo-4-chloro-3-indolyl-beta-D-galacto-pyranoside
Y	**YOPD**	young-onset PD
	6-His tag	6-histidines tag
	6-OHDA	6-hydroxydopamine
	°C	degree Celsius

1 | INTRODUCTION

1.1. PARKINSON'S DISEASE

Parkinson's disease (PD) is the second most common progressive neurodegenerative disorder (after Alzheimer's disease) and profoundly affects movement [1-2]. This disease was first described in 1817 by James Parkinson in the classic ''Essay on the Shaking Palsy'' [3].

Parkinson's disease is age-related and its prevalence, similar worldwide, is about 1% in people over the age of 60 and 4% over the age of 85 [4-5]. The onset of sporadic PD has a marked increase after the age of 60 [4]. Rare early-onset PD (EOPD) occurs before the age of 50, with an incidence of about 5%-10% of all cases, and has usually a monogenic origin [4]. EOPD can be divided in two groups: young-onset Parkinson's disease (YOPD), with an age of onset between 21 and 40 years, and juvenile-onset PD (JOPD), with onset before the age of 20 years [6].

The cardinal symptoms of PD (usually described as ''parkinsonism'') are resting tremor, bradykinesia, rigidity, and postural imbalance [1, 4]. Nevertheless, many non-motor symptoms of PD, such as autonomic insufficiency, cognitive impairment, depression, olfactory deficits, psychosis, and sleep disturbance have been described [5]. Moreover, dementia affects about 40% of PD patients [7] and depression nearly 50% [8].

Classical PD is characterized pathologically by degeneration of the dopaminergic neurons of the *substantia nigra pars compacta* (SNpc) leading to loss of dopamine (DA) in the striatum, in association with the appearance of Lewy bodies (LB) (Figure 1.1) and Lewy neurites in the surviving neurons [2, 9-10]. Lewy bodies are deposits of fibrils of insoluble polymers of α-synuclein in the cell body of neurons [11]. However, some monogenic forms of PD lack this typical LB pathology [12]. Clinical signs of PD are evident when approximately 80% of striatal dopamine and 50% of nigral neurons are lost [13].

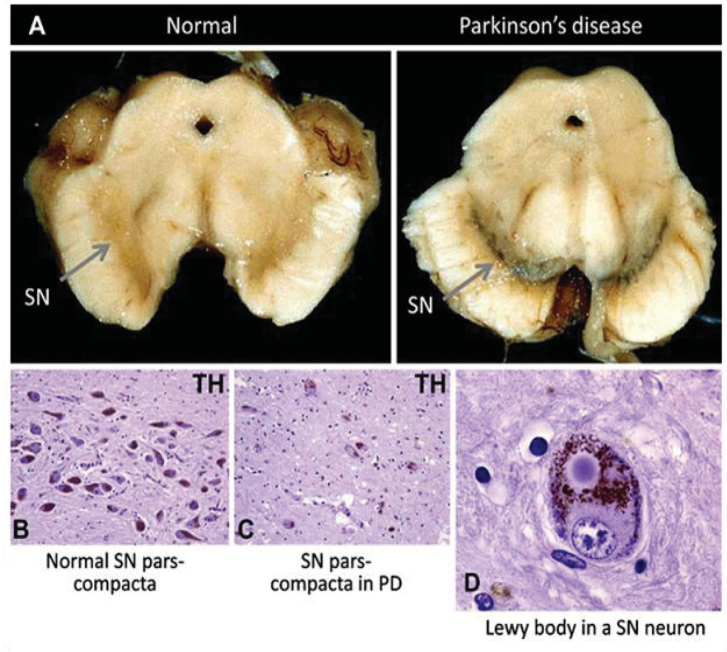

FIGURE 1.1| *SUBSTANTIA NIGRA* DEGENERATION IN PD WITH LEWY BODIES. The loss of SNpc neurons in advanced PD results in depigmentation of the SNpc (A), and in loss of the DA synthesising enzyme tyrosine-hydroxylase (TH) (B-C). The depositis of α-synuclein fibrils in the neuronal cell body are called Lewy bodies (D). Adapted from [11].

PD is multifactorial, likely arising from a combination of genetic susceptibility, ageing and gender (men are slightly more prone to PD [14]), environmental exposures, and gene-environment interactions [5, 15-16]. Many of the familial forms display clinical features that are considered atypical for PD, such as young onset, dystonia, or early occurrence of dementia [4].

The diagnosis of PD is based on clinical criteria, mainly parkinsonian symptoms and a definite diagnosis is only achieved by autopsy [2, 17]. Neuroimaging can be also helpful when patient's history or clinical findings are atypical [17].

Oral levodopa (LD) therapy is still the most efficient symptomatic treatment of Parkinson's disease and responsiveness to it has become a key diagnostic criterion [5, 18 and references there in]. However, neuroprotective treatment that delays or arrests neurodegeneration in PD remains an unaccomplished goal, due to the lack of knowledge about the specific molecular events that provoke neurodegeneration in PD [19-20]. Until the late 90's, most of the hypothesis of the etiology and pathogenesis of PD was postulated based on post-mortem tissue or neurotoxic animal models, such as using 1-methyl-4-phenyl-1,2,3,6-tetrahydropyridine (MPTP) as inductor of

dopaminergic degeneration [21]. These studies evidence three types of cellular dysfunction that seem to be important in PD pathogenesis: oxidative stress, mitochondrial respiration defect, and abnormal protein aggregation [20]. The knowledge about the disease only changed in 1997, when mutations in the gene encoding for α-synuclein [22], and then other PD-causing genes, were described as a cause of inherited PD [20].

1.1.1. ETIOLOGY OF PD

The etiology of Parkinson's disease is not well understood but seems to involve both genetic and environmental factors [2].

Environmental risks for PD include exposure to pesticides, rural living, drinking well water, heavy metal and solvent exposure, welding and mining [15]. In 1983, several people developed typical signs of PD after intravenous injection of drugs contaminated with MPTP. Subsequently, it was found that MPTP selectively damages dopaminergic cells in the *substantia nigra* [23] (Figure 1.2) favouring the hypothesis that exposure to environmental toxins might be related to the risk of PD. MPTP, as well as the herbicide paraquat and the pesticide rotenone, is a selective complex-I inhibitor and induce dopamine depletion in animal studies [24].

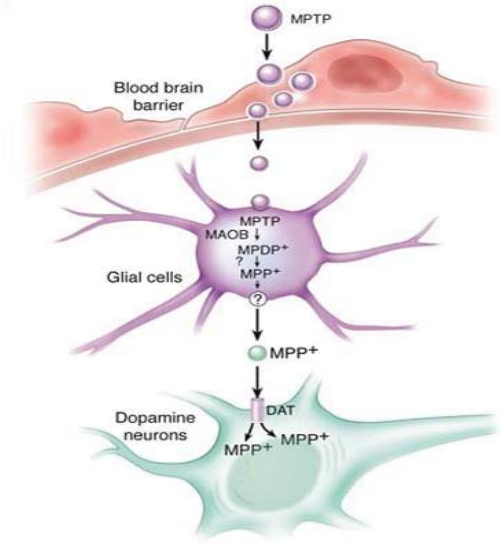

FIGURE 1.2| SCHEMATIC REPRESENTATION OF MPTP METABOLISM. After systemic administration, MPTP crosses the blood-brain barrier. Once in the brain, MPTP is converted to $MPDP^+$ by MAO-B within nondopaminergic cells, such as glial cells, and then to MPP+ by an unknown mechanism. After that, MPP^+ is released, again by an unknown mechanism, into the extracellular space. MPP^+ is concentrated into dopaminergic neurons via the dopamine transporter (DAT). Adapted from [20].

Many epidemiological studies have shown a reduced risk of PD among cigarette smokers [25-27]. Several mechanisms have been proposed to explain the potential neuroprotective effect of cigarette smoking. The most likely explanations involve nicotine, because nicotine may stimulate dopamine release, act as an antioxidant, or alter monoamine oxidase B activity [28]. Other possible protective factors include caffeine consumption and use of anti-inflammatory agents [29]. Nevertheless, the normal metabolism of DA can be a cause of neurodegeneration by generation of ROS (reactive oxygen species) [20, 30].

The majority of PD forms results from complex interactions among genes, and between genes and environmental factors [31]. The identification of distinct genetic *loci* at which pathogenic mutations are associated with parkinsonism (Table 1.1) contributes to the advance in the understanding of the mechanisms underlying PD pathogenesis [1]. Many pathogenic mutations produce variable pathological and clinical phenotypes distinct from typical PD (Table 1.1).

TABLE 1.1| GENES AND LOCI ASSOCIATED WITH MONOGENIC PARKINSONISM [1, 31-32].

PARK locus	*Gene*	Map position	Clinical phenotype	Mutations	Pathology	Inheritance
Well-validated loci/genes						
PARK1/4	*SNCA*	4q21	EO, parkinsonism with common dementia	A30P, E46K, A53T, Genomic duplications/triplications	LB	AD and sporadic
PARK2	*parkin*	6q25-q27	EO and juvenile, slowly progressing parkinsonism	>100 mutations (point mutations, exonic rearrangements)	LB	AR and sporadic
PARK6	*PINK1*	1p35-p36	EO, slowly progressing parkinsonism	>40 point mutations, rare large deletions	One case exhibiting LB	AR
PARK7	*DJ-1*	1p36	EO parkinsonism	>10 point mutations and large deletions	Unknown	AR
PARK8	*LRRK2*	12q12	LO parkinsonism	>40 missense variants, >7 of them pathogenic, including the common G2019S	LB (usually)	AD and sporadic
PARK9	*ATP13A2*	1p36	Jvenile and EO parkinsonism with Kufor-Rakeb syndrome	>5 point mutations	Unknown	AR
Not assigned	VPS35	16q11.2	LO parkinsonism			AD and sporadic
Not assigned	EIF4G1	3q27.1	LO parkinsonism			AD
Putative loci/genes						
PARK3	Unknown	2p13	LO parkinsonism	Not identified	LB	AD
PARK5	*PARK5*	4p14	LO parkinsonism	One mutation in a single PD sibling pair	Unknown	AD
PARK10	Unknown	1p32	Unclear	Not identified	Unknown	Not clear
PARK11	*GIGYF2*	2q36-q37	LO parkinsonism	Seven missense variants	Unknown	AD
PARK13	*Omi/HTRA2*	2p13	Unclear	Two missense variants	Unknown	Not clear
PARK12	Unknown	Xq	Unclear	Not identified	Unknown	Not clear
PARK14	*PLA2G6*	22q13.1	Juvenile and parkinsonism with additional features	Two missense mutations	LB	AR
PARK15	*FBX07*	22q12-q13	EO parkinsonism and parkinsonian-pyramidal syndrome	Three point mutations	Unknown	AR

Abreviations: PD – Parkinson's Disease; EO - early-onset; LO - late-onset; AD - autosomal dominant; AR - autosomal recessive; LB - Lewy bodies

1.1.2. MONOGENIC FORMS OF PD

Although PD was long considered a non-genetic disorder of 'sporadic' origin, 5 to 10% of patients are now known to have monogenic forms of the disease [4]. Several *loci* have been associated with both autosomal dominant [SNCA/PARK1/4 and Leucine-rich repeat kinase 2 (LRRK2)/PARK8] and autosomal recessive PD [parkin/PARK2, PTEN-induced kinase 1 (PINK1)/PARK6, DJ-1/PARK7, ATP13A2/PARK9] (Table 1.1) [1, 31-32]. Mutations in two other genes [vacuolar protein sorting 35 (VPS35) and eukaryotic translation initiation factor 4G1 (EIF4G1)], segregate in large families with dominant late-onset PD, but they are not assigned as PARK loci yet [33-34] (Table 1.1).

Genome-wide association studies (GWAS) have been helpful to identify *loci* at which common genetic variants increase risk of developing apparently sporadic disease [1].

1.1.2.1. *SNCA*

α-synuclein is a 140 kDa protein encoded by the *SNCA* [1] and is the major component of Lewy bodies [31]. *SNCA* is crucial to the pathophysiology of familial and sporadic PD [31].

Although rare, three missense mutations were identified in this gene: A53T, A30P and E46K (Figure 1.3). In the case of the A53T mutation, different studies showed that it leads to an early onset age (<50 years), rapid disease progression, atypical symptoms such as prominent cognitive deterioration, central hypoventilation, myoclonus and severe postural hypotention [12 and references there in]. The A30P mutation causes a typical PD phenotype with neuronal loss in the SNpc and LB pathology, and dementia late in the disease course [35]. The third *SNCA* missense mutation was described as leading to parkinsonism with Lewy bodies formation that progressed to dementia with visual hallucinations and fluctuations in consciousness [36].

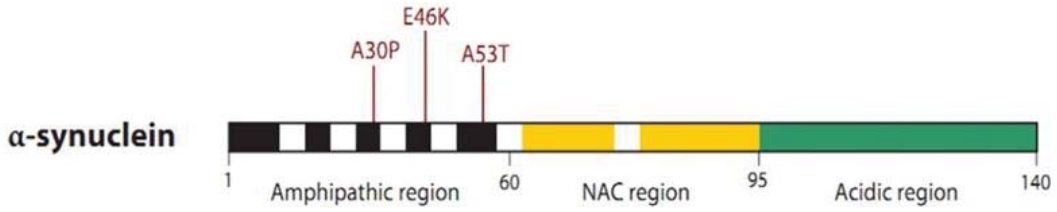

FIGURE 1.3| α-SYNUCLEIN DOMAINS AND MISSENSE MUTATIONS: A53T, A30P AND E46K. A number of imperfect KTKEGV repeat sequences (white stripes) are shown in the N-terminal region and central NAC (nonamyloid component) region. Mutations that segregate with PD are annotated at their approximate position along the protein's length. Adapted from [1].

Numerous studies have also established a link between familial PD and duplications or triplications in the *SNCA* gene [37]. Indeed, multiplication of this gene appears to be a more common cause of PD than point mutations [12 and references there in]. Duplication of *SNCA* are associated with familial PD with a classical phenotype and an earlier onset age [38]. Gene triplication leads to earlier onset and faster progression of disease than duplication, indicating that disease severity is dependent on α-synuclein expression levels [1]. All these studies indicates that there is a relationship between α-synuclein expression levels and the appearance of PD [1].

1.1.2.2. *LRRK2*

LRRK2 mutations are more frequently found in sporadic cases of PD than in autosomal dominant parkinsonism [31]. This gene encodes a leucine-rich repeat kinase 2 (LRRK2), also called as Dardarin [39], that has been suggested to be involved in protein-protein interactions, maintenance of neurites, and regulation of neuronal survival [40]. This protein is expressed in the striatum, suggesting that LRRK2 malfunction is relevant for PD pathogenesis [40]. Several mutations in *LRRK2* have been described as segregating with PD in large families worldwide with autosomal dominant PD, such as Y1699C, I2020T, R1441C, and R1441G (Figure 1.4) [41]. However, the most common mutation in this gene is the G2019S mutation (Figure 1.4) which segregates with familial and sporadic PD [42].

Overall, mutations in LRRK2 are estimated to account for up to 10% of autosomal dominant familial PD cases and 0.6-1.6% of sporadic PD [43-44]. Patients

with LRRK2 mutations typically have late disease onset and exhibit a wide range of pathologies that can differ between or within families [40].

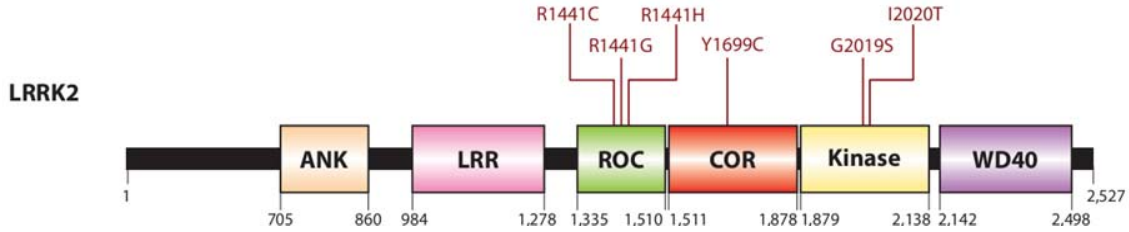

FIGURE 1.4| LRRK2 DOMAINS AND PATHOGENIC MUTATIONS: Y1699C, I2020T, R1441C, R1441G, AND G2019S. Ank (ankyrin-like repeats), LRR (leucine-rich repeats), ROC (Ras of complex proteins) GTPase domain, COR (C-terminal of ROC), kinase, and WD40. Mutations that segregate with PD are annotated at their approximate position along the protein's length. Adapted from [1].

1.1.2.3. *PARKIN*

Parkin is an ubiquitin E3 ligase responsible for the addition of ubiquitin to specific substrates, targeting them for degradation by the proteasome or lysosome [45-46].

Parkin may play a role in sporadic PD through common and frequent mutations (Figure 1.5) [45]. Moreover, parkin is inactivated by nitrosative, dopaminergic, and oxidative stress, which indicates that loss of parkin function plays a role not only in sporadic forms of the disease but also in autosomal recessive parkinsonism [45]. Accumulation of parkin substrates is thought to contribute to DA neurodegeneration due to parkin inactivation in the pathogenesis of PD [1].

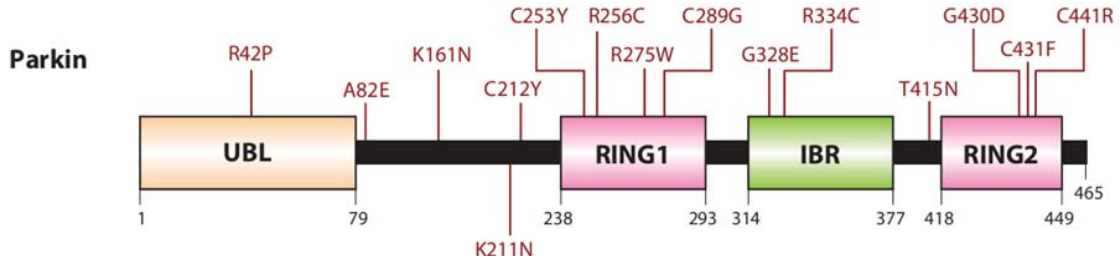

FIGURE 1.5| PARKIN DOMAINS AND PATHOGENIC MUTATIONS. UBL (ubiquitin-like) and two RING domains separated by an IBR (in-between RING) domain. Mutations that segregate with PD are annotated at their approximate position along the protein's length. Adapted from [1].

PD-linked parkin mutations give rise to early-onset parkinsonism (10 to 15% of the cases), often with the absence of Lewy bodies, and account for a large proportion of the familial PD cases (for up to 50% of the cases) [45, 47].

1.1.2.4. *PINK1*

The PINK1 protein is a putative serine/threonine kinase (PTEN-induced putative kinase-1) involved in mitochondrial response to cellular and oxidative stress [47]. In 2009, Whitworth and Pallanck, suggest a mitochondrial quality-control pathway that fails in PD in which PINK1 and parkin are involved, leading to cellular dysfunction and death [48].

Mutations in *PINK1* gene (Figure 1.6) were identified as a cause of autosomal recessive early-onset parkinsonism [47], with a prevalence below 4% [12 and references there in].

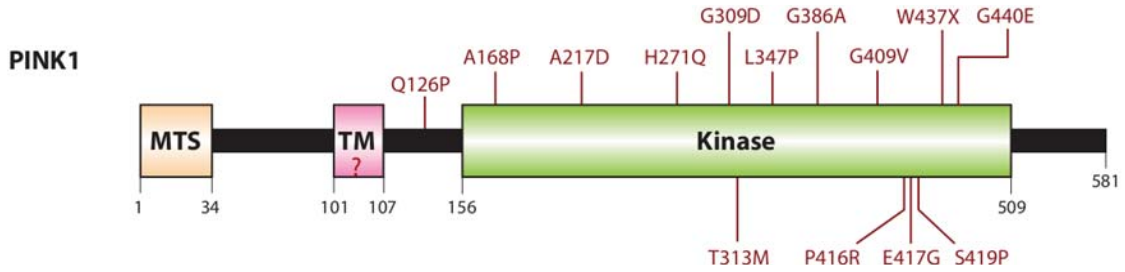

FIGURE 1.6| PINK1 DOMAINS AND PATHOGENIC MUTATIONS. MTS (mitochondrial targeting sequence), TM (putative transmembrane domain), and serine/threonine kinase Mutations that segregate with PD are annotated at their approximate position along the protein's length. Adapted from [1].

1.1.2.5. *ATP13A2*

ATP13A2 is a lysosomal membrane protein with an ATPase domain [49]. Loss-of-function mutations in *ATP13A2* gene underlying an autosomal recessive form of early-onset parkinsonism with pyramidal degeneration and dementia (Kufor-Rakeb syndrome) [49-50]. The unstable truncated mutant proteins were retained in the endoplasmic reticulum and degraded by the proteasome [49].

1.1.2.6. *DJ-1*

DJ-1 was first described as an oncogene [51], but nowadays the protein encoded by this gene is seen as a multifunctional protein. DJ-1 protein has been suggested to participate in response to oxidative stress and mutations in this protein lead to cell death, as observed in PD [52]. DJ-1 also seems to have chaperone activity in response to protein misfolding [53]. DJ-1-deficient mice show hypersensitivity to oxidative stress and DA neuron loss following treatment with MPTP, an oxidative stress-inducing compound [54]. DJ-1 was found to be responsive to hydrogen peroxide (H_2O_2) suggesting that it can act as a sensor for oxidative stress, for example, dopamine toxicity [55].

Despite the low frequency of pathogenic *DJ-1* mutations in early-onset PD (*DJ-1* mutations seem not to contribute to the late-onset cases of PD), these mutations are the second most common known genetic cause of PD [56], being the age of onset before 40 years [56-57]. Two homozygous mutations in the *DJ-1* gene have been shown to cause early-onset autosomal recessive Parkinson's disease in families in the Netherlands and Italy: a 14kb deletion removing exons 1 to 5 and a missense mutation (L166P) (Figure 1.7) [58]. The typical phenotype caused by these mutations is characterized by slow progression of the disease, good response to dopaminergic therapy, psychiatric disturbances, dystonic features, and clinical heterogeneity in disease severity [57].

FIGURE 1.7| DJ-1 GENE AND PATHOGENIC MUTATIONS. Mutations that segregate with PD are annotated at their approximate position along the protein's length. Adapted from [1].

1.1.3. PATHOGENESIS OF PD

As stated above, toxicological studies of PD models and the knowledge of the function of genes involved in PD suggest two major hypotheses regarding the disease's pathogenesis: protein misfolding and aggregation as a cause of SNpc dopaminergic neurons death, and the mitochondrial dysfunction with the consequent oxidative stress, including toxic oxidized DA species [20].

The protein deposition in brain tissues is a trait of age-related neurodegenerative disorders, like PD, suggesting that this fact is toxic to neurons [20]. Despite that, protein aggregation can be a defensive manner of the cell to remove toxic soluble misfolded proteins by inducing chaperones [59]. However, if chaperones are unable to properly refold proteins, they are target to proteosomal degradation by polyubiquitination [59]. On the other hand, the failure of the ubiquitine-proteosome system is a common pathway of neurodegeneration that underlies the development of familial and sporadic PD [60]. Even in sporadic PD, protein modifications, chaperones or proteosome dysfunction may lead to the accumulation of misfolded proteins, and the oxidative stress seems to have a key role in the pathogenesis of this form of disease too [20]. These facts are consistent with the genetic discoveries previously mentioned.

As reported, several mutations can lead to neurodegeneration and development of PD pathogenesis (Figure 1.8). Moreover, misfolded proteins may contribute to PD neurodegeneration by overloading the ubiquitin proteasomal and lysosomal degradation pathways [61]. When proteins involved in these pathways are mutated (e.g. α-synuclein and parkin), the ability of the cell's machinery to detect and degrade misfolded proteins is impaired [61]. Mutations in DJ-1 may alter its putative chaperone activity, leading to the accumulation of unwanted proteins and, consequently, to neurodegeneration [61]. Mitochondrial dysfunction and dopamine metabolism generate oxidative stress that can also promote protein misfolding and neurodegeneration [17, 61]. The reduced capacity of DJ-1 to detoxify ROS, may also originate oxidative stress in PD, and DJ-1 and PINK1 mutations can lead to mitochondrial dysfunction [61-62].

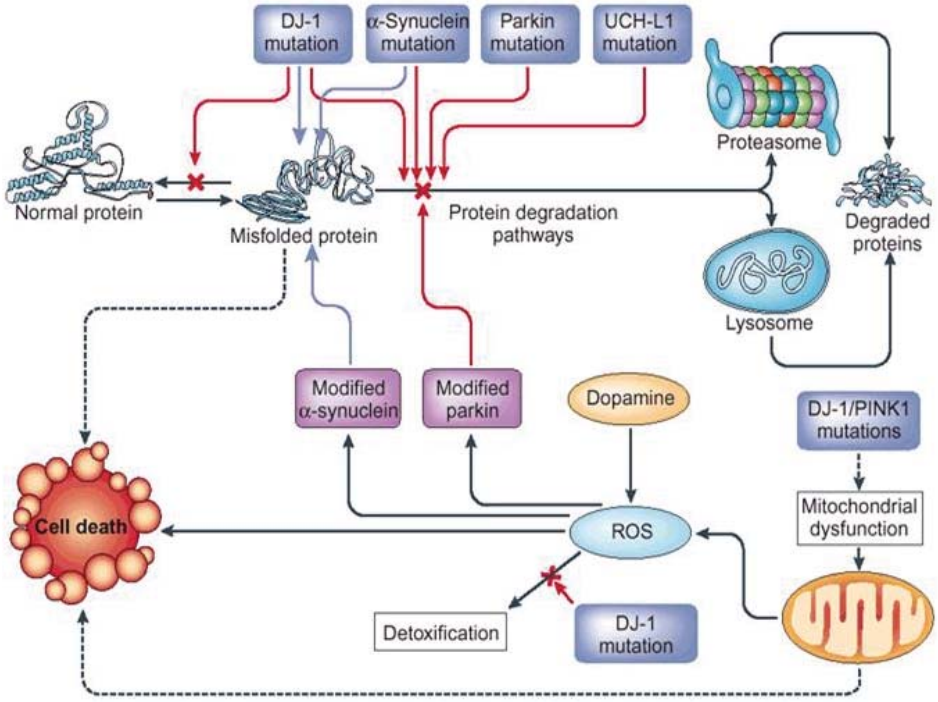

FIGURE 1.8| GENETIC MUTATIONS AND THE PATHOGENESIS OF PD. Red arrows represent the targeting and delivery of damaged proteins for degradation. Dashed arrows correspond to unknown mechanisms. Blue arrows represent misfolded proteins [61].

More recent evidence in mammalian cells implicate parkin and PINK1 in the regulation of autophagy, with parkin being recruited from the cytosol to damaged mitochondria [63-64]. These events trigger mitochondria autophagy, when PINK1 is accumulated in this organelle [63-64]. Thus, mutations in parkin and PINK1 impaired this process, leading to the accumulation of defective mitochondria and, ultimately, neurodegeneration in Parkinson's disease [63-64]. Moreover, DJ-1 was also correlated with the PINK1/parkin pathway to control mitochondrial function and autophagy [62, 65].

Thus, protein misfolding, mitochondrial dysfunction, oxidative stress, and autophagy are connected in the hypothetical pathogenic pathway of PD. The mechanisms of mitochondrial dysfunction and oxidative stress related to Parkinson's disease have been extensively studied over the last years.

1.1.3.1. MITOCHONDRIAL DYSFUNCTION AND OXIDATIVE STRESS

Mitochondria are ubiquitous organelles, critical for cell survival [66]. Their main function is to support aerobic respiration and to provide energy substrates for

intracellular metabolic pathways, but they are also involved in cell signalling, particularly in signalling for apoptotic cell death [66].

A dysfunction of mitochondrial energy metabolism leads to low levels of ATP production, impaired calcium buffering, and high levels of ROS generation [67]. It is known that the generation of ROS is related to aging and neurodegenerative disorders, including PD [67].

Several studies suggest that there is widespread oxidative damage in the brain of PD patients [68]. Evidence for mitochondrial metabolism impairment come from studies in autopsy and other tissue samples, and *in vitro* cell cultures derived from PD patients [69]. These studies revealed a decreased mitochondrial complex I activity in the *substantia nigra* [70] and in the frontal cortex [71]. The complex I deficiency in *substantia nigra* of PD patients supports the proposition that complex I deficiency may be directly involved in dopaminergic cell death in this disease [72].

Further, loss of activity of complex I induced by neurotoxins, such as MPTP and rotenone, produces parkinsonism in humans and animals [23, 73-74]. The complex I inhibition causes an increased free radical generation and protein oxidation, and could contribute to oxidative damage that is involved in PD and other neurodegenerative disorders [66, 75]. On the other hand, free radicals can damage the respiratory chain, leading to further production of ROS [20, 66].

A complex I defect could also contribute to cell degeneration through decreased ATP synthesis and a bioenergetic deficit [68]. The reduction of the mitochondrial membrane potential impairs proton pumping, including complex I, leading to mitochondrial permeability, with the release of small mitochondrial proteins that engage apoptosis. Complex I inhibition can also decrease the activity of the energy-dependent proteasome, suggesting a possible mechanism by which the ubiquitin proteasomal system (UPS) might be impaired in sporadic PD [75]. The presence of ROS also increase the amount of misfolded proteins hindering the proteasome activity [20]. Several studies indicate that mitochondrial DNA (mtDNA) mutations could contribute to the impairment of the respiratory chain in PD, but in fact, no abnormality of this genome has been consistently identified in PD patients [76]. Nevertheless, studies in which mtDNA from PD patients is introduced into

mtDNA-depleted cells (cybrid studies) show reduced mitochondrial respiration [77-78], and the appearance of Lewy bodies and Lewy neurites in cybrid cells, linking the mtDNA expression to neuropathology [78].

Other proteins can also play a role on mitochondrial activity (and in other cell compartments), such as PINK1, parkin, α-synuclein, and DJ-1 [76]. PINK1 has an N-terminal mitochondrial signal and an intramitochondrial location [76]. It was reported that loss of PINK1 results in mitochondrial dysfunctions in mice, reduced activities of complex I, complex II and aconitase [79]. Furthermore, PINK1 protects mitochondria from both intrinsic stress (e.g., dopamine metabolism and aging) and environmental insults (e.g., H_2O_2 and heat shock) [79]. This protective role of PINK1 in mitochondria might be explained by its involvement in the regulation of mitochondrial fission and fusion [79-80] or by the activation of mitochondrial chaperonin, such as TRAP1 and HtrA2 [81-82]. Moreover, parkin interplays dynamically with PINK1 in the regulation of mitochondrial morphology via mitochondrial fission/fusion [83-84].

Mutations in parkin result in a E3 ubiquitin ligase loss-of-function leading to the accumulation of parkin substrates within dopaminergic neurons, and consequently to nigral neuronal death [85]. Cells from parkin-knockout mice show an impaired aggresome (a specific cellular response to sequester potentially toxic misfolded proteins) formation [86], suggesting a direct involvement of parkin in the formation of Lewy bodies [46]. Mutations in parkin observed in PD patients were also suggested to prevent the formation of these protective inclusion bodies, possibly leading to the rapid onset and progression of the disease [46]. Parkin knockout mice revealed a decreased abundance of a number of proteins involved in mitochondrial function or oxidative stress, and reductions in respiratory capacity of striatal mitochondria [87]. In addition, *parkin* gene inactivation in mice leads to motor and cognitive deficits, and inhibition of amphetamine-induced dopamine release and glutamate neurotransmission [88].

α-synuclein is a predominantly cytosolic protein, but a fraction of it was identified in mitochondria membrane [89]. This binding of α-synuclein to the membrane of mitochondria could be related to its pathological role in mitochondrial dysfunction in PD [89]. α-synuclein inhibits complex I activity in a dose dependent

manner and is differentially expressed in mitochondria in different rat brain regions, suggesting that this protein might be important in neurodegeneration [90]. In addition, transgenic A53T mutant mice showed neuronal mitochondrial DNA damage and degeneration, and consequently mitochondrial structure and function abnormalities [91].

DJ-1 was found in cytosol, nucleus, microsomes (endoplasmic reticulum [ER] and Golgi), and in mitochondria (in mitochondrial matrix and inter-membrane space) [92-94]. Under oxidative stress conditions, DJ-1 translocates from the cytoplasm to mitochondria and nucleus, possibly to exert its protective role against oxidative stress [95-96]. It was reported that DJ-1 is important in the maintenance of the mitochondrial complex I activity [97]. Additionally, DJ-1 acts as an oxidative stress sensor within cells [11, 98], and DJ-1-deficient cells display an increased sensitivity to oxidative stress, leading to increased apoptosis due to the high levels of ROS [99-100], and proteasomal inhibition [100]. DJ-1 functions as a redox-sensitive molecular chaperone and inhibits α-synuclein aggregate formation [101-102].

The inhibition of DJ-1α in flies, a Drosophila homologue of human DJ-1, causes accumulation of ROS, hypersensitivity to oxidative stress, and dysfunction and degeneration of dopaminergic and photoreceptor neurons [103]. In DJ-1 null mice, nigrostriatal dopaminergic function is altered and motor deficits are present [104].

As previously mentioned, the DA metabolism produces ROS, such as hydrogen and superoxide radicals, and auto-oxidation of DA produces DA-quinone, a molecule that damages proteins by reacting with cysteine residues [20].

All together, these evidence show the importance of mitochondria and oxidative stress in the pathogenesis of PD.

1.2. ROLE OF DJ-1 IN NEUROPROTECTION

The *DJ-1* gene encodes a 189 amino acid protein with ≈20kDa and multiple putative functions [105, 106 and references there in]. DJ-1 has attracted attention because of its involvement in certain cases of familial early onset Parkinson's disease [57, 107-108]. A homozygous deletion, missense mutations (L166P, M26I), and a

compound heterozygous mutation in *DJ-1* gene have been reported to be directly related to EOPD, and loss or reduction of DJ-1 protein function has been considered to cause this phenotype [56, 58, 109]. DJ-1 is a member of the ThiJ/PfpI superfamily, and has homologues in most (if not all) organisms [107].

As mentioned above, *DJ-1* was originally identified as a novel oncogene in collaboration with active *ras* [51], related to fertilization [110], and later found to be a PD causative gene [58]. Additionally, many functions have been attributed to DJ-1, including transcriptional regulation [111], molecular chaperone [102, 112], peroxiredoxin-like peroxidase activity [113], modulator of autophagy and mitochondrial quality control [114-116], oxidative stress modulation [52], and important roles in the activation of pro-survival [103, 117-120] and inhibition of pro-apoptotic pathways [121-123].

In addition to a cytosolic localization, DJ-1 is also localized in the mitochondrial matrix and inter-cellular space of neurons. DJ-1 has a widespread distribution in the brain and peripheral tissues [93, 106], unlike parkin and α-synuclein, which have a more restricted tissue distribution [93]. Nevertheless, neurodegeneration associated with DJ-1 mutations remains mainly confined to the *substantia nigra* [106]. DJ-1 is expressed in neurons (dendritic, cytoplasmic, and nuclear distribution) of different neurotransmitter phenotypes and in all glial cell types: astrocytes, microglia and oligodendrocytes [106, 124]. The localization of DJ-1 in mitochondria suggests that it may play important roles in mitochondrial function [93]. As stated above, it was reported that upon an oxidative insult, more DJ-1 translocates to mitochondria [95], which could be related to a neuroprotective role of the protein.

DJ-1 protects neurons against oxidative stress-induced cell death and loss of DJ-1 may lead to Parkinson's disease by conferring hypersensitivity to dopaminergic insults [52, 54, 103, 125]. Moreover, mitochondria isolated from DJ-1 deficient mice produce more ROS compared with control animals [115]. All these findings suggest that DJ-1 has an antioxidant activity or can act as a free radical scavenger. Nevertheless, DJ-1 seems to be a weaker free radical scavenger when compared with peroxidases, hence its antioxidant activity might be due to other additional indirect activities of the protein [103, 113]. For example, DJ-1 has been described to up-

regulate the antioxidant glutathione synthesis [126] and to stabilize the transcription factor Nrf2, a major regulator of antioxidant genes [127].

In addition, DJ-1 deficiency in cell lines, cultured neurons, mouse brain and lymphoblast cells derived from PD patients showed abnormal mitochondrial morphology [115]. This phenotype contributes to the oxidative stress sensitivity caused by DJ-1 loss, which can be rescued by the expression of Pink1 and parkin [115]. Moreover, DJ-1 deficiency leads to altered autophagy in murine and human cells [115], and it has been implicated in mitochondrial quality control [114, 116].

In 2003, Yokota and colleagues demonstrated that downregulation of endogenous DJ-1 increases neuronal cell death, induced by H_2O_2, and neurons were rescued by overexpression of wild-type (WT) DJ-1 but not by the L166P mutant DJ-1 [125]. Again, this finding suggests that DJ-1 has antioxidant activity and this mutation (which causes a loss of function) consequently can be responsible for neuronal cell death in PD patients [125]. In the same study, it was shown that down regulation of endogenous DJ-1 enhanced ER-stress and proteasome inhibition, and its overexpression slightly suppresses these mechanisms [125].

An important finding from crystallography studies is that DJ-1 exists as an homodimer [112, 128-129]. The L166P mutation appears to disrupt the C-terminal domain and the dimerization capability, suggesting that the dimerization is functionally important [112, 128-129]. On the other hand, Baulac and colleagues, showed that this mutated DJ-1 does not prevent dimer formation, but apparently, forms oligomers or higher molecular weight structures (analogous to aggregates) [106]. These observations can be related to the aggregation of several proteins into insoluble intracellular inclusions (Lewy bodies) implicated in neurodegenerative diseases, including PD [106]. Some of these proteins are α-synuclein and parkin [130-131], and apparently, DJ-1 is not a major component of Lewy bodies [132]. However, it was shown that DJ-1 is present in Tau inclusions from tauopathies disorder cases, suggesting that abnormal DJ-1 aggregation is implicated in neurodegenerative disease mechanisms [133]. Another group reported the presence of DJ-1 in a large molecular complex, and provided evidence for an interaction between endogenous DJ-1 and α-synuclein [134]. It was also demonstrated that DJ-1 can act as a redox-sensitive

chaperone protein which can increase the solubility of α-synuclein, preventing its aggregation [102]. α-synuclein is also mutated in forms of inherited parkinsonism [35-36], so its interaction with DJ-1 may play an important role in PD [134]. Nevertheless, this interaction does not seem to be direct, and there are candidate proteins to anchor α-synuclein and DJ-1 such as mortalin, nucleolin, calnexin, grp94, and clathrin [135].

Still regarding the L166P mutation of DJ-1, it was also shown that this mutant is polyubiquitinated or binds to polyubiquitinated proteins [106, 136]. Moreover, several groups have found that the L166P mutation reduces protein stability, being quickly degraded through the proteasome [92, 108, 136-137], although proteasomal degradation may be only one of the mechanisms for DJ-1 turnover [137]. On the other hand, M26I mutated protein is as stable as WT DJ-1, has normal expression levels, and is not polyubiquitinated [106]. Another interesting feature of this mutated form is the ability to self-interact and to form homo-oligomers [108]. The DJ-1 mutant E64D was found to have a similar half-life, structure and dimer formation capacity compared to WT DJ-1 and was not subjected to accelerated proteasomal degradation, however the structure rigidity of the mutated protein seems to be higher than WT protein [137].

Another important structural aminoacid of DJ-1 is the cysteine-106 (C106), which is a highly conserved residue located at the ‘‘nucleophile elbow’’ region (Figure 1.9), extremely sensitive to radiation, which suggests that it may also be a favoured target of modification by ROS generated by oxidative stress [128]. It was reported that under oxidative conditions, the C106 residue of DJ-1 was oxidized, whereas C46 and C53 remained in their reduced state [98]. It was reported that DJ-1 may be activated by a complex mechanism dependent on its redox center C106 and modulated by the peripheral cysteine residues, and that impairment of oxidative-induced activation of DJ-1 might contribute to the pathogenesis of PD (Figure 1.10) [123]. Furthermore, inhibition of mitochondrial complex I is abolished by overexpression of WT DJ-1, but not by the C106 DJ-1 mutant [98]. Moreover, studies with a variant of C106, where the cystein residue was substituted by an alanine residue, showed resistance to oxidation of the protein and incapacity to localize in mitochondria under oxidative stress conditions, suggesting that cysteine mutations might affect the ability of DJ-1 to protect against cell death [98]. Another report indicates that C106 oxidation is crucial

for the protection of cells from mitochondrial damage by DJ-1 [111]. Taken together, these findings suggest that C106 may be a site of regulation of DJ-1 activity by oxidation, making the protein a potential sensor of oxidative stress [98, 128].

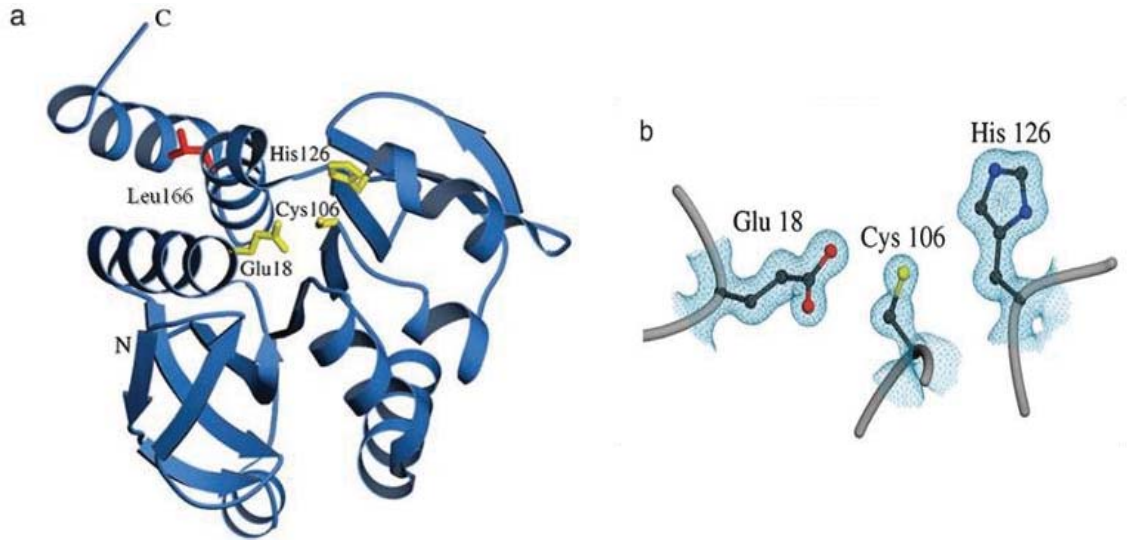

FIGURE 1.9| DJ-1 MONOMER STRUCTURE. Representation of DJ-1 monomer, with residues Glu-18, Cys-106, and His-126 in yellow (a). The Leu-166 residue in red is mutated to proline in *PARK7* familial PD. A closer view of the "nucleophile elbow" region (b). Adapted from [128]**.**

The C106 residue has been indicated to facilitate secretion of DJ-1 through cellular membrane microdomains in cultured cells [138]. This study also showed that DJ-1 was detected in the culture media of all types of cells examined (human SH-SY5Y and HeLa cells, and mouse Flp-In™ NIH3T3 cells) [138]. In the same study it was shown that DJ-1 was located in microdomains containing caveolin, and the treatment of cells with an inhibitor of non-classical pathways suggests that a portion of DJ-1 is secreted through microdomains [138]. Another evidence of this work is that oxidation of DJ-1 at C106 seems to facilitate its secretion [138].

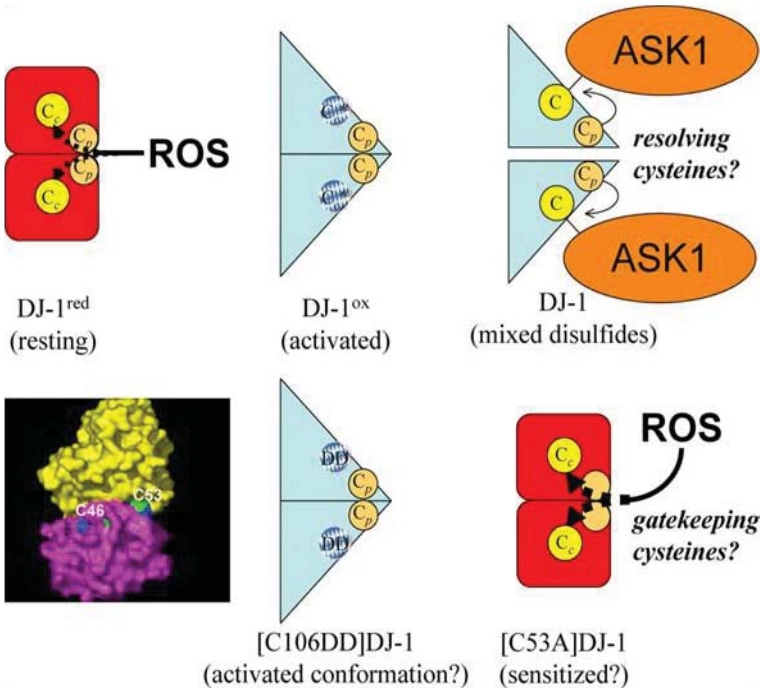

FIGURE 1.10| SCHEMATIC REPRESENTATION OF PROPOSED DJ-1 ACTIVATION STATES. The surface contour plot of the DJ-1 dimer (lower left) shows the cysteine side chains of each monomer (green residues belong to the yellow homomer, blue residues to the purple monomer). The Cys-53 side chains are prominently localized at the edge of the dimer interface. The Cys-106 residues are deeply buried within each DJ-1 monomer, necessitating a channel for ROS to enter the central active site Cys-106 (Cc). A peripheral (Cp) redox center that appears to comprise Cys-53 and perhaps other oxidizable and/or structural residues (Cys-46 and Met-26) could gate the accessibility of reactive oxygen species to Cys-106 and activate the central site (Cc*). Peripheral redox center mutants might be sensitized due to deregulated gating of reactive oxygen species, allowing unquenched access to the active center. Alternatively, Cp might function as "resolving cysteines," reducing transiently formed mixed disulfide bonds of Cys-106 with effector proteins. Formation of Cc* might "open" the DJ-1 conformation, allowing access of the buried Cys-106 to cysteines of other proteins [123].

In PD brain tissues, DJ-1 is expressed in reactive astrocytes at high levels, whereas non-disease astrocytes express this protein at very low levels, and this expression is sensitive to oxidative stress conditions [132-133]. Yanagida and colleagues showed that oxidative stress induces the release of DJ-1 protein from astrocytes, which may contribute to astrocyte-mediated neuroprotection [139]. In fact, DJ-1 knock-down in astrocytes impaired the astrocyte-mediated neuroprotection against rotenone, and its overexpression enhances their capacity to protect neurons [140-141]. Recently, DJ-1 deficiency was also found to impair astrocyte mitochondrial physiology [142]. On the other hand, a recombinant GST-DJ-1 has been shown to be incorporated into cells when it was injected into the *substantia nigra* of rats with neurodegeneration induced by 6-OHDA (6-hydroxydopamine) with a protective effect,

even when the administration was post-treatment [143]. In the same study, the uptake of recombinant DJ-1 was demonstrated (in the presence or absence of oxidative stress stimuli) as well as the inhibition of ROS production and cell death of SH-SY5Y cells after treatment with 6-OHDA [143]. This incorporation of recombinant DJ-1 was not seen in L166P mutant DJ-1 [143], maybe due to its instability and/or insoluble form [144-145]. DJ-1 has also been observed in serum, plasma and cerebrospinal fluid of PD patients [146-148]. All these findings suggest that DJ-1 shuttles between the inside and outside of cells [138]. However, some questions remain to be answered:

- If DJ-1 enter into neurons, which mechanisms are responsible for DJ-1 internalization?
- Is there any DJ-1 specific membrane receptor?
- Are there extracellular proteins interacting with DJ-1?
- Are these mechanisms involved in neuroprotection?
- Does DJ-1 act only as an extracellular first-line defence of ROS?

In order to address the DJ-1 entry mechanisms into neurons, it is necessary to understand the uptake processes of macromolecules through the cellular membrane.

1.3. PROTEIN INTERNALIZATION MECHANISMS

The cell membrane allows the communication between the cytoplasm and the extracellular environment by regulating the entry and exit of molecules from cells [149]. Macromolecules must be packed into membrane vesicles derived by the invagination of the plasma membrane in a process termed endocytosis [149]. Endocytosis has an important role in development, immune response, neurotransmission, intracellular communication, signal transduction, and cellular and organismal homeostasis [149]. Endocytosis occurs by multiple mechanisms that can be divided in two broad categories: phagocytosis, which is the uptake of large particles, and pinocytosis, the uptake of fluid and solutes (Figure 1.11) [149]. Phagocytosis is typically performed by specialized mammalian cells, whereas pinocytosis occurs in all cells in general [149]. Pinocytosis may occur by at least four mechanisms:

macropinocytosis, clathrin-mediated endocytosis (CME), caveolin-mediated endocytosis, and clathrin- and caveolin-independent endocytosis (Figure 1.11) [149].

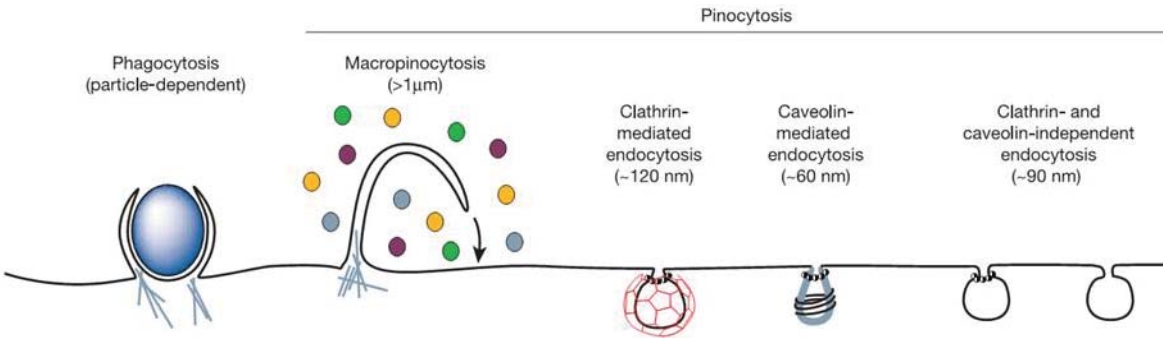

FIGURE 1.11| MULTIPLE PORTALS OF ENTRY INTO THE MAMMALIAN CELL. The endocytic pathways differ in the size of the endocytic vesicle, the nature of the cargo (ligands, receptors and lipids) and the vesicle formation mechanism [149].

Caveolae mediate the transport of serum proteins from the bloodstream to tissues across the endothelial cell layer [149]. Calveolae are present in many cells, and bound cholesterol and sphingolipid-rich microdomains of the plasma membrane, where various signalling molecules and membrane transporters are present [149-150]. Caveolin, a dimeric protein that binds cholesterol, is responsible for the shape and structural organization of caveolae [149] that typically appear as rounded plasma membrane invaginations of 50-80 nm in diameter [151]. Caveolae-mediated endocytosis seems to be highly regulated by the cargo molecules [149]. Although, the molecular basis of the cargo molecules and caveolae-localized receptors remain to be clarified [149].

Rafts are other type of cholesterol-rich microdomains on the plasma membrane that have 40-50 nm in diameter and diffuse freely on the cell surface [152-153]. Most probably these small rafts are captured and internalized by an endocytic vesicle, such as clathrin-coated vesicles (CCVs) [149, 154], or through a clathrin- and caveolin-independent manner [149, 155]. In neurons and neuroendocrine cells, clathrin-dependent mechanisms are crucial to the normal synaptic activity, but there are also clathrin-independent mechanisms of endocytosis that rapidly makes the recovery of membrane proteins after stimulated secretion [149, 156]. The caveolae- and clathrin-

independent endocytosis mechanisms remain poorly understood, whereas the molecular mechanisms of CME are better understood [149].

CME occurs constitutively in all mammalian cells and is responsible for the continuous uptake of essential nutrients [149]. This mechanism is fundamental for intercellular communication during development [157], and during the organism's life as it modulates the signal transduction by controlling the levels of surface signalling receptors, and by mediating the rapid clearance and downregulation of activated signalling receptors [149]. The assembly of CCVs under physiological conditions requires assembly proteins (APs) and numerous accessory proteins, such as dynamin, AP-2, and Eps15, which have been implicated in CME [149, 158]. Clathrin-coated vesicles mediate the sorting and selective transport of membrane-bound proteins, the endocytosis of transmembrane receptors, and the transport of newly synthesized lysosomal hydrolases from the trans-Golgi to the lysosomes [159]. CME occurs in endocytic "hotspots" in the plasma membrane that are constrained by the actin cytoskeleton [160], despite that, actin assembly doesn't seem to play an obligatory role in endocytic coated vesicle formation [161].

1.4. EXTRACELLULAR INTERACTOME

The study of cellular membrane or inter-cellular proteins interactome may contribute to understand the mechanisms of action of proteins released from cells possibly involved in protecting cells against oxidative stress conditions [139]. In fact, there is evidence for DJ-1-mediated neuroprotection involving DJ-1 downstream molecules through DJ-1 expressed by astrocytes [140]. Thus, the study of extracellular or cellular membrane interactors is fundamental to the knowledge about the neuroprotective mechanisms mediated by DJ-1 expressed and secreted by astrocytes.

In order to identify specific interactors in the cellular membrane, as specific receptors, or in the inter-cellular space of cells, crosslinking strategies can be used to link a protein of interest to interacting proteins in a stable form [162-163]. Another possibility is the pull-down of proteins contained in conditioned medium by using immunopurification or tag-affinity strategies.

1.5. OBJECTIVES

As stated above, DJ-1 plays an important role in neuroprotection mechanisms, such as those observed in oxidative stress conditions. Moreover, the protein is expressed in neurons and astrocytes, and its release from astrocytes is enhanced in oxidative stress conditions [139]. So, DJ-1 secretion by astrocytes [139] may further play a neuroprotective role in target neurons, with evidence for its uptake by SH-SY5Y cells [143]. Although several mechanisms of protein internalization can be used, none have been associated with DJ-1 neuronal internalization. Furthermore, no membrane receptor or extracellular interactors that can be related to DJ-1-mediated neuroprotection have been identified yet.

This study intends to provide some insight about the neuroprotective mechanisms of the exogenously added DJ-1. The study of these mechanisms will further elucidate how the protein shuttles between cells and how astrocytes can promote neuronal rescue under oxidative stress conditions.

2| METHODS

2.1. RECOMBINANT DJ-1 PRODUCTION

2.1.1. DJ-1 CLONING

The synthetic DNA coding for the human protein DJ-1 with the codons optimized for *E. coli* expression was obtained from GeneArt® (Invitrogen) and it was amplified by polymerase chain reactions (PCR) using the following primers: forward primer: **GCTAGC**AAACGTGCACTGGTTATTCTG and reverse primer: **CTCGAG**TCAATCTTTCAGAACCAGCGGTG. The forward and reverse primers introduced a Nhe I and Xho I sites respectively at the ends of the amplified sequence (restriction sites are represented in bold and the STOP codon is underlined).

The PCR was performed in a volume of 100 µl, in the presence of 50 ng of template DNA, 100 pmoles of forward and reverse primers, and 5 Units of recombinant Taq DNA polymerase (GE Healthcare), 10 nmoles of dNTP's, and the PCR was performed using the following cycling parameters: a first step of 5 min at 95 °C, followed by 35 cycles of 30 sec at 95 °C, 30 sec at 57 °C, and 1 min at 72 °C. After confirming the size of the amplified product by an agarose gel electrophoresis, the DNA band of the corresponding product was purified using the NZYGelpure gel extraction kit from NZYTech. The purified product was bound to pGEM®-T-easy vector system (Promega) according to the manufacture's protocol and the resultant construction was transformed in TOP10F´ competent cells (Invitrogen) that were then plated in 9 cm (diameter) Petri dishes with Luria-Bertani (LB) agar medium supplemented with 50 µg/ml ampicillin, 4 µmoles of isopropyl β-D-1-thiogalactopyranoside (IPTG), and 3 µmoles of 5-bromo-4-chloro-3-indolyl-beta-D-galacto-pyranoside (X-Gal) for blue/white colony selection. White colonies were picked and grown in liquid LB supplemented with 50 µg/ml ampicilin, and the DNA was isolated using the High Pure Plasmid Isolation Kit from Roche.

The subcloning of the DJ-1 coding DNA from pGEM-T-Easy vector to pSKB-3 vector (DJ-1_pSKB-3) was performed by digesting 1 µg of each pGEM-T-Easy construction and pSKB-3 with 2.5 Units of both Nhe I and Xho I (New England Biolabs,

Inc.), in buffer 50 mM potassium acetate, 20 mM Tris-acetate, 10 mM magnesium acetate, 1 mM ditiothreitol, pH 7.9, supplemented with 0.1 mg/ml Bovine Serum Albumin followed by agarose gel electrophoresis, where the correct size bands were cut, purified with NZYGelpure gel extraction kit (NZYTech) and the digested DNA fragments were ligated using T4 DNA Ligase (New England Biolabs, Inc.), according to the manufacturer's instructions. The ligated DNA molecules were then used to transform NZYStar competent cells (NZYTech), that were grown at 37 °C in LB/agar plates supplemented with kanamycin (50 µg/ml) and tetracycline (15 µg/ml). Two colonies were picked and grown in liquid LB supplemented with kanamycin (50 µg/ml), the DNA was isolated using the High Pure Plasmid Isolation Kit (Roche) and the DNA sequence was confirmed by Sanger DNA Sequencing at STAB Vida.

2.1.2. DJ-1 EXPRESSION

The DJ-1_pSKB-3 construct (Figure 2.1) was transformed into competent *E. coli* BL21star (DE3) strain and plated into LB/agar supplemented with 50 µg/ml kanamycin. One colony was used to inoculate 100 ml of LB supplemented with 50 µg/ml kanamycin sulphate that was grown overnight at 37 °C, from where 25 ml were used to inoculate 1 L of LB supplemented with 50 µg/ml kanamycin. The cells were allowed to grow at 37 °C with shaking. When the optical density at 600 nm reached 0.5, the temperature of the incubator was decreased to 18 °C and one hour later the protein expression was induced by the addition of IPTG to a final concentration of 1 mM. The protein expression was allowed to occur for another 16 hours.

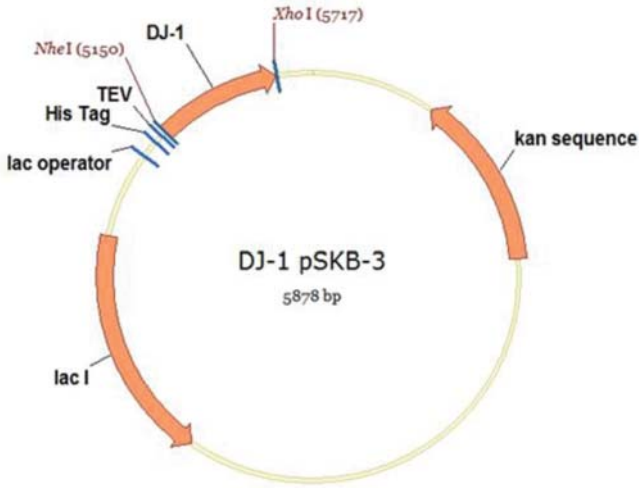

FIGURE 2.1| MAP OF THE CONSTRUCT OF DJ-1_PSKB-3. Representation of the DJ-1_pSKB-3 construct which contains: lac I – lac repressor gene; His Tag – hexahistidine tag; TEV – tobaco etch virus protease recognition site; kan – kanamycin resistance gene; the *DJ-1* cDNA (optimized for *E. coli* expression) cloned between Nhe I and Xho I restriction endonuclease sites. The vector pSKB-3 corresponds to pET-28a where thrombin recognition site was modified to TEV recognition site.

2.1.3. DJ-1 PURIFICATION

The cell suspension was centrifuged (20 min, 9,000×*g*, 4 °C), the cellular pellet was suspended in 50 ml of 20 mM sodium phosphate, 500 mM NaCl, 10 mM Imidazole, pH 7.2, and disrupted through a high pressure homogenizer EmulsiFlex-C3 (AVESTIN), with 3 passages at 1000 bar. The cellular extract was clarified by centrifugation (20 min, 9,000×*g*, 4 °C), the supernatant was filtered through 0.2 µm syringe filters and the protein was applied to a 5 ml HisTrap HP column (GE Healthcare) using a Bio-Rad BioLogic LP (Bio-Rad) low-pressure chromatography system. After column loading, the column was extensively washed with loading buffer (20 mM sodium phosphate, 500 mM NaCl, 10 mM Imidazole, pH 7.2) and protein elution was obtained by stepwise increasing of imidazole concentration up to 500 mM.

The eluted fractions containing DJ-1 were quantified by using the 2-D Quant Kit (GE Healthcare) and analysed by Coomasie Brilliant Blue R-250 and silver stained SDS-PAGE [4-20% polyacrylamide gel (Bio-Rad)]. The fraction which contained the highest amount of DJ-1 was dialysed [dialysis membrane with cut-off of 12-14,000 Da (Medicell International Ltd)] against PBS (8 mM K_2HPO_4, 2 mM $NaH_2PO_4 \cdot H_2O$, 150 mM NaCl), quantified by measuring absorption at 280 nm using a Nanodrop ND-1000

Spectrophotometer (Thermo Fisher Scientific) and stored at -80 °C in PBS with 10 % glycerol.

2.1.4. GEL BAND PROCESSING

Bands from the gel used to analyse the eluted fractions were excised, sliced in small pieces, and transfered to microcentrifuge tubes with 1 mL of de-ionized water (to prevent gel bands dehydration). Gel slices were then destained by removing water and adding 1 mL of destaining solution (50 mM ammonium bicarbonate and 30% acetonitrile). The destaining step was performed in a thermomixer (comfort, Eppendorf) at 850 rpm for 15 min. The destaining solution was removed, and the process was repeated if the gel pieces remained blue. Otherwise 1mL of water was added and the tubes were shaken in the thermomixer at 850 rpm for 10 minutes. After this washing step, the water was removed and the gel bands were dehydrated on Concentrador Plus (Eppendorf) for 1 hour at 60 °C. Then, enough volume of trypsin (15 ng/µL in 10 mM ammonium bicarbonate) was added to cover the dried gel bands and incubated for 10 minutes, on ice, in order to rehydrate the gel. After this period, 10 mM ammonium bicarbonate was added to cover gel bands again, and incubated overnight at room temperature in the dark to perform the in-gel digestion. The tryptic solution (containing trypsin and peptides) was collected to low binding microcentrifuge tubes (Eppendorf) and the remaining peptides were sequentially extracted from gel pieces by adding 40 µL of 30%, 50%, and 98% of acetonitrile (ACN) in 1% formic acid (FA), with agitation in the thermomixer at 1050 rpm for 15 min. Each solution was collected to the tube containing the initial tryptic solution. Peptides mixtures were concentrated by rotary evaporation, using the Concentrator Plus at 60 °C, and resuspended to 100 µL in a solution of 5% FA. Peptides were desalted using C18 Bond Elut OMIX tips (Agilent technology). Briefly, tip columns were hydrated with 30 µL of 90% ACN and 5% of FA and equilibrated with 180 µL of 5% FA. Peptides were loaded to the columns and this step was repeated twice, followed by a washing step with 60 µL of 5% FA solution and elution to new tubes with 120 µL of 90 % ACN and 5% of FA. Eluates were concentrated using the Concentrator Plus at 60 °C. Sample volume was adjusted to 30 µL in a solution of 2 % ACN and 0.1 % FA and transferred into vials for

posterior Liquid Chromatography coupled to tandem mass spectrometry (LC-MS/MS) analysis.

2.1.5. PROTEIN IDENTIFICATION BY LC-MS/MS

Peptides were resolved by liquid chromatography (nanoLC Ultra 2D, Eksigent) on a ChromXPTM C18 reverse phase column (300 µm ID × 15cm length, 3 µm particles, 120 Å pore size, Eksigent) at 5µL/min. Peptides were eluted into the mass spectrometer with an acetonitrile gradient in 0.1% FA (5% to 98% ACN, in a multiple step gradient for 25 min), using an electrospray ionization source (DuoSpray™ Source, ABSciex). The mass spectrometer (Triple TOF™ 5600 System; ABSciex) was programmed for information dependent acquisition (IDA) scanning full spectra (350-1250 m/z), followed by 20 MS/MS on multiple charged ions (+2 to +5) and performed one MS/MS before adding those ions to the exclusion list for 15 s (mass spectrometer operated by Analyst® TF 1.5.1, ABSciex).

Peptide identification was performed using Protein Pilot software (v4.5, ABSciex). Search parameters used were the following: SwissProt database, against *Homo sapiens*, *E. coli* and all species, and the recombinant protein sequence database, trypsin digestion, acrylamide as cysteine alkylating reagent, special factor gel-based ID, thorough ID search effort, and 0.05 Unused ProtScore (10% confidence score) as detected protein threshold. Data analysis was based on an independent False Discovery Rate analysis (FDR) using the target-decoy approach. Positive identifications were considered when proteins present 95% confidence (5% local FDR) with more than one peptide hit with individual confidence above 95% or with a single peptide hit with an individual confidence above 95% and a minimum sequence tag of 3 amino acids (4 consecutive peaks in the MS/MS spectrum).

2.1.6. HPLC-SIZE EXCLUSION CHROMATOGRAPHY

High-performance liquid chromatography (HPLC)-size exclusion chromatography (SEC) was performed using a Prominence Shimadszu system (Shimadzu Scientific Instruments) and a Superdex 200 5/150 GL column (GE

Healthcare), and data were collected and analyzed by LC Solution Software (Shimadzu Scientific Instruments). The mobile phase was composed by PBS with 10 % glycerol – buffer in which the purified protein was stored. Absorbance of the eluant was monitored over the wavelength 220 nm. Retention times were calibrated with the following protein molecular mass standards: aprotinin (6.5 kDa) (AppliChem), Ribonuclease A (13.7 kDa), Carbonic anhydrase (29 kDa), Ovalbumin (43 kDa), Conalbumin (75 kDa), Aldolase (158 kDa), and Ferritin (440 kDa) (all from GE Healthcare).

2.1.7. LC-MS OF INTACT DJ-1

The purified DJ-1 was cleaned and desalted using Strong Cation Exchage (SCX) followed by C4 Bond Elut OMIX tips (Agilent technology). SCX tips were wetted with 200 µL of 0.1% FA and equilibrated with 400 µL of 1% FA. Protein (185 µg in 0.1 % FA) was bind to the column (in 3 cycles of aspirate-dispense) and washed with 400 µL of a 0.1 % FA solution in methanol. Finally, protein was eluted with 30% methanol in 0.1 M solution of NaOH.

Then, sample was desalted using C4 tips. Sample was pre-treated with FA to adjust the solution to 5% FA. C4 tips were hydrated with 30 µL of 90% ACN and 5% of FA and equilibrated with 180 µL of 5% FA. Protein molecules were loaded to the columns (in 3 cycles of aspirte-dispense), followed by a washing step with 60 µL of 5% FA solution and elution to new tubes with 120 µL of 90 % ACN and 5% of FA. The eluted protein molecules were concentrated using the Concentrator Plus (Eppendorf) at 60 °C. Sample volume was adjusted to 30 µL in a solution of 2 % ACN and 0.1 % FA and transferred into vials for posterior LC-MS/MS analysis.

Proteins were resolved by liquid chromatography (nanoLC Ultra 2D, Eksigent) on a ChromXP™ C18 reverse phase trap-column (350 µm ID × 0.5mm length, 3 µm particles, 120 Å pore size, Eksigent) at 7 µL/min. Proteins were eluted into the mass spectrometer with an acetonitrile gradient in 0.1% FA (2% to 98% ACN, in a multiple step gradient for 12 min), using an electrospray ionization source (DuoSpray™ Source, ABSciex). The mass spectrometer (Triple TOF™ 5600 System; ABSciex) was

programmed for scanning full spectra (600-1250 m/z, operated by Analyst® TF 1.5.1, ABSciex).

Intact mass was determined using BioAnalyst™ Software (ABSciex). Briefly, the deconvolution of the spectra was obtained by Baesian Protein Reconstruct of the average of the maximum spectra possible, with the following parameters: mass range from 15 to 30 kDa (determined according with the expected protein molecular weight), spectrum limit range from 620 to 1000 m/z (determined according with protein charge envelope profile), signal to noise threshold of 10 (according with the ration from the less intense peak used in calculation to the noise determined by a script present in Analyst). From the deconvoluted sprectrum it was chosen a peak from the isotopic distribuition for modelling the data that was then used to calculate the molecular weight of the protein.

2.2. SH-SY5Y CELL CULTURE

Human neuroblastoma SH-SY5Y cells were cultured in Dulbecco's modified Eagle medium (DMEM) with Glutamax™ and low glucose (1 g/L) (Gibco), supplemented with fetal bovine serum (FBS) (Gibco) (10 %), amphotericin B solution (Invitrogen) (1.25 µg/mL) and penicilin-streptomycin solution (Pen-Strep) (Cambrex) (1 %). In order to facilitate the reading this supplemented culture medium will be referred only as DMEM with the reference to the percentage of FBS contained. For cell passage, cells were washed with Dulbecco's phosphate buffered saline (DPBS) (Cambrex, Charles City, IA) and detached with trypsin-EDTA (0.05 % solution in phosphate buffered saline (PBS)) (Invitrogen).

Cells were maintained at 37 °C, 5 % CO_2/95 % air in a humidified incubator (Shel Lab 3517-2) (Sheldon Manufacturing, Inc.).

2.3. Cell Viability Under Oxidative Stress

2.3.1. Cell Culture

SH-SY5Y cells were seeded at 46.9×10^3 cells/cm^2 in DMEM with 10 % FBS in 96-well plates (Corning) at 37 °C, 5 % CO_2/95 % air in a humidified incubator (Sheldon Manufacturing, Inc.).

2.3.2. Oxidative Stress Stimuli

Four hours after plating, cells were stimulated with different concentrations (25-10,000 μM) of H_2O_2 (Sigma-Aldrich) in DMEM with 0.1% of FBS for 24 h. The culture medium was totally exchanged to the referred above H_2O_2 solutions, freshly made. Control condition consisted in exchange the culture medium to DMEM with 0.1% of FBS.

2.3.3. Cell Viability Assessment

Cell viability was assessed by using the Cell Titer-Glo® Luminescent assay (Promega) in white opaque 96-well plates (Corning). The luminescent signal was detected by a LUMIstar Galaxy automated microplate luminescence reader (BMG Labtech), according to the manufacturer's instructions.

2.4. DJ-1-mediated Neuroprotection

2.4.1. Oxidative Stress and DJ-1 Stimuli

Four hours after plating (as described on section 2.3.1) cells were stimulated with different concentrations (25, 50, 100 and 200 μM) of H_2O_2 (Sigma-Aldrich) in DMEM with 0.1 % of FBS in the presence or absence of recombinant His-tagged human DJ-1 protein (1 or 5 μM) or the corresponding vehicle (PBS with 10 % of glycerol) for 24 h. Control condition consisted in exchange the culture medium to DMEM with 0.1% of FBS.

2.5. Activation of Akt and ERK1/2 Signalling Pathways

2.5.1. Cell Culture and DJ-1 Stimuli

SH-SY5Y cells were seeded at 75×10^3 cells/well in DMEM with 10 % FBS in 12-well plates (Corning) at 37 °C, 5 % CO_2/95 % air in a humidified incubator (Sheldon Manufacturing, Inc.). Twenty-four hours after plating, cells were serum starved by changing the culture medium to DMEM with 0.1 % FBS. After 16 h of serum starvation, cells were treated with 1 μM of recombinant DJ-1 (or equivalente volume of vehicle – PBS with 10% glycerol) for 0, 15, 30 and 60 min. Starved cells were also treated with 200 μM or 1 mM of H_2O_2, in the presence or absence of 1 μM of recombinant DJ-1 for 15 min. The positive control condition for Akt and ERK1/2 activation was the addition of 15 % of FBS to the culture medium of starved cells. Stimulation was terminated by aspiration of the medium and performing the cellular protein extracts.

2.5.2. Cellular Protein Extracts

Cells were washed and then scraped with ice-cold PBS supplemented with Complete Mini protease inhibitor mixture and Complete Mini phosphatase inhibitor mixture (inhibitors cocktail) (Roche) using rubber cells scraper (TPP, Switzerland). Cells were collected to microcentrifuge tubes and centrifuged at 500×*g* for 5 min at 4 °C. Pellets were resuspended in ice-cold RIPA buffer (50 mM Tris-HCl, pH 7.4; 1% (v/v) Igepal; 0.25% (v/v) sodium-deoxycholate; 150 mM NaCl; 1 mM DTT; 1 mM EDTA and the inhibitors cocktail). After three freeze-thaw cycles, cell lysates were centrifuged at 20,000×*g* for 15 min at 4 °C and the supernatant was collected to a new tube and stored at -20 °C, until further use. The protein concentration of each protein extract was determined by using the BCA protein determination assay (Thermo Fisher Scientific).

2.5.3. Immunoblot Detection

The cellular extracts (50 μg of total protein) were denatured with sample buffer (6×) [0.35 M Tris-HCl, pH 6.8 with 0.4 % SDS (v/v), 30 % glycerol (v/v), 10 % SDS (w/v),

9.3 % DTT (w/v) and 0.01 % bromophenol blue (w/v)] by boiling at 95°C for 5 min and then electrophoretically separated on a 10 % SDS-polyacrylamide gel (Bio-Rad) using a Mini-PROTEAN Tetra Electrophoresis System (Bio-Rad). Proteins were transferred to Trans-Blot® Turbo™ polyvinylidene fluoride (PVDF) membranes (Bio-Rad) using a Trans-Blot® Turbo™ Transfer System (Bio-Rad). After transfer, the membranes were blocked for 1 hour at room temperature (RT) with 5% (w/v) skimmed milk powder dissolved in PBS with 0.1 % (v/v) Tween-20 (PBS-T) (Bio-Rad).

Membranes were then incubated with primary antibodies against the total form of Akt and ERK1/2: rabbit Anti-total ERK1/2 (1:500) [Cell Signaling Technology, Inc.(# 9272)], mouse Anti- total ERK1/2 (1:500) [Cell Signaling Technology, Inc.(#4695)]; or against the phosphorylated form of Akt and ERK1/2: rabbit Anti-P-Akt (Ser473) (1:500) [Cell Signaling Technology, Inc.(#9271)] and rabbit Anti-P-ERK1/2 (Thr202/Tyr204) (1:500) [Cell Signaling Technology, Inc.(#4377)] in 5% (w/v) skimmed milk powder dissolved in PBS-T – overnight at 4 °C followed by 1 hour at RT. Primary antibodies were removed and membranes were washed with PBS-T (3 times for 15 min and under agitation). Blots were then incubated for 2 hour at RT with the secondary antibodies conjugated with alkaline phosphatase [anti-rabbit (1:3,000) and anti-mouse (1:10,000), both from Jackson ImmunoResearch Laboratories, Inc.], in 5% (w/v) skimmed milk powder dissolved in PBS-T, followed by three washes as above. After the incubation of membranes with the phospho- and total-specific antibodies, they were stripped and re-probed with a mouse antibody against glyceraldehyde 3-phosphate dehydrogenase (GAPDH) (sc-47724) (Santa Cruz Biotechnology, Inc.) used as protein loading control.

To observe protein-immunoreactive bands, membranes were incubated with “Enhanced Chemifluorescence (ECF) detection system” (GE Healthcare) and visualized using a Molecular Imager FX System (Bio-Rad). The adjusted volumes (total intensities in a given area with local background subtraction) for each band were obtained using Quantity One® version 4.6 software (Bio-Rad).

2.6. DJ-1 INTERNALIZATION

2.6.1. OXIDATIVE STRESS STIMULI

SH-SY5Y cells were seeded in 148 cm^2 plates (Corning) at 5×10^6 cells/plate in DMEM with 10 % FBS and maintained in culture for 48h at 37 °C, 5 % CO_2/95 % air in a humidified incubator (Sheldon Manufacturing, Inc.). Cells were treated with 1 μM of recombinant DJ-1 in the presence or absence of H_2O_2 (Sigma-Aldrich) (200 μM) in DMEM with 0.1 % FBS and they were incubated for 4 h at 37 °C, 5 % CO_2/95 % air in a humidified incubator. The control condition consisted in the same condition except the addition of DJ-1 and H_2O_2.

2.6.2. CELLULAR FRACTIONATION AND PROTEIN EXTRACTS

The culture medium (in the presence or absence of the recombinant DJ-1 or DJ-1 and H_2O_2) was removed and cells were washed with PBS four times. Then, cells were treated with 1.5 mM of DTSSP (crosslinker) (Thermo Fisher Scientific) for 30 min at 37 °C, 5 % CO_2/95 % air in a humidified incubator (Sheldon Manufacturing, Inc.). The crosslinker was quenched by incubation with Tris-HCl (15 mM, pH 7.4) for 15 min at 37 °C, 95 % air and 5 % CO_2 in humidified incubator.

After removing the crosslinker and Tris-HCl solution, cells were scraped and pulse-sonicated (1 sec pulses for 10 sec with 40 % amplitude) (Vibra-Cell™ VCX130) (Sonics & Materials) in Tris-HCl (50 mM, pH 7.4) with Complete Mini protease inhibitor mixture and Complete Mini phosphatase inhibitor mixture (inhibitors cocktail) (Roche). Cellular debris were removed by a centrifugation at 1,000×g for 5 min. The supernatant was centrifuged at 126,000×g for 1h at 4 °C to separate it into the cytosolic (supernatant) and membrane (pellet) fractions. The membrane fraction was washed with ice-cold PBS suplemmented with inhibitors cocktail and then centrifuged again at 126,000×g for 1h at 4 °C. The pellet was resuspended in RIPA buffer (50 mM Tris-HCl, pH 7.4; 1% (v/v) Igepal; 0.25% (v/v) sodium-deoxycholate; 150 mM NaCl; 1 mM DTT; 1 mM EDTA and inhibitors cocktail) and both fractions were incubated with the His-trap resin (GE Healthcare) for 1h at 4 °C at 1400 rpm in the thermomixer (Eppendorf).

Samples were then centrifuged at 1,000×g for 3 minutes, the supernatant containing proteins that did not bind to His-trap resin was collected to a new tube and the resin was denaturated with sample buffer (2×), without DTT (to avoid the cleavage of DTSSP) at 95 °C, for 15 minutes with agitation. Proteins eluted from the resin were collected after a centrifugation at 1,000×g for 3 minutes. All fractions were stored at -20 °C until further use. Fractions of proteins that did not bind to His-trap resin were concentrated using concentrators with a cut-off of 5 kDa (500 µL) (Sartorius). Protein content was determined in all samples using the RC-DC method (Bio-Rad), according to the manufacturer's instructions.

2.6.3. IMMUNOBLOT DETECTION

Samples were denaturated with sample buffer (6×) with DTT at 95 °C for 5 min and then electrophoretically separated on 12.5 % SDS-polyacrylamide gel (equal amounts of protein per lane) using a Mini-PROTEAN Tetra Electrophoresis System (Bio-Rad). Proteins were transferred to Trans-Blot® Turbo™ polyvinylidene fluoride (PVDF) membranes (Bio-Rad) using a Trans-Blot® Turbo™ Transfer Starter System (Bio-Rad). After transfer, the membranes were blocked for 1 hour at room temperature (RT) with 5% (w/v) skimmed milk dissolved in PBS with 0.1 % (v/v) Tween-20 (PBS-T) (Bio-Rad). Membranes were then incubated with primary antibodies: goat Anti-DJ-1 C-16 (1:200) [Santa Cruz Biotechnology, Inc. (sc-27006)], in 5% (w/v) skimmed milk powder dissolved in PBS-T, overnight at 4°C followed by 1 hour at RT or mouse Anti-His Tag TM0243 (1:5,000) (GenScript), in 5% (w/v) skimmed milk powder dissolved in PBS-T, for 1 hour at RT. Primary antibodies were removed and membranes were washed with PBS-T (3 times for 15 min under agitation). Blots were then incubated for 1 hour at RT with the secondary antibodies conjugated with alkaline phosphatase (anti-goat (1:1,000) and anti-mouse (1:10,000) both from Jackson ImmunoResearch Laboratories, Inc., respectively), in 5% (w/v) skimmed milk powder dissolved in PBS-T, followed by three washes as above. To observe protein-immunoreactive bands, membranes were incubated with "Enhanced Chemifluorescence (ECF) detection system" (GE Healthcare) and visualized in a Molecular Imager FX System (Bio-Rad).

2.7. EXTRACELLULAR DJ-1 INTERACTOME

2.7.1. CELL CULTURE AND PULL-DOWN ASSAY

SH-SY5Y cells were seeded at 25×10^3 cells/cm^2 in 148 cm^2 plates (Corning) in DMEM with 10 % FBS and maintained in culture for 48h at 37 °C, 5 % CO_2/95 % air in a humidified incubator (Sheldon Manufacturing, Inc.). Then, cells were washed four times with PBS and twice with DMEM without FBS, warmed at 37 °C. Then, cells were maintained in culture with DMEM without FBS for further 48h at 37 °C, 5 % CO_2/95 % air in a humidified incubator. The conditioned medium and culture medium that was not in contact with cells (negative control) were concentrated using 5 kDa cut-off concentrators (20 mL) (Sartorius). Cells were scraped with ice-cold PBS with the inhibitors cocktail (Roche) using rubber cells scraper (TPP), and collected to microcentrifuge tubes and centrifuged at 500×*g* for 5 min at 4 °C. Pellets were resuspended in ice-cold RIPA buffer. After three freeze-thaw cycles, cell lysates were centrifuged at 20,000×*g* for 15 min at 4 °C and the supernatant was collected to a new tube and store at -20 °C, until further use.

Concentrated culture mediums and total protein extracts (positive control) were then incubated with 100 µL of His-trap resin with or without recombinant DJ-1 overnight at 4 °C at 1400 rpm in the thermomixer (Eppendorf).

Following a centrifugation at 1,000×g for 3 minutes, the supernatant containing proteins that did not bind to His-trap resin was collected to a clean tube and the resin was denaturated with sample buffer (2×) at 95 °C, for 15 minutes with agitation. Proteins eluted from the resin were collected after a centrifugation at 1,000×*g* for 3 minutes. All fractions were stored at -20 °C until further use.

2.7.2. SDS-PAGE AND COOMASIE STAINING

Samples were electrophoretically separated in a pre-cast 4-20 % SDS-polyacrylamide gel (Bio-Rad) using a Mini-PROTEAN Tetra Electrophoresis System (Bio-Rad) and stained with Coomasie Brilliant Blue G-250 (Bio-Rad). The gel band processing was done as described in section 2.1.4 and protein identification as described on section 2.1.5. Peptide identification was also performed using Protein Pilot software

(v4.5, ABSciex), as described on section 2.1.5., but searching using the SwissProt database, against *Homo sapiens* and all species.

2.8. STATISTIC ANALYSIS

Statistical analysis of results from cell viability was performed using SPSS (Statistical Package for the Social Sciences) version 17.0 (IBM®). Statistical significance was considered relevant for *p < 0.05, **p < 0.01 and ***p < 0.001 using Two-way ANOVA (Analysis Of Variance). The ANOVA analysis was followed by Tukey HSD post hoc test for comparison among experimental conditions. Parametric assumptions (data normality and homoscedasticity) were tested using Shapiro-Wilk Test and Levene's Test, respectively. Data presented as mean ± standard error of the mean (S.E.M.) Every experimental condition was tested in four sets of independent experiments, unless specified.

3| RESULTS

DJ-1 has been associated with familial early onset Parkinson's disease [57, 107-108] as DJ-1 dysfunction leads to neurodegeneration [56, 58, 109]. The exact mechanisms by which DJ-1 confers neuroprotection remain to be clarified, but this protein has been suggested to participate in oxidative stress response [52] and to act as a sensor for oxidative stress [55]. A DJ-1 astrocyte-mediated neuroprotection has been suggested [139] highlighting the potential of extracellular neuroprotective mechanisms of this protein. In order to mimic the presence of extracellular DJ-1 secreted by astrocytes, the first task of this project consisted in the production of a recombinant DJ-1 protein to study the effect of an exogenous addition of this protein to neuronal cells, under normal or oxidative stress conditions.

3.1. RECOMBINANT DJ-1 PRODUCTION AND CHARACTERIZATION

Recombinant DJ-1 was expressed in *E. coli* BL21star (DE3) strain and purified by chromatography, using a His-Trap column (Figure 3.1), since the produced protein contains a His-tag. The amount of protein in fractions from DJ-1 expression and purification steps, including fractions corresponding to the higher intensity peaks (fractions 1, 2, 3 and 4 - Figure 3.1) were quantified using the 2-D Quant kit, electrophoretically separated and stained with Colloidal Coomassie Brilliant Blue G-250 (Bio-Rad) and silver (only fraction 3 and fraction of purified DJ-1, after the dialysis) to observe the protein content profile (Figure 3.2). The most concentrated fraction - fraction 3 - (corresponding to the highest chromatographic peak and eluted at 300 mM Imidazole - Figure 3.1) was dialysed against PBS and stored at -80 °C in PBS with 10 % of glycerol at a final concentration of 1.85 µg/µL.

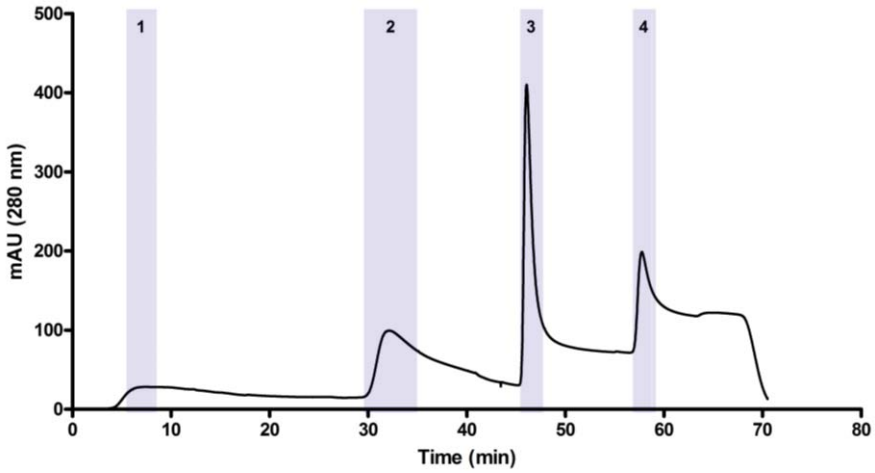

FIGURE 3.1| CHROMATOGRAM OF DJ-1 PURIFICATION BY AFFINITY CHROMATOGRAPHY. The chromatography was performed in an His-Trap column. Fractions represented by grey bars correspond to the collected fractions of each elution step. Fraction 1 - eluted fraction with 10 mM Imidazole; fraction 2 - eluted fraction with 50 mM Imidazole; fraction 3 - eluted fraction with 100 mM Imidazole; and fraction 4 eluted fraction with 300 mM Imidazole.

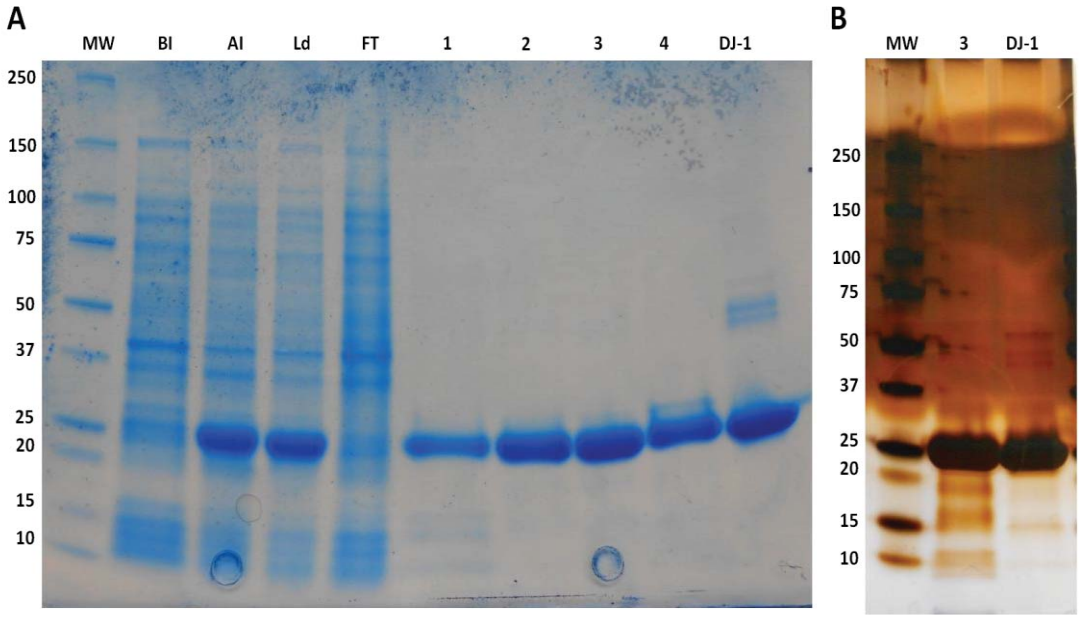

FIGURE 3.2| SDS-PAGE OF DIFFERENT FRACTIONS OF RECOMBINANT DJ-1 PURIFICATION. A - SDS-PAGE followed by coomassie staining. MW – molecular weight marker; BI – before expression induction; AI – after expression induction; Ld – loaded on the his-trap column; FT – flow-through of the his-trap column; 1 – eluted fraction 1; 2 – eluted fraction 2; 3 – eluted fraction 3; 4 – eluted fraction 4; DJ-1 – purified DJ-1 after dialysis of fraction 3. **B** - SDS-PAGE followed by silver staining. 3 – eluted fraction 3; DJ-1 – purified DJ-1 after dialysis of fraction 3.

The results indicate that before the protein expression induced with IPTG (BI), there is not a highly intense band at ≈22 kDa (expected mass of a DJ-1 monomer) (Figure 3.2, A). On the other hand, after the induction of DJ-1 expression (AI), a higher

intensity band appears at this molecular weight, as in the fraction loaded on the His-trap column (Ld) (Figure 3.2, A). Moreover, in the flow through (FT) of the His-trap column, the highly intense band disappeared, indicating that almost all the recombinant protein was captured by the column (Figure 3.2, A). All the analysed eluted fractions (1, 2, 3 and 4 – higher chromatogram peaks) presented this band (Figure 3.2, A). The fraction of stored protein (after the dialysis step) has a highly intense band at ≈22 kDa, as expected (Figure 3.2, A and B). However, fraction 3 and the final fraction of purified DJ-1 (after dialysis) presented other bands (Figure 3.2, B). In order to understand what was the content of these fractions besides DJ-1, bands were digested and analysed by LC-MS/MS.

3.1.1. PROTEIN IDENTIFICATION BY LC-MS/MS

The produced recombinant protein has some protein contaminants in both analysed fractions: fraction 3 and the final fraction of purified DJ-1 (after dialysis of fraction 3) (Figure 3.1 and Figure 3.2). The analysis of gel bands digests by LC-MS/MS (Table 3.1) shows that most of the protein contaminants are bovine proteins, probably contained in the LB medium used in bacterial culture, and *Escherichia coli* proteins, which was the host for the cloning and expression of the desired protein. Nevertheless, a high number of DJ-1 peptides were identified with a sequence coverage of 97.88 % (Table 3.1). The sequence coverage of recombinant DJ-1 relatively to the human protein is not 100% because the N-terminal of the recombinant DJ-1 was engineered to contain an hexahistidine tag and a TEV cleavage sequence, hence the differences to the human protein (Figure 3.3 - Protein Alignment using the ClustalW2 tool). Although some alterations in protein folding and/or function may happen when a tag is added, in the case of DJ-1 the insertion of a tag in the C-terminal could be more prejudicial than in the N-terminal, because the putative DJ-1 active site is occluded by the C-terminal helix-kink-helix motif [164]. Moreover, the most deleterious DJ-1 point mutation, L166P, occurs in this C-terminal motif [164]. In addition, as DJ-1 is a relatively small protein, the used tag (an hexahistidine tag) is also a small one to

minimize the possible negative effects of its addition in terms of protein structure and function.

TABLE 3.1| PROTEINS IN PURIFIED FRACTIONS OF THE RECOMBINANT PROTEIN.

Protein ID			F 3		DJ-1	
Name	**Accessions**	**Specie**	**Unique Peptides**	**Cov (95%)**	**Unique Peptides**	**Cov (95%)**
Protein DJ-1	Q99497|PARK7_HUMAN	*Homo sapiens*	104	97.88	118	97.88
Kappa-casein	P02668|CASK_BOVIN	*Bos taurus*	14	45.79	18	46.32
Alpha-S1-casein	P02662|CASA1_BOVIN	*Bos taurus*	15	61.21	12	57.01
Beta-casein	P02666|CASB_BOVIN	*Bos taurus*	14	68.75	13	60.27
Beta-lactoglobulin	P02754|LACB_BOVIN	*Bos taurus*			15	59.55
Alpha-S2-casein	P02663|CASA2_BOVIN	*Bos taurus*	10	33.78	7	27.93
Serum albumin	P02769|ALBU_BOVIN	*Bos taurus*	8	10.54	6	8.57
Glycosylation-dependent cell adhesion molecule 1	P80195|GLCM1_BOVIN	*Bos taurus*	3	22.88	3	27.45
Lactadherin	Q95114|MFGM_BOVIN	*Bos taurus*			2	3.28
Alpha-lactalbumin	P00711|LALBA_BOVIN	*Bubalus bubalis*	1	7.04	2	7.04
50S ribosomal protein L2	P60422|RL2_ECOLI	*Escherichia coli*	23	62.27	11	38.83
50S ribosomal protein L28	P0A7M2|RL28_ECOLI	*Escherichia coli*	5	33.33	1	12.82
50S ribosomal protein L17	P0AG44|RL17_ECOLI	*Escherichia coli*	4	20.47		
Ferric uptake regulation protein	P0A9A9|FUR_ECOLI	*Escherichia coli*	3	27.03	3	30.41
FKBP-type peptidyl-prolyl cis-trans isomerase slyD	P0A9K9|SLYD_ECOLI	*Escherichia coli*			2	10.2
Beta-galactosidase	P00722|BGAL_ECOLI	*Escherichia coli*	1	1.94		
Uncharacterized protein yqjI	P64588|YQJI_ECOLI	*Escherichia coli*	1	4.35		
50S ribosomal protein L21	P0AG48|RL21_ECOLI	*Escherichia coli*	1	11.65		

```
6-His-DJ-1              MGSSHHHHHHDYDIPTTENLYFQGHMASKRALVILAKGAEEMETVIPVDV 50
sp|Q99497|PARK7_HUMAN   ------------------------MASKRALVILAKGAEEMETVIPVDV 25
                                                 *************************

6-His-DJ-1              MRRAGIKVTVAGLAGKDPVQCSRDVVICPDASLEDAKKEGPYDVVVLPGG 100
sp|Q99497|PARK7_HUMAN   MRRAGIKVTVAGLAGKDPVQCSRDVVICPDASLEDAKKEGPYDVVVLPGG 75
                        ***************************************************

6-His-DJ-1              NLGAQNLSESAAVKEILKEQENRKGLIAAICAGPTALLAHEIGFGSKVTT 150
sp|Q99497|PARK7_HUMAN   NLGAQNLSESAAVKEILKEQENRKGLIAAICAGPTALLAHEIGFGSKVTT 125
                        ***************************************************

6-His-DJ-1              HPLAKDKMMNGGHYTYSENRVEKDGLILTSRGPGTSFEFALAIVEALNGK 200
sp|Q99497|PARK7_HUMAN   HPLAKDKMMNGGHYTYSENRVEKDGLILTSRGPGTSFEFALAIVEALNGK 175
                        ***************************************************

6-His-DJ-1              EVAAQVKAPLVLKD 214
sp|Q99497|PARK7_HUMAN   EVAAQVKAPLVLKD 189
                        **************
```

FIGURE 3.3| SEQUENCE ALIGNMENT OF THE PRODUCED RECOMBINANT DJ-1 AND THE HUMAN PROTEIN. "*" means that the residues in that position are identical in both sequences. Red - small and hydrophobic residues; blue - acidic residues; magenta - basic residues; green - residues with hydroxyl, amine or basic groups in its lateral chain.

The recombinant DJ-1 sequence was found with 100 % of coverage in the case of DJ-1 fraction (fraction of the purified protein after dialysis of fraction 3) and with 99.6% in the case of fraction 3 (Figure 3.4). This fact must be due to the lack of the initial methionine in the final sequence, probably removed by *E. coli* methionyl-aminopeptidase [165]. Actually the initial methionine could be identified in DJ-1 sequence of DJ-1 fraction, which can be due to the overexpressing system used that can overload the capacity of removing the initial methionine.

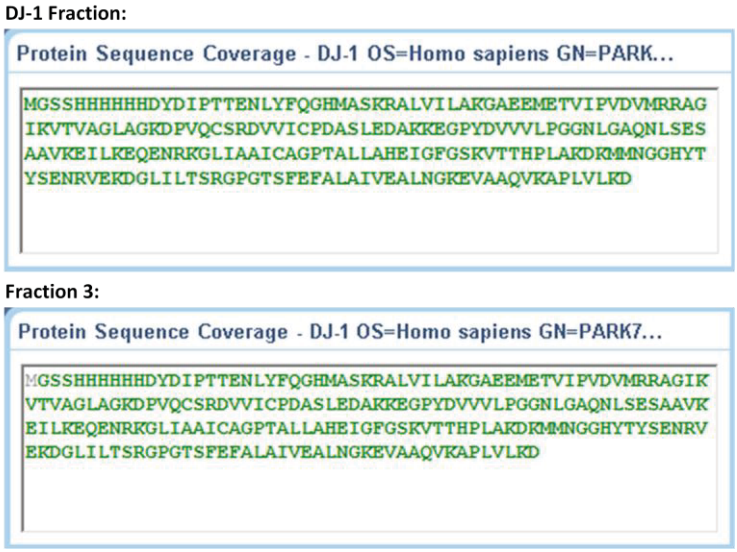

FIGURE 3.4| COVERAGE OF THE RECOMBINANT DJ-1 SEQUENCE IN FRACTION 3 AND DJ-1 FRACTION. Green - residues identified in peptides with at least 95% confidence; grey - unidentified residues.

3.1.2. MOLECULAR SIZE EXCLUSION CHROMATOGRAPHY

DJ-1 exists as homodimer [112] and this seems to be the functionally relevant form of the protein [128-129]. In order to assess the form of the purified protein, an HPLC-size exclusion chromatography was performed. Standards retention time were used to perform a calibration curve (Figure 3.5 and Supplementary Figure 7.1) and the molecular weight of purified DJ-1 was determined using the retention time of DJ-1 sample (Figure 3.5). The molecular weight of the purified DJ-1 is ≈43 kDa, which corresponds to the dimer form [105].

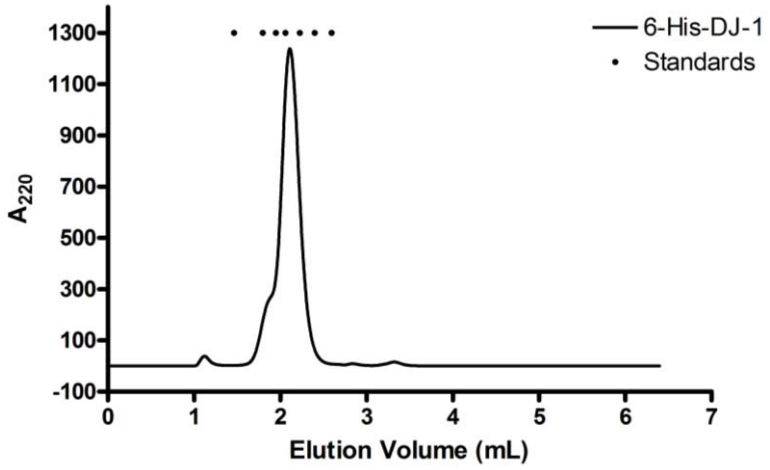

FIGURE 3.5| HPLC-SIZE EXCLUSION PURIFIED DJ-1 CHROMATOGRAM AND STANDARDS CALIBRATION. Standards from left to right: Ferritin (440 kDa); Aldolase (158 kDa); Conalbumin (75 kDa); Ovalbumin (43 kDa); Carbonic Anhydrase (29 kDa); Ribonuclease A (13.7 kDa); Aprotinin (6.5 kDa).

To confirm the molecular weight of the monomeric form of DJ-1 protein, the purified protein was analysed by LC-MS.

3.1.3. LC-MS OF INTACT DJ-1

The theoretical molecular weight (average) of recombinant DJ-1 produced, without the initial methionin, calculated using the Mass Calculator tool (Bioinformatics Solutions, Inc.), was 22739.998 Da. The molecular weight predicted using the mass spectrum of protein charge envelop of intact DJ-1 (Figure 3.6) and the BioAnalyst™ Software was 22739.1091 Da, which is a very proximal value (a shift of

0.8889 Da). Thus, the produced recombinant DJ-1 has the predicted molecular mass of the protein and is present, in solution, as a dimer (Figure 3.6 and Figure 3.5).

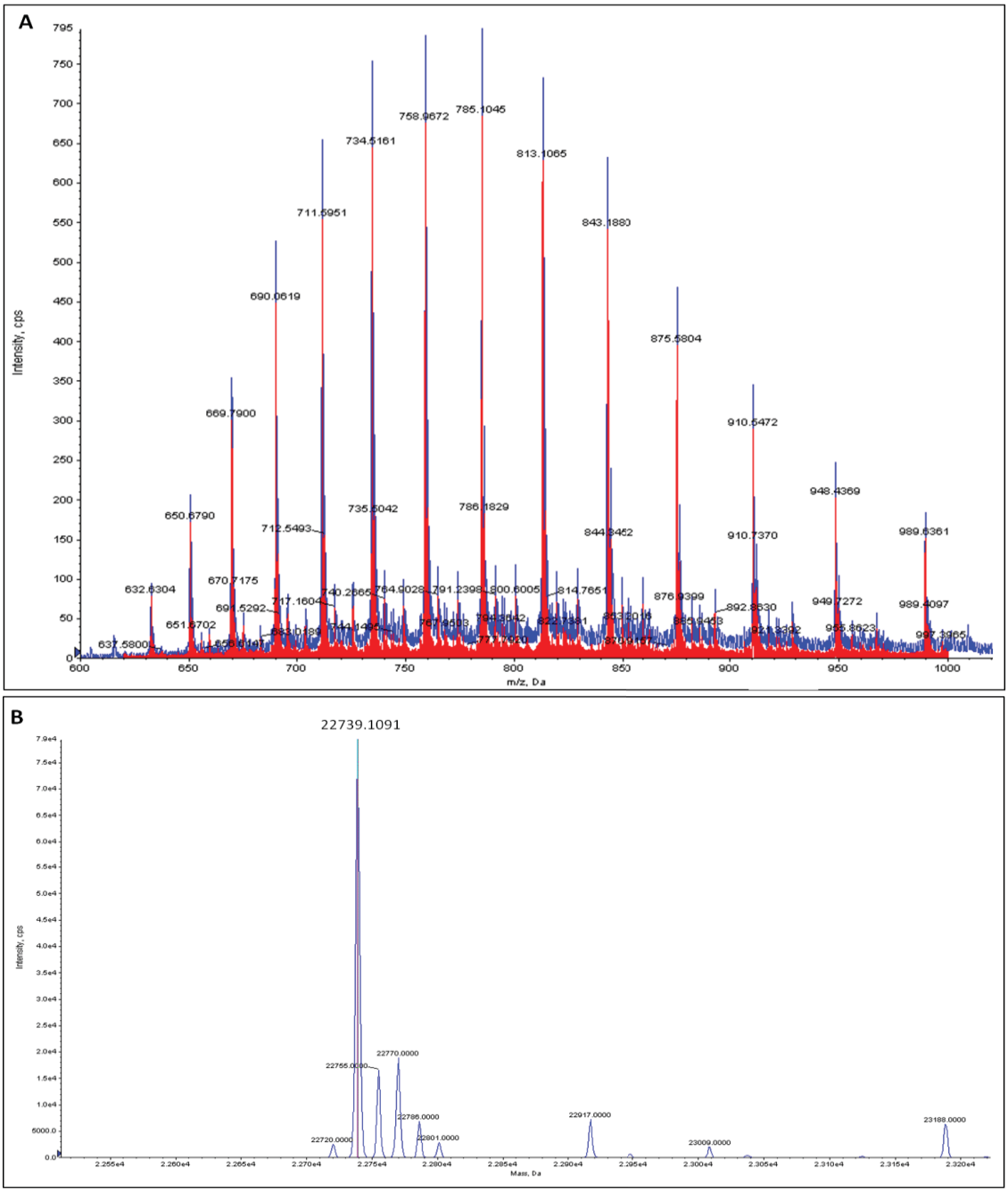

FIGURE 3.6| ESI-MS ANALYSIS OF INTACT DJ-1. A – Blue - Mass spectrum of protein charge envelop of intact DJ-1. Red – Deconvoluted mass spectrum of protein charge envelop of intact DJ-1. **B** – Graphic of deconvoluted masses using BioAnalyst™.

In order to address if the recombinant DJ-1 is functional, its neuroprotective capacity against oxidative stress was tested.

3.2. CELL VIABILITY UNDER OXIDATIVE STRESS

The human neuroblastoma SH-SY5Y cell line has been widely used as an *in vitro* model of dopaminergic neurons for Parkinson's disease [166] and, is known to be responsive to oxidative stress caused by hydrogen peroxide [139, 167-169]. SH-SY5Y cells were sensitive to the oxidative stress-inducer hydrogen peroxide in a dose dependent manner (Figure 3.7), as expected, with a LD50 value of 247.4 µM. This dose-response curve (Figure 3.7) allowed the choice of hydrogen peroxide concentrations used in further assays.

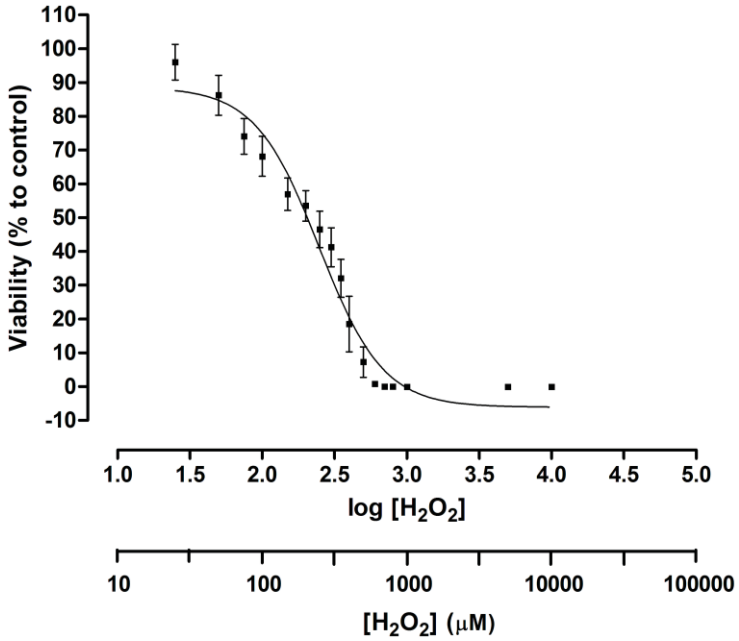

FIGURE 3.7| H_2O_2-INDUCED CELL DEATH. SH-SY5Y cells were treated with various concentrations of hydrogen peroxide, 4 h after plating. After 24 h, cell viability was assessed using the Cell Titer-Glo® assay. Data are the mean±SEM of four determinations. 100% viability was based on untreated cultures.

3.3. DJ-1-MEDIATED NEUROPROTECTION

Reports have shown the inhibition of H_2O_2-induced cell death by the exogenous addition of recombinant DJ-1 protein [139, 170]. To address this, cells were treated

with different concentrations of H_2O_2 in the presence of 1 µM DJ-1 (or 5 µM – Supplementary Figure 7.3) (or the corresponding volume of vehicle). The results indicate a significant inhibition of cell death as a result of DJ-1 action (Figure 3.8), indicating that DJ-1 is in its functional form.

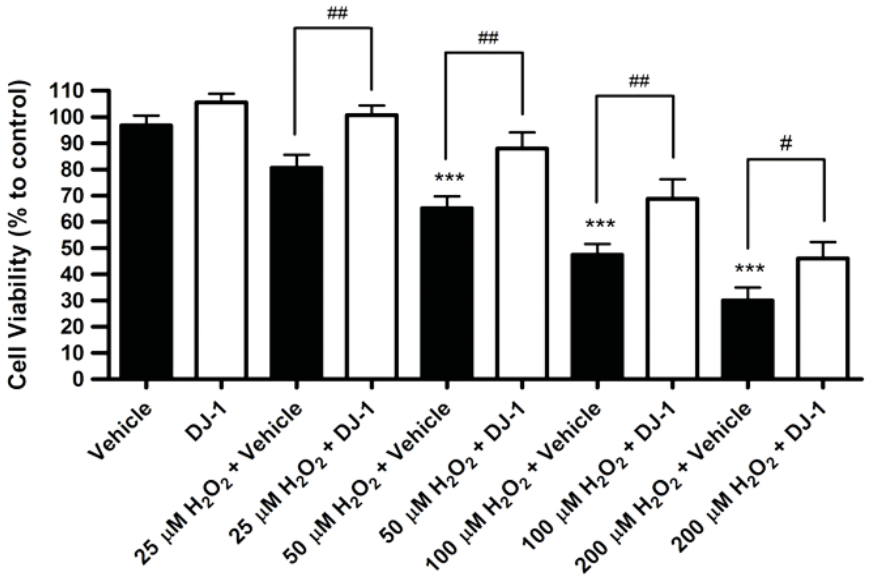

FIGURE 3.8| PROTECTIVE EFFECT OF RECOMBINANT DJ-1 AGAINST H_2O_2-INDUCED OXIDATIVE STRESS. SH-SY5Y cells were treated with H_2O_2 (25, 50, 100 and 200 µM) in the presence or absence of recombinant His-tagged human DJ-1 protein (1 µM) or vehicle, 4h after plating. After 24 h, cell viability was assessed by the Cell Titer-Glo assay. Data are the mean±SEM of four determinations, based on untreated cultures as 100% of viability. Significance (Tukey HSD post hoc comparisons after Two-way ANOVA): ***$p < 0.001$ treatment with H_2O_2 and vehicle vs. treatment with vehicle alone. #$p < 0.05$, ##$p < 0.01$ treatment with H_2O_2 and DJ-1 vs. corresponding treatment with H_2O_2 and vehicle.

The treatment of SH-SY5Y cells with 50, 100 and 200 µM H_2O_2 induced cell death (Figure 3.8 black bars) in presence of the protein's vehicle. In contrast, the presence of 1 µM His-tagged recombinant human DJ-1 protein significantly increased cell viability in all the corresponding conditions (Figure 3.8 white bars).

The neuroprotective effect of DJ-1 against H_2O_2-induced cell death has been associated with the activation of pro-survival [103, 117-120] and inhibition of pro-apoptotic pathways [121-123], such as Akt and ERK1/2 signalling pathways. Thus, another task of this project was to observe if these signalling pathways were activated by DJ-1 under normal or oxidative stress conditions.

3.4. ACTIVATION OF AKT AND ERK1/2 SIGNALLING PATHWAYS

There are reports suggesting that DJ-1 activates Akt [103, 120] and ERK1/2 [117] signalling pathways. All of them showed a DJ-1 mediated activation of these signalling pathways, using strategies of DJ-1 over-expression, inhibition of its expression or function, inside the cells. In order to assess if the purified DJ-1 can also activate these signalling pathways in SH-SY5Y cells when it is exogenously added (which has never been reported), under normal or oxidative stress conditions, immunoblot experiments using phospho-specific antibodies were performed.

SH-SY5Y cells were first serum starved to reduce the basal level of activation of Akt and ERK1/2 signalling pathways, induced by several soluble factors present in the serum. Then, cells were treated with 1 μM of recombinant DJ-1 (or the vehicle) for 0, 15, 30 and 60 min (Figure 3.9 and Figure 3.10), and with 200 μM or 1 mM of H_2O_2, in the presence or absence of recombinant DJ-1 for 15 min (Figure 3.11 and Figure 3.12). The time-points of the experiment were determined based on a previous work (Sandra Anjo's master project – unpublished data) (Supplementary Figure 7.12).

Although these are preliminary results, they show an apparent increase in phosphorylation of Akt (Figure 3.9), ERK1 and ERK2 (Figure 3.10) upon incubation of SH-SY5Y cells with recombinant DJ-1 (this increase was not observed when cells were treated with the vehicle alone). In the case of immonoblot detection of Akt phosphorylation, an increase of phosphorylation by exogenous DJ-1 was observed in all time-points, with maximum activation after 60 minutes of treatment (Figure 3.9).

Phosphorylation levels of ERK1 and ERK2 were also increased by the exogenous addition of DJ-1 in all time-points, with maximum activation at 60 min of treatment in the case of ERK1, and at 30 min in the case of ERK2 (with a slight decrease at 60 min) (Figure 3.10).

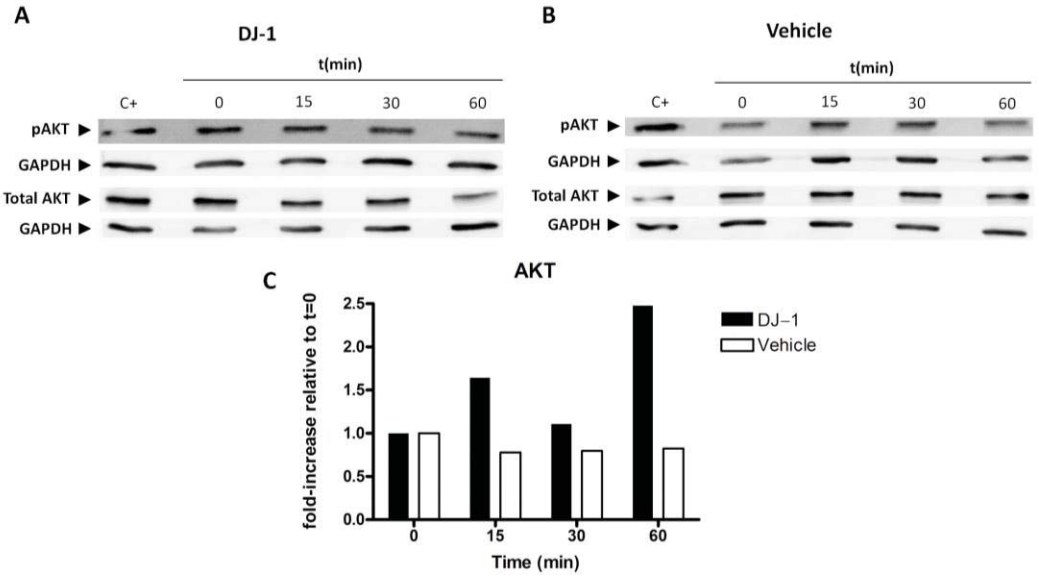

FIGURE 3.9| TIME-COURSE PROFILE FOR DJ-1-INDUCED AKT ACTIVATION IN SH-SY5Y CELLS. Serum-starved SH-SY5Y cells were treated with 1 µM of 6-His-DJ-1 (or vehicle) for the indicated periods of time and equal amounts of protein extract were analysed for Akt (60 kDa) activation by Western blot using phospho-specific Akt (Ser473) antibody or anti-total Akt, and anti-GAPDH antibodies to check protein loading. **A** - representative Western blot for the treatment with the recombinant protein; **B** - representative Western blot for the treatment with the vehicle; **C** - graphic representation of the measured adjusted volume of each band. Data was normalized to the positive control (C+ - 15% FBS stimulation) for each western-blot.

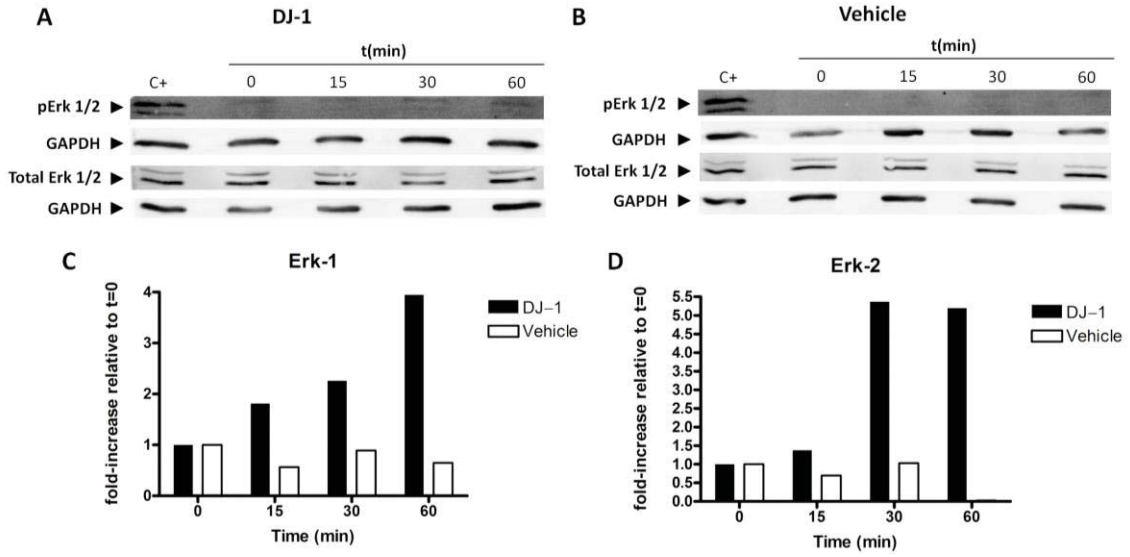

FIGURE 3.10| TIME-COURSE PROFILE FOR DJ-1-INDUCED ERK1/2 ACTIVATION IN SH-SY5Y CELLS. Serum-starved SH-SY5Y cells were treated with 1 µM of 6-His-DJ-1 (or the vehicle) for the indicated periods of time and equal amounts of protein extract were analysed for ERK1 (44 kDa) and ERK2 (42 kDa) activation by Western blot using phospho-specific ERK1/2 (Thr202/Tyr204) antibody or anti-total ERK1/2, and anti-GAPDH antibodies to check protein loading. **A** - representative Western blot for the treatment with the recombinant protein; **B** - representative Western blot for the treatment with the vehicle; **C** - graphic representation of the measured adjusted volume of each ERK1 corresponding band; **D** - graphic representation of the measured adjusted volume of each ERK2 corresponding band. Data was normalized to the positive control (C+ - 15% FBS stimulation) for each western-blot.

Although an activation of these pathways was already observed when SH-SY5Y cells were treated with H_2O_2 (1 mM) for different time periods [171], the activation of these pathways by a simultaneous incubation with exogenous DJ-1 and H_2O_2 was never tested. An increase of Akt (Figure 3.11) and both ERK1 and ERK2 (Figure 3.12) phosphorylation was observed after 15 min of treatment with 200 µM of H_2O_2, in the presence or absence of recombinant DJ-1 (1 µM). The Akt activation after 15 min of treatment had been shown in DJ-$1^{+/+}$ cortical neurons treated with 100 µM of H_2O_2, and not observed in DJ-$1^{-/-}$ cortical neurons in the same conditions [120]. Moreover, using 1 mM of H_2O_2 the activation of both pathways was not observed, in the presence or absence of the recombinant protein (Figure 3.11 and Figure 3.12). Nevertheless, an activation of Akt and ERK1/2 activation in SH-SY5Y cells treated with 1 mM of H_2O_2 was already observed after 5, 10 and 20 minutes [171], so these results must be validated.

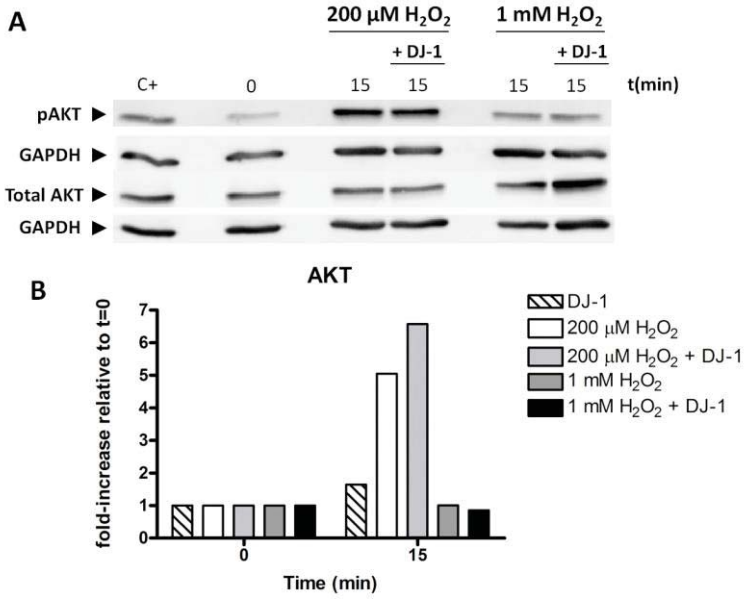

FIGURE 3.11| H_2O_2-INDUCED AKT ACTIVATION, IN THE PRESENCE OR ABSENCE OF THE RECOMBINANT DJ-1, IN SH-SY5Y CELLS. Serum-starved SH-SY5Y cells were treated with 200 µM or 1 mM of H_2O_2, in the presence or absence of 1 µM of 6-His-DJ-1, during 15 minutes. Equal amounts of protein extract were analysed for Akt (60 kDa) activation by Western blot using phospho-specific Akt (Ser473) antibody or anti-total Akt, and anti-GAPDH antibodies to check protein loading. **A** - representative Western blot for the treatment with 200 µM or 1 mM of H_2O_2, in the presence or absence of 1 µM of 6-His-DJ-1; **B** - graphic representation of the measured adjusted volume of each band. Data was normalized to the positive control (C+ - 15% FBS stimulation) for each western-blot.

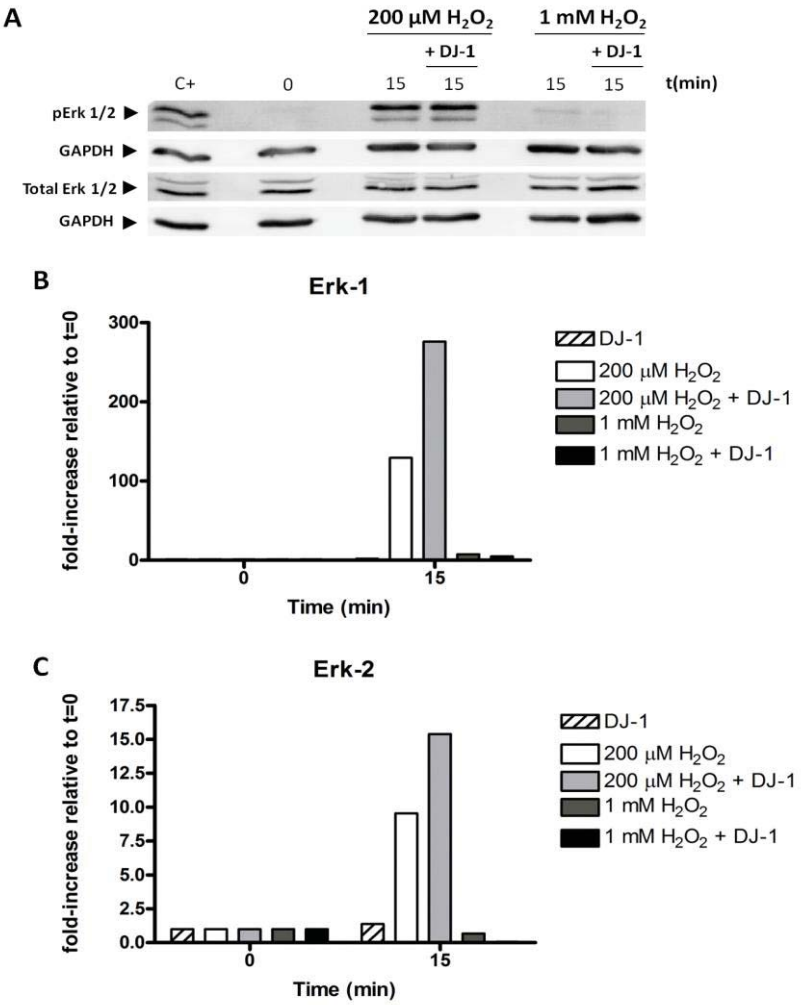

FIGURE 3.12| H_2O_2-INDUCED ERK1/2 ACTIVATION, IN THE PRESENCE OR ABSENCE OF THE RECOMBINANT DJ-1, IN SH-SY5Y CELLS. Serum-starved SH-SY5Y cells were treated with 200 µM or 1 mM of H_2O_2, in the presence or absence of 1 µM of 6-His-DJ-1, during 15 minutes. Equal amounts of protein extract were analysed for ERK1 (44 kDa) and ERK2 (42 kDa) activation by Western blot using phospho-specific ERK1/2 (Thr202/Tyr204) antibody or anti-total ERK1/2, and anti-GAPDH antibodies to check protein loading. **A** - representative Western blot for the treatment with 200 µM or 1 mM of H_2O_2, in the presence or absence of 1 µM of 6-His-DJ-1; **B** - graphic representation of the measured adjusted volume of each ERK1 corresponding band; **C** - graphic representation of the measured adjusted volume of each ERK2 corresponding band. Data was normalized to the positive control (C+ - 15% FBS stimulation) for each western-blot.

Another question that remains to be answered is if recombinant DJ-1 is exerting its neuroprotective effect in the extracellular space or if it has to be internalized by cells to accomplish this effect.

3.5. DJ-1 INTERNALIZATION

The secretion of DJ-1 from astrocytes is enhanced under oxidative stress conditions, with a potential role in astrocyte-mediated neuroprotection [139]. Moreover, the DJ-1 uptake by SH-SY5Y cells was already observed using a GST-tagged recombinant protein [143]. An hypothesis that remains to be clarified is whether secretion of DJ-1 from astrocytes may further be uptaken to play its neuroprotective role in target neurons.

To answer this question, a first task was performed to attempt to detect the DJ-1 internalization in SH-SY5Y cells, as described in section 2.6. A protein enrichment step was performed for cytosolic and membrane proteins by performing an ultracentrifugation at 126,000×*g*. This enrichment step allows to distinguish roughly if DJ-1 was internalized to the intracellular space, by observing if it is present in the cytosolic-enriched fraction, or if it interacts with any extracellular membrane protein, if it is present in the membrane-enriched fraction. In order to observe the efficiency of the experimental procedure, the sediment of the ultracentrifugation was confirmed to be enriched in membrane proteins (Figure 7.8) while the supernatant was enriched in cytosolic proteins (Figure 7.7), by immunoblott detection using specific antibodies against a cytosolic (GAPDH) and a membrane protein (transferrin receptor).

Both fractions were used in a pull-down assay against the 6-His tag, using an His-trap resin and analyzed by western-blot, using specific antibodies against DJ-1 and against the His-tag (Figure 3.13). The use of both antibodies allows to have a more refined and accurate result, as if the recombinant DJ-1 is internalized or if it interacts with any membrane protein, it should be present in the cytosolic-enriched fraction or in the membrane-enriched fraction, respectively, in the immunobloting using each antibody.

In the end of the pull-down using the His-trap resin, three different groups of samples were obtained:

1. Fraction with all of the proteins that did not bind to the His-trap resins, in which it is expected to be the endogenous DJ-1, but not the recombinant DJ-1 that was exogenously added;

2. Fraction with proteins eluted from the His-trap resin – proteins that bound to the resin during the incubation period;
3. Fraction of proteins that remained bound to the resin – if the elution step was not efficient.

In the case of proteins that did not bind to the His-trap resin, in both protein-enriched fractions, using the primary antibody anti-His (Figure 3.13, left panel), only the positive control (an SH-SY5Y total protein extract with the addition of 0.6 μg of the recombinant protein) presents a band corresponding to the recombinant DJ-1 protein (≈22 kDa). This means that there was no recombinant DJ-1 in the fraction of proteins that did not bind to the resin, as expected. So, if the recombinant DJ-1 is present - if it was uptake by SH-SY5Y cells and is present in the cytosolic-enriched fraction, or if it interacts with any membrane protein and is present in the membrane-enriched fraction - it must remain bound to the His-trap resin.

In the cytosolic fraction (Figure 3.13 upper panel), in the case of the result with the primary antibody anti-DJ-1, all fractions present a band corresponding to DJ-1, because the endogenous protein does not bind to the His-trap resin. Thus, the endogenous DJ-1 is present in the first supernatant which contains proteins that did not bind to resin. In addition, the positive and the negative controls also presents a band corresponding to DJ-1 as they are SH-SY5Y total proteins extracts, so they contain the endogenous DJ-1, and the positive control contain even the recombinant protein added.

In the case of the membrane fraction (Figure 3.13 bottom panel), with the primary antibody anti-DJ-1, only the positive and negative controls present a band corresponding to the endogenous DJ-1, as these are SH-SY5Y total protein extract (the positive control has also the addition of 0.6 μg of the recombinant DJ-1 to the extract). There are some unspecific bands between 75 and 30 kDa already observed with these antibodies.

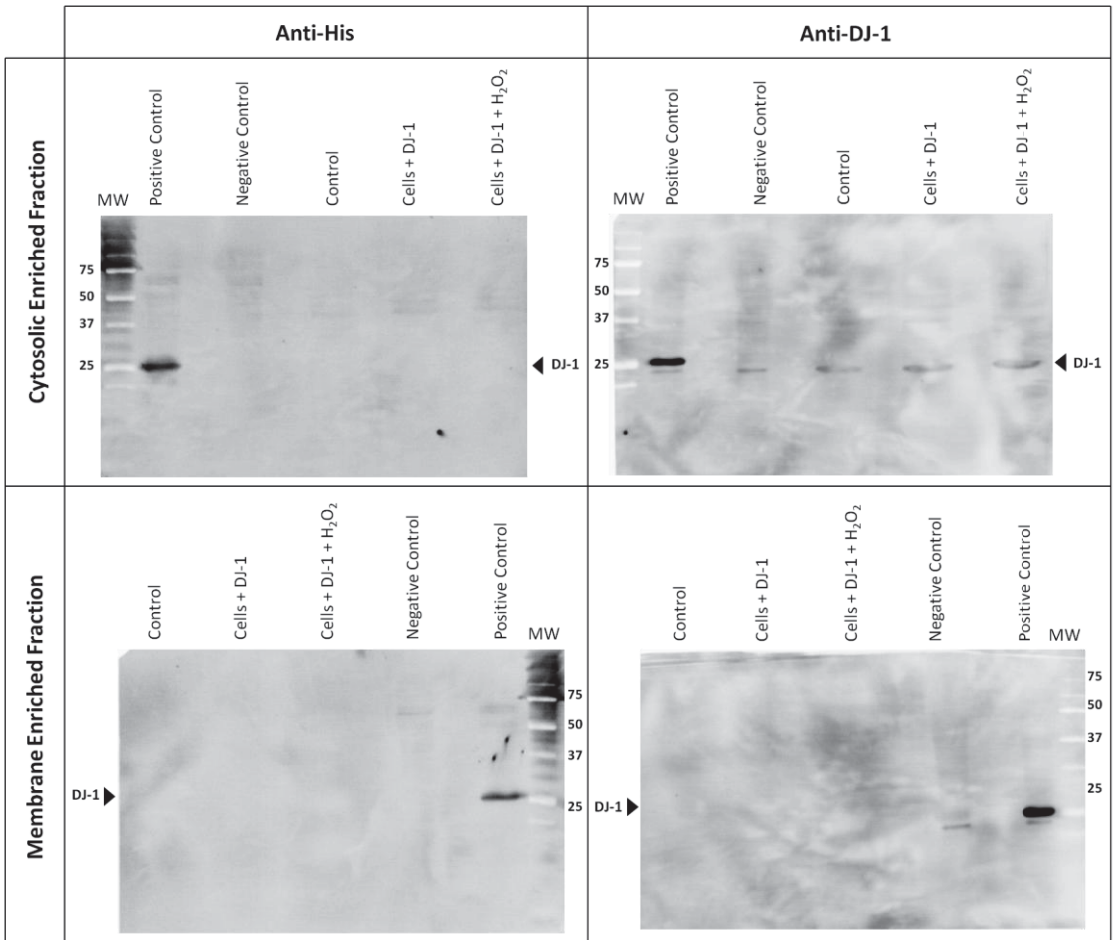

FIGURE 3.13| IMMUNOBLOT RESULTS FROM CYTOSOLIC AND MEMBRANE PROTEIN FRACTIONS THAT DID NOT BIND TO THE HIS-TRAP RESIN. SH-SY5Y cells were treated with 1 µM or with 200 µM H_2O_2 and 1 µM DJ-1 of DJ-1, for 4h. The control condition was cells maintained in culture only with DMEM. Cellular extracts were performed by scraping cells and cell fractionation was performed by ultra-centrifugation. Cytosolic and membrane enriched fractions were incubated with the His-trap resin and western-blots were performed using an anti-DJ-1 and an anti-His antibody. The negative control is an SH-SY5Y total protein extract and the positive control is the same extract with the addition of 0.6 µg of the recombinant DJ-1.

The upper results can indicate that the recombinant DJ-1 must be still bound to the resin, if it was internalized by SH-SY5Y cells or if it interacted with any membrane protein. Although, there is no evidence for a DJ-1 uptake by SH-SY5Y cells upon its exogenous addition, under normal or oxidative stress conditions, or even to its interaction with membrane proteins, as there are any reactive band corresponding to the recombinant protein is present in both cytosolic and membrane proteins eluted from the resin (supernatant after resin denaturation – proteins that bound to the His-trap resin) (Figure 3.14).

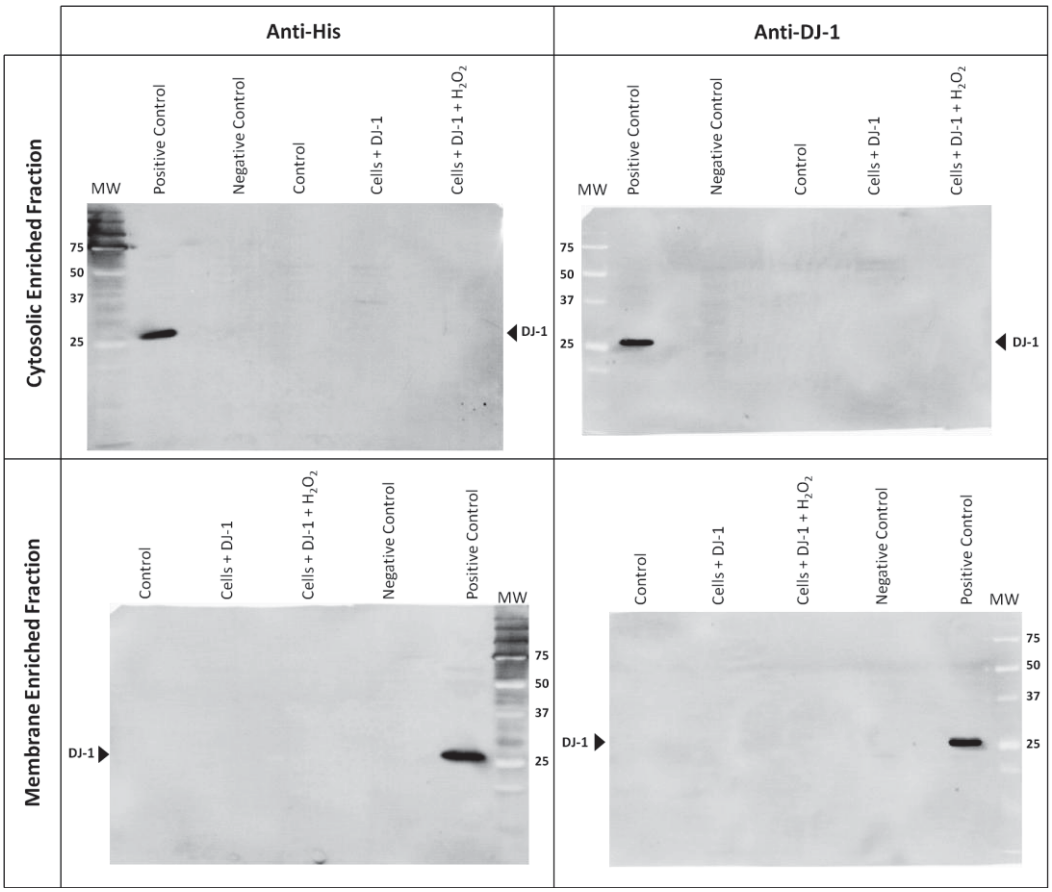

FIGURE 3.14| IMMUNOBLOT RESULTS FROM CYTOSOLIC AND MEMBRANE PROTEIN ELUTED FROM THE HIS-TRAP RESIN. SH-SY5Y cells were treated with 1 µM or with 200 µM H_2O_2 and 1 µM DJ-1 of DJ-1, for 4h. The control condition was cells maintained in culture only with DMEM. Cellular extracts were performed by scraping cells and cell fractionation was performed by ultra-centrifugation. Cytosolic and membrane enriched fractions were incubated with the His-trap resin and western-blots were performed using an anti-DJ-1 and an anti-His antibody. The negative control is an SH-SY5Y total protein extract and the positive control is the same extract with the addition of 0.6 µg of the recombinant DJ-1.

Only positive controls present a reactive band corresponding to the recombinant DJ-1 protein (≈22 kDa) (Figure 3.14). As previously indicated, there are some unspecific bands between 75 and 30 kDa already observed with this antibodies.

In order to confirm that the recombinant protein didn't remain bound to the resin, resins were also analysed by SDS-PAGE followed by western-blot (Figure 3.15), using the same specific antibodies used to analyse the other fractions of the pull-down against the His-trap resin. If the recombinant protein remained bound to the His-trap resin, it means that the elution step was not efficient.

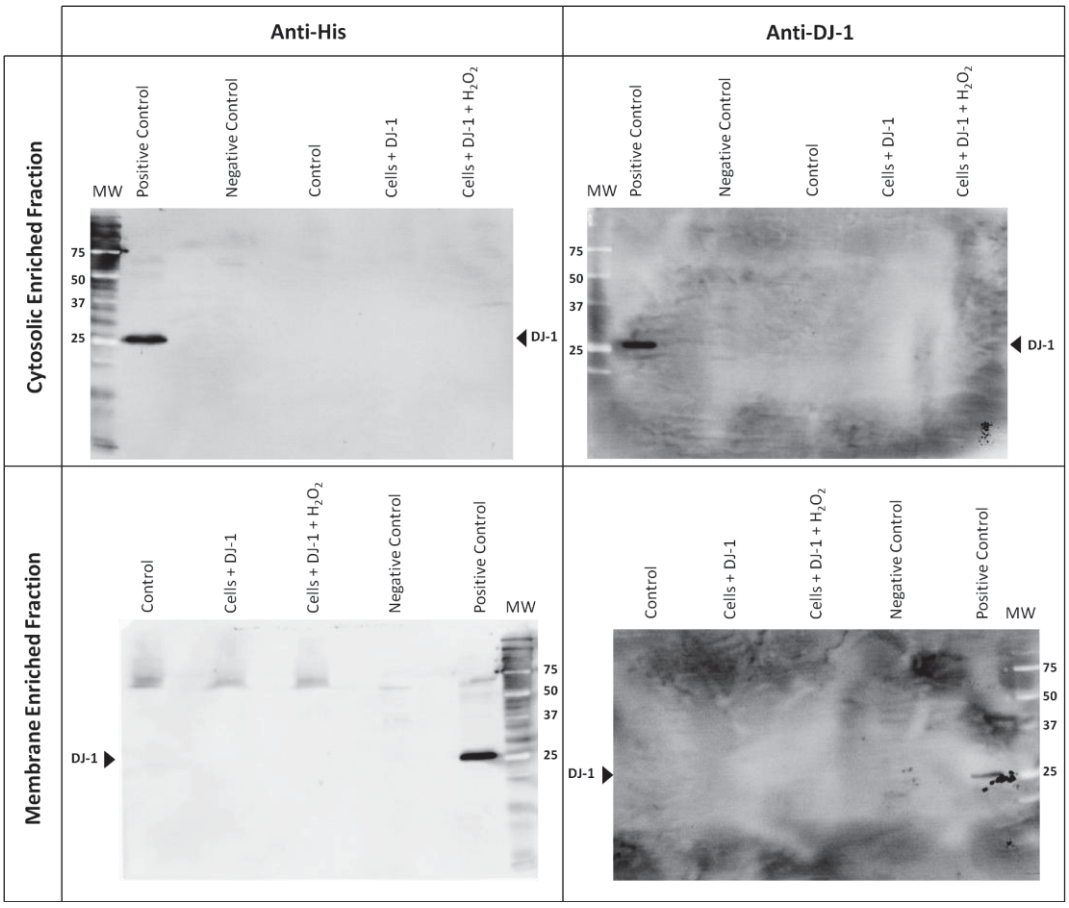

FIGURE 3.15| IMMUNOBLOT RESULTS FROM CYTOSOLIC AND MEMBRANE PROTEIN STILL BOUNDED TO THE HIS-TRAP RESIN. SH-SY5Y cells were treated with 1 µM or with 200 µM H_2O_2 and 1 µM DJ-1 of DJ-1, for 4h. The control condition was cells maintained in culture only with DMEM. Cellular extracts were performed by scraping cells and cell fractionation was performed by ultra-centrifugation. Cytosolic and membrane enriched fractions were incubated with the His-trap resin and western-blots were performed using an anti-DJ-1 and an anti-His antibody. The negative control is an SH-SY5Y total protein extract and the positive control is the same extract with the addition of 0.6 µg of the recombinant DJ-1.

Although, there is no recombinant DJ-1 bound to the resin (Figure 3.15), which means that the absence of a reactive band corresponding to DJ-1 in all samples was not due to a problem in the elution step. Only the positive control presents a band corresponding to the recombinant DJ-1, as it corresponds to a SH-SY5Y total protein extract with the addition of 0.6 µg of the recombinant DJ-1 directly to the whole cell extract. In summary, there is no evidence for DJ-1 uptake by SH-SY5Y cells and neither any evidence for DJ-1 interaction with any membrane protein.

Other attempts were performed to try to observe the internalization of the recombinant DJ-1 in SH-SY5Y cells, as reported using a GST-DJ-1 [143], but none shown the uptake of this protein (Figure 7.4, Figure 7.5 and Figure 7.6).

Altogether, these results do not show any evidence for recombinant His-DJ-1 uptake by SH-SY5Y cells, in contrast to what was reported by others using GST-DJ-1 [143] and neither an interaction of DJ-1 with any membrane protein, as hypothesized.

3.6. EXTRACELLULAR INTERACTOME OF DJ-1

Without having any evidence for a DJ-1 internalization or even any interaction with membrane proteins, strategies to find DJ-1 extracellular interactors that could be related with DJ-1 neuroprotective effect observed (Figure 3.8) and previously reported [139, 170], were carried out.

The conditioned medium of SH-SY5Y cells was used to perform a pull-down assay against recombinant DJ-1 previously bound to a His-trap resin. One of the control conditions consisted in a similar pull-down assay against the His-trap resin, without any DJ-1 bound. This control condition allowed discarding proteins that bound only to the resin and not to the protein. Other control conditions were similar pull-down assays performed with the culture medium (DMEM), without being in contact with cultured cells, against the His-trap resin with or without DJ-1 bound. This control condition allowed discarding identified proteins possibly present in the culture medium.

This type of approach can identify some indirect interactors because the identified proteins can be interacting with other DJ-1 interactors and not directly with DJ-1. Moreover, in the future, other control condition that must be included is a pull-down assay performed against the His-tag bound to the resin, as some identified proteins could be also interacting only with this region of the recombinant protein, which is not present in the human protein.

The coomassie staining showed some differences in protein bands between the sample of the pull-down of proteins contained in the conditioned medium against the His-trap resin with DJ-1 bound to it and control conditions (Figure 3.16), which can be an indication for a DJ-1 interaction with different proteins.

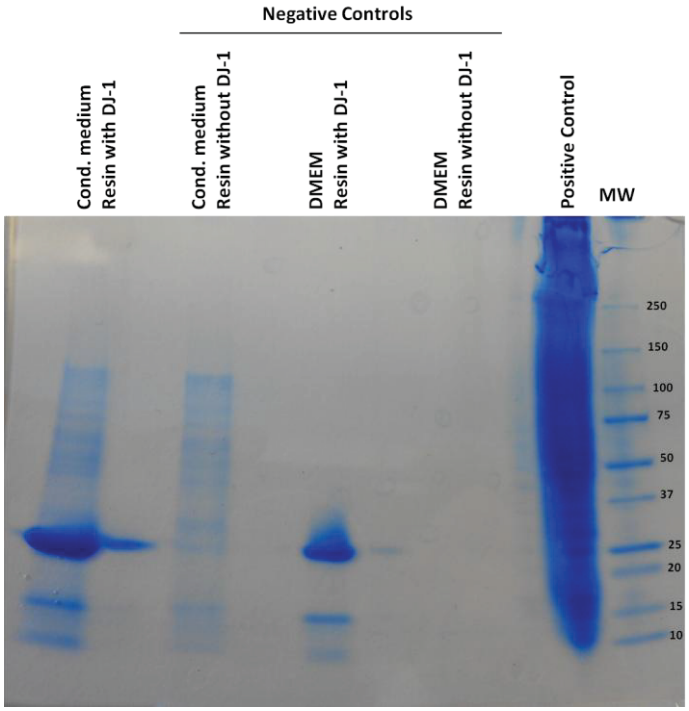

FIGURE 3.16| EXTRACELLULAR INTERACTORS. SDS-PAGE stained with coomassie of samples of the extracellular interactors experiment. In the first lane there is the sample corresponding to the conditioned medium incubated with resin with DJ-1. Negative controls: conditioned medium incubated with resin without DJ-1; DMEM (culture medium that was not in contact with cultured cells) incubated with resin with DJ-1; DMEM incubated with resin without DJ-1. The positive control is the sample of the total protein extract incubated with resin with DJ-1.

The analysis of the gel lanes by LC-MS/MS reveals the identity of proteins that putatively interact with exogenous recombinant DJ-1 in the extracellular space of cells (Table 3.2). Proteins present in control conditions were not considered as possible DJ-1 interactors. The identified proteins were separated in secreted and non-secreted (Supplementary Table 7.2 and Table 7.3), and its relevant biological processes for this study were assessed, based on the Gene Ontology (GO) Annotation available on the Uniprot database. Among the identified proteins there are cell adhesion proteins, proteins involved in cellular processes, such as, axon guidance, cell migration and proliferation, carbohydrate metabolism, synaptic process and positive or negative regulation of signalling pathways (Table 3.2).

TABLE 3.2| PROTEINS FROM THE CONDITIONED MEDIUM PULL-DOWN WITH DJ-1.

Name	Accessions	Relevant Biological Process	Unique Peptides
Probable carboxypeptidase X1	Q96SM3|CPXM1_HUMAN	cell adhesion proteolysis	6
Annexin A2	P07355|ANXA2_HUMAN	positive regulation of vesicle fusion	6
Neurocan core protein	O14594|NCAN_HUMAN	axon guidance carbohydrate metabolic process cell adhesion chondroitin sulfate catabolic process regulation of synapse structural plasticity small molecule metabolic process	6
Carboxypeptidase E	P16870|CBPE_HUMAN	cellular protein modification process neuropeptide signaling pathway protein localization to membrane proteolysis	6
Semaphorin-3C	Q99985|SEM3C_HUMAN	axon guidance immune response neural crest cell migration neural tube development response to drug	6
Inter-alpha-trypsin inhibitor heavy chain H2	P19823|ITIH2_HUMAN	hyaluronan metabolic process	5
Complement component C7	P10643|CO7_HUMAN	complement activation, alternative pathway complement activation, classical pathway cytolysis innate immune response	3
Insulin-like growth factor-binding protein 2	P18065|IBP2_HUMAN	aging cellular response to hormone stimulus regulation of cell growth response to drug response to glucocorticoid stimulus response to lithium ion response to mechanical stimulus response to retinoic acid response to stress signal transduction	3
Vitronectin	P04004|VTNC_HUMAN	cell adhesion mediated by integrin immune response negative regulation of endopeptidase activity positive regulation of peptidyl-tyrosine phosphorylat ion positive regulation of protein binding positive regulation of receptor-mediated endocytosis positive regulation of smooth muscle cell migration	2

		positive regulation of vascular endothelial growth factor receptor signaling pathway positive regulation of wound healing smooth muscle cell-matrix adhesion	
Fibronectin	P02751|FINC_HUMAN	acute-phase response peptide cross-linking regulation of cell shape substrate adhesion-dependent cell spreading	2
Nidogen-1	P14543|NID1_HUMAN	cell-matrix adhesion glomerular basement membrane development positive regulation of cell-substrate adhesion	2
Integral membrane protein 2B	Q9Y287|ITM2B_HUMAN	apoptotic process induction of apoptosis nervous system development	1
Glia-derived nexin	P07093|GDN_HUMAN	long-term synaptic potentiation negative regulation of cell growth negative regulation of cell proliferation negative regulation of phosphatidylinositol 3-kinase cascade positive regulation of astrocyte differentiation positive regulation of neuron projection development regulation of synaptic transmission, glutamatergic secretory granule organization	1
Testican-1	Q08629|TICN1_HUMAN	cell adhesion central nervous system neuron differentiation neuron migration signal transduction	1

In addition, some proteins were found both in the pull-down assay performed using the recombinant protein bound to the His-trap resin, and using the His-trap resin without the addition of the recombinant protein. As one of these identified proteins was the endogenous DJ-1 protein, maybe some of these identified proteins can be interacting not only with the His-trap resin, but also with the endogenous DJ-1. So, some of these proteins could also be DJ-1 interactors in the extracellular space. Thus, proteins identified in both fractions are presented in the Supplementary Data (Table 7.1). The experimental design of this experience must be improved to avoid the presence of the endogenous DJ-1 in this control condition. One of the possible improvements that can be done is the increase of the number of washing steps.

4| DISCUSSION

Parkinson's disease is a progressive neurodegenerative disorder which etiology and pathology are not completely understood [2, 61]. DJ-1, a multifunctional protein [105-106] in which mutations have been associated with familial Parkinson's disease [56, 58, 108], has been highly studied over the last years. DJ-1 protein has been suggested to participate in response to oxidative stress [52] and to act as a sensor of oxidative stress [55]. This protein is expressed in neurons and in all glial cell types [106, 124] and its expression and release from astrocytes was suggested to contribute to astrocyte-mediated neuroprotection [139]. Taking these facts together, this study intended to give some insights about the neuroprotective mechanisms of exogenous DJ-1, mimicking its release from astrocytes, in SH-SY5Y cells, a cell line widely used as an *in vitro* model of dopaminergic neurons for Parkinson's disease studies [166].

Recombinant DJ-1 was produced in order to be used in further studies of DJ-1-mediated neuroprotection against H_2O_2-induced cell death, DJ-1-mediated activation of signalling pathways, DJ-1 internalization and DJ-1 extracellular interactome. The sequence of DJ-1 coding DNA in the pSKB-3 vector was confirmed by Sanger DNA Sequencing, and the purified protein was ≈43 kDa (Figure 3.5), corresponding to its dimer form [105], which is an important functional feature of the protein [112, 128-129]. There are some contaminant proteins in the final DJ-1 purification fraction, but these are mainly proteins from the LB medium, used for bacterial cultures and proteins from the host (*E. coli*) used to clone and express the protein of interest (Table 3.1). On the other hand, the amino-acid sequence of the purified protein only lacks the initial methionine (Figure 3.4), due to a natural post-translational process, having the predicted molecular weight of its monomers (Figure 3.6).

When SH-SY5Y cells were treated with H_2O_2, the cell viability decreased in a dose-dependent manner (Figure 3.7), but when cells were treated simultaneously with DJ-1, the H_2O_2-induced cell death was significantly inhibited in almost all conditions (Figure 3.8 white bars). This protective effect of DJ-1 was previously reported [139, 170], and could be explained by a direct or indirect antioxidant capacity of DJ-1 [52, 113, 126-127] or by its action as an oxidative stress sensor [11, 98]. Although a direct

antioxidant capacity has been proposed, other evidence showed a weaker antioxidant capacity of this protein when compared with peroxidases [103, 113]. Its antioxidant activity must be due to other additional factors, such as up-regulation of the antioxidant glutathione [126] and stabilization of the transcription factor Nrf2 (a major regulator of antioxidant genes) [127]. Some studies suggest a role for intracellular DJ-1 in the activation of pro-survival [103, 117-120] and inhibition of pro-apoptotic signalling pathways [121-123], which could also be related with the neuroprotective effect of DJ-1 against H_2O_2-induced cell death. Therefore, DJ-1-mediated activation of Akt and ERK1/2 was tested in this study using a different approach, in which cells were incubated with recombinant DJ-1 in the extracellular milieu.

The mitogen activated protein kinases (MAPK) signalling pathways, in particular ERK, contribute to neuronal survival [172]. Moreover, activation of ERK1/2 promotes a basal dopaminergic cell survival and protects dopaminergic neurons from oxidative stress [173]. On the other hand, Akt, also known as protein kinase B (PKB), is an anti-apoptotic protein and the PI3K-Akt signalling pathway plays a critical role in mediating neuronal survival [174]. In the present study, the activation of the Akt and ERK1/2 signalling pathways was observed when SH-SY5Y cells were treated with 1 μM of recombinant DJ-1 exogenously added to the medium (an observation that had never been reported - Figure 3.9 and Figure 3.10), which complements other studies showing the ability of intracellular DJ-1 to activate these pathways [103, 117-120].

As the ERK1/2 signalling pathway is crucial to protect cells against oxidative stress, the increased ERK1/2 phosphorylation caused by DJ-1 could be related to the role of DJ-1 in neuroprotection, as already reported [117]. In fact, that same report showed that the neuroprotective capacity of DJ-1 against H_2O_2-induced cell death was depleted when cells were pre-treated with a MEK1/2 inhibitor, suggesting that this DJ-1 neuroprotective effect was mediated by the activation of this signalling pathway [117]. Another study of the same research group, suggested that DJ-1 exerts its neuroprotective role by activating the ERK1/2 pathway and suppressing mTOR (a major negative regulator of autophagy after phosphorylation by PIK3) in dopaminergic cells, leading to enhanced autophagy, more efficient clearance of damaged mitochondria, and reduced apoptosis [175]. Antother recent study showed a possible

action of DJ-1 in the upregulation of the tyrosine hydroxylase (TH) (a rate-limiting enzyme in dopamine synthesis) gene expression by activating its transcriptional factor Nurr1 via the ERK1/2 pathway [176].

The activation of the Akt and ERK1/2 signalling pathways was already observed when SH-SY5Y cells were treated with 1 mM of H_2O_2 [171], but in this study there is no evidence of this activation. Nevertheless, the activation of both signalling pathways upon H_2O_2 treatment, observed in this study when cells were treated with 200 µM of H_2O_2 for 15 minutes (Figure 3.11 and Figure 3.12), was already reported using 300 µM of H_2O_2 after 15 minutes of stimulation in cortical neurons [177].

The activation of Akt and ERK1/2 signalling pathways was also observed when cells treated with 200 µM of H_2O_2, in the presence of 1 µM of exogenous recombinant DJ-1 (Figure 3.11 and Figure 3.12), and the activation of Akt signalling pathway by DJ-1 was already been reported using 100 µM of H_2O_2 at the same time-point (15 min) [120]. Although, this has never been tested in the case of activation of ERK1/2 signalling pathway. These results are an indication that DJ-1 potentiates the activation of Akt and ERK1/2 signalling pathways under oxidative stress conditions, which could be a very important mechanism of induction of neuroprotection in neuronal cells.

All these results, although preliminary, open the opportunity for a DJ-1 mediated neuroprotection after its release from astrocytes by the activation of Akt and ERK1/2 signalling pathways in dopaminergic neurons.

An hypothesis that remains to be clarified is whether DJ-1 secretion from astrocytes may further play a neuroprotective role in target neurons after its putative uptake. Although there is evidence for DJ-1 uptake by SH-SY5Y cells [143], these results could not be confirmed in our study (Figure 3.14 upper panel), hence there is still a need for confirmation of this observation from other reports. The recombinant DJ-1 used in the mentioned study was engineered with an N-terminus GST-tag. However, the GST-tag alone was also uptaken by the target cells, which raises the question of whether the GST-DJ-1 fusion protein was internalized by cells in a mechanism that relied on GST internalization or if it was specific for DJ-1. Moreover, in our understanding, GST is a very large tag (≈26 kDa) when compared with the size of DJ-1 (≈22 kDa in its monomeric form and ≈43 kDa in its dimeric form), hence we chose to

use a smaller tag (a six histidines tag) in the N-terminal of the recombinant protein produced in this study.

Considering the neuroprotective effect of exogenous DJ-1 towards oxidative stress insults and that no protein internalization was observed, it was hypothesized that DJ-1 could bind and/or activate membrane receptors receptors that might transduce signals that could activate Akt and ERK1/2 (Figure 3.9, Figure 3.10, Figure 3.11 and Figure 3.12). A pull-down assay followed by western-blot analysis did not reveal any protein from the membrane-enriched fraction bound to DJ-1 (Figure 3.14 bottom panel), so there is no evidence for an interaction of DJ-1 with any protein from the cytoplasmic membrane.

Once no evidence indicates DJ-1 internalization or even its interaction with any membrane protein, a different strategy was used to find DJ-1 extracellular interactors possibly related with DJ-1 neuroprotective mechanisms. Therefore, the conditioned medium of SH-SY5Y was used to identify putative DJ-1 extracellular interactors in a pull-down assay. Among the identified proteins (Table 3.2), there are some particularly interesting ones. The identified proteins: probable carboxypeptidase X1, annexin A2, neurocan core protein, vitronectin, fibronectin, nidogen-1 and testican-1 are proteins mainly involved in cell adhesion, growth and migration [178-183]. Semaphorin-3C, is also involved in the axonal guidance of neurons and cell survival [184].

More interestingly, carboxypeptidase E, also identified in this study, seems to be involved in the biotransformation of dynorphin A (1-17), an endogenous opioid peptide related to the striatonigral pathway [185]. Actually different dynorphin A-derived peptides were identified in the striatum following a unilateral 6-OHDA-induced lesion, correlating them with parkinsonism [185]. Another study showed the colocalization of somatostatin protein with prohormone convertase 1, prohormone convertase 2 and carboxypeptidase E in rat brain, and somatostatin plays an important role in neurological disorders such as Alzheimer's disease and Huntington's disease [186]. Thus, perhaps DJ-1 has also a role in the striatonigral pathway by its interaction with carboxipeptidase E or upstream/downstream molecules. In fact, DJ-1 was found in both striatum and *substantia nigra* [124]. Another possibility is the occurrence of the same type of interactions with the proteins already associated with other

neurological diseases, including somatostatin protein, prohormone convertase 1, prohormone convertase 2 and carboxypeptidase E, giving some clues about similar molecular mechanisms possibly related with PD.

Complement proteins, such as the identified complement C7, are present in Lewy bodies in the *substantia nigra*, with a predominant activation of the classical complement cascade, amplifying the proteolytic cascade and opsonizing tissue for phagocytosis [187]. Possibly, if DJ-1 can interact with the complement component C7, or upstream/downstream molecules, it can be a regulator of the complement cascade.

Another identified protein was the insulin-like growth factor-binding protein 2 which has been related to aging, increasing in serum of adults over the age of 60, and during starvation periods [188]. This protein seems to be regulated by several mechanisms, although the exact mechanism that regulates its concentrations remains unclear [188]. One possibility is the involvement of DJ-1 in this regulation mechanism, as it is also present in serum [146].

In the case of fibronectin, besides its adhesion properties, this protein has been implicated in pathological conditions of the central nervous system (CNS) by exerting a strong angiogenic influence on endothelial cells, via MAP kinase signalling pathway [189]. This signalling pathway seems to be affected by DJ-1, possibly to protect neurons from oxidative stress conditions by its activation, as suggested by the results presented in this study (Figure 3.10) and as previously reported [117].

Additionally, mutations in the integral membrane protein 2B, also known as BRI2, were found in families with dementia associated with amyloidopathies, linking this protein with neurodegenerative disorders [190]. This protein was also detected in Lewy neurites in cases of dementia with Lewy bodies and PD, suggesting that it might also be involved in Lewy body formation [191]. DJ-1 might also play a role in the process of Lewy bodies formation. In fact, DJ-1 has already been reported as a redox-sensitive molecular chaperone and as inhibitng α-synuclein (a protein present in Lewy bodies [11]) aggregate formation [101-102].

The identified glia-derived nexin was found to interact with vitronectin (also identified in this study), potentiating the neurite-promoting activity [192], so maybe these proteins come together (in a complex with DJ-1) in the pull-down assay. On the

other hand, the glia-derived nexin, also known as protease nexin-1, is a serine protease inhibitor and neurite outgrowth promoter expressed in the rat CNS [193-194]. After the induction of *substantia nigra* and nigrostriatal pathway degeneration with 6-hydroxydopamine, the *de novo* synthesis of this protein occurred in the dopamine depleted *caudate putamen* but not in the *substantia nigra* [193-194]. So, it was postulated that the oxidative inactivation of protease nexin-1 in the brain may be involved in neurodegeneration [194]. As DJ-1 can have an antioxidant activity [113] it might be protecting protease nexin-1 from oxidation. Moreover, the protease nexin-1 counteracts the cellular effects of thrombin, inhibiting mitogenic activity and inducing neurite extension in neurons, leading to the hypothesis that neuronal morphology is governed by its interplay [195]. Thrombin activates MAP kinases [196], including the phosphoinositide 3-kinase (PI3K) [195], suggesting that thrombin may be involved in the neuropathological processes of dopaminergic neuronal cell death that occur in PD [196]. Furthermore, there is evidence that injury and disease-related events trigger protease nexin-1 production to levels which ultimately abolish the thrombin effects [195]. On the other hand, thrombin can have differential effects *in vivo*, after injury, depending on its concentration [195]. For example, at a low concentration, thrombin may contribute to the repair processes, and the protease nexin-1 might participate in these processes by regulating the levels of active thrombin in the surrounding environment of both neurons and astrocytes [195]. As DJ-1 related with MAPK signalling pathways activation [as suggested by the results from the present study (Figure 3.10) and as previously reported [117]], maybe DJ-1 can also be interacting with protease nexin-1 or other up- or down-stream molecules leading to the activation of the mentioned signalling pathway.

5| CONCLUSIONS

The main goal of this study was to give some clues about the neuroprotection mechanisms of exogenous DJ-1, mimicking its release from astrocytes to the extracellular space. To achieve this, a recombinant DJ-1 was produced to exogenously add it to cultured SH-SY5Y cells, a model cell line to study Parkinson's disease.

This research project allowed the production of a dimeric and functional recombinant DJ-1 that conferred neuroprotection to SH-SY5Y cells under H_2O_2-induced oxidative stress conditions, as already reported.

Moreover, this study provided some preliminary data regarding the activation of Akt and ERK1/2 signalling pathways, induced by exogenous DJ-1, under normal or oxidative stress conditions. Therefore, the activation of pro-survival signalling pathways by DJ-1 remains one of the possible mechanisms of neuroprotection induced by this protein.

Two of the hypotheses raised were the internalization of DJ-1 by neurons, in which the protein could exert its neuroprotective effects in the intracellular milieu, or alternatively, through membrane receptor-mediated activation of signalling pathways. This study did not reveal any evidence for DJ-1 internalization, neither any evidence for an interaction with any membrane protein. So, the mechanism by which DJ-1 mediates neuroprotection in the extracellular space of cells remains to be clarified.

The pull-down assay used to identify some possible DJ-1 extracellular interactors, allowed the identification of some secreted proteins that can be interacting with DJ-1 in the extracellular space mediating its neuroprotective effect. These results must be validated in the future by improving the experimental design of the approach and by performing complementary assays, such as co-immunoprecipitation.

In summary all the results presented in this study contribute to a better understanding of the molecular mechanisms leading neuroprotection conferred by DJ-1 against oxidative stress-induced neuronal death, which is one of the most relevant insults in Parkinson's disease pathology. Hence, these findings may contribute to future strategies for the treatment and prevention of the disease.

6| REFERENCES

1. Martin, I., V.L. Dawson, and T.M. Dawson, *Recent advances in the genetics of Parkinson's disease.* Annu Rev Genomics Hum Genet, 2011. **12**: p. 301-25.
2. Wirdefeldt, K., et al., *Epidemiology and etiology of Parkinson's disease: a review of the evidence.* Eur J Epidemiol, 2011. **26 Suppl 1**: p. S1-58.
3. Parkinson, J., *An essay on the shaking palsy. 1817.* J Neuropsychiatry Clin Neurosci, 2002. **14**(2): p. 223-36; discussion 222.
4. de Lau, L.M.L. and M.M.B. Breteler, *Epidemiology of Parkinson's disease.* The Lancet Neurology, 2006. **5**(6): p. 525-535.
5. Bekris, L.M., I.F. Mata, and C.P. Zabetian, *The genetics of Parkinson disease.* J Geriatr Psychiatry Neurol, 2010. **23**(4): p. 228-42.
6. Muthane, U.B., et al., *Early onset Parkinson's disease: are juvenile- and young-onset different?* Mov Disord, 1994. **9**(5): p. 539-44.
7. Emre, M., *Dementia associated with Parkinson's disease.* Lancet Neurol, 2003. **2**(4): p. 229-37.
8. McDonald, W.M., I.H. Richard, and M.R. DeLong, *Prevalence, etiology, and treatment of depression in Parkinson's disease.* Biol Psychiatry, 2003. **54**(3): p. 363-75.
9. Dickson, D.W., et al., *Neuropathological assessment of Parkinson's disease: refining the diagnostic criteria.* Lancet Neurol, 2009. **8**(12): p. 1150-7.
10. Waragai, M., et al., *alpha-Synuclein and DJ-1 as Potential Biological Fluid Biomarkers for Parkinson's Disease.* International Journal of Molecular Sciences, 2010. **11**(11): p. 4257-4266.
11. Mandel, S., et al., *Biomarkers for prediction and targeted prevention of Alzheimer's and Parkinson's diseases: evaluation of drug clinical efficacy.* The EPMA Journal, 2010. **1**(2): p. 273-292.
12. Crosiers, D., et al., *Parkinson disease: Insights in clinical, genetic and pathological features of monogenic disease subtypes.* J Chem Neuroanat, 2011. **42**(2): p. 131-41.
13. Fearnley, J.M. and A.J. Lees, *Ageing and Parkinson's disease: substantia nigra regional selectivity.* Brain, 1991. **114 (Pt 5)**: p. 2283-301.
14. Baldereschi, M., et al., *Parkinson's disease and parkinsonism in a longitudinal study: two-fold higher incidence in men. ILSA Working Group. Italian Longitudinal Study on Aging.* Neurology, 2000. **55**(9): p. 1358-63.
15. Hindle, J.V., *Ageing, neurodegeneration and Parkinson's disease.* Age and Ageing, 2010. **39**(2): p. 156-161.
16. Elbaz, A. and F. Moisan, *Update in the epidemiology of Parkinson's disease.* Current Opinion in Neurology, 2008. **21**(4): p. 454-460.
17. Samii, A., J.G. Nutt, and B.R. Ransom, *Parkinson's disease.* Lancet, 2004. **363**(9423): p. 1783-93.
18. Zappia, M., C. Colosimo, and W. Poewe, *Levodopa: back to the future.* J Neurol, 2010. **257**(Suppl 2): p. S247-8.
19. Jankovic, J., *An update on the treatment of Parkinson's disease.* Mt Sinai J Med, 2006. **73**(4): p. 682-9.

20. Dauer, W. and S. Przedborski, *Parkinson's disease: mechanisms and models.* Neuron, 2003. **39**(6): p. 889-909.
21. Jackson-Lewis, V., et al., *Time course and morphology of dopaminergic neuronal death caused by the neurotoxin 1-methyl-4-phenyl-1,2,3,6-tetrahydropyridine.* Neurodegeneration, 1995. **4**(3): p. 257-69.
22. Polymeropoulos, M.H., et al., *Mutation in the alpha-synuclein gene identified in families with Parkinson's disease.* Science, 1997. **276**(5321): p. 2045-7.
23. Langston, J.W., et al., *Chronic Parkinsonism in Humans Due to a Product of Meperidine-Analog Synthesis.* Science, 1983. **219**(4587): p. 979-980.
24. Betarbet, R., et al., *Chronic systemic pesticide exposure reproduces features of Parkinson's disease.* Nat Neurosci, 2000. **3**(12): p. 1301-6.
25. Grandinetti, A., et al., *Prospective study of cigarette smoking and the risk of developing idiopathic Parkinson's disease.* Am J Epidemiol, 1994. **139**(12): p. 1129-38.
26. Paganini-Hill, A., *Risk factors for parkinson's disease: the leisure world cohort study.* Neuroepidemiology, 2001. **20**(2): p. 118-24.
27. Hernan, M.A., et al., *Cigarette smoking and the incidence of Parkinson's disease in two prospective studies.* Ann Neurol, 2001. **50**(6): p. 780-6.
28. Quik, M., *Smoking, nicotine and Parkinson's disease.* Trends Neurosci, 2004. **27**(9): p. 561-8.
29. Powers, K.M., et al., *Combined effects of smoking, coffee, and NSAIDs on Parkinson's disease risk.* Mov Disord, 2008. **23**(1): p. 88-95.
30. Andersen, J.K., *Oxidative stress in neurodegeneration: cause or consequence?* Nat Med, 2004. **10 Suppl**: p. S18-25.
31. Lesage, S. and A. Brice, *Parkinson's disease: from monogenic forms to genetic susceptibility factors.* Hum Mol Genet, 2009. **18**(R1): p. R48-59.
32. Lesage, S. and A. Brice, *Role of mendelian genes in "sporadic" Parkinson's disease.* Parkinsonism Relat Disord, 2012. **18 Suppl 1**: p. S66-70.
33. Chartier-Harlin, M.C., et al., *Translation initiator EIF4G1 mutations in familial Parkinson disease.* American Journal of Human Genetics, 2011. **89**(3): p. 398-406.
34. Zimprich, A., et al., *A mutation in VPS35, encoding a subunit of the retromer complex, causes late-onset Parkinson disease.* American Journal of Human Genetics, 2011. **89**(1): p. 168-75.
35. Seidel, K., et al., *First appraisal of brain pathology owing to A30P mutant alpha-synuclein.* Ann Neurol, 2010. **67**(5): p. 684-9.
36. Zarranz, J.J., et al., *The new mutation, E46K, of alpha-synuclein causes Parkinson and Lewy body dementia.* Ann Neurol, 2004. **55**(2): p. 164-73.
37. Nuytemans, K., et al., *Genetic etiology of Parkinson disease associated with mutations in the SNCA, PARK2, PINK1, PARK7, and LRRK2 genes: a mutation update.* Hum Mutat, 2010. **31**(7): p. 763-80.
38. Ibanez, P., et al., *Causal relation between alpha-synuclein gene duplication and familial Parkinson's disease.* Lancet, 2004. **364**(9440): p. 1169-1171.
39. Paisan-Ruiz, C., et al., *Cloning of the gene containing mutations that cause PARK8-linked Parkinson's disease.* Neuron, 2004. **44**(4): p. 595-600.

40. Belin, A.C. and M. Westerlund, *Parkinson's disease: a genetic perspective.* FEBS J, 2008. **275**(7): p. 1377-83.
41. Zimprich, A., et al., *Mutations in LRRK2 cause autosomal-dominant parkinsonism with pleomorphic pathology.* Neuron, 2004. **44**(4): p. 601-7.
42. Dachsel, J.C. and M.J. Farrer, *LRRK2 and Parkinson disease.* Arch Neurol, 2010. **67**(5): p. 542-7.
43. Berg, D., et al., *Type and frequency of mutations in the LRRK2 gene in familial and sporadic Parkinson's disease*.* Brain, 2005. **128**(Pt 12): p. 3000-11.
44. Gilks, W.P., et al., *A common LRRK2 mutation in idiopathic Parkinson's disease.* Lancet, 2005. **365**(9457): p. 415-6.
45. Dawson, T.M. and V.L. Dawson, *The role of parkin in familial and sporadic Parkinson's disease.* Mov Disord, 2010. **25 Suppl 1**: p. S32-9.
46. Chin, L.S., J.A. Olzmann, and L. Li, *Parkin-mediated ubiquitin signalling in aggresome formation and autophagy.* Biochemical Society Transactions, 2010. **38**: p. 144-149.
47. Valente, E.M., et al., *PINK1 mutations are associated with sporadic early-onset parkinsonism.* Ann Neurol, 2004. **56**(3): p. 336-41.
48. Whitworth, A.J. and L.J. Pallanck, *The PINK1/Parkin pathway: a mitochondrial quality control system?* J Bioenerg Biomembr, 2009. **41**(6): p. 499-503.
49. Ramirez, A., et al., *Hereditary parkinsonism with dementia is caused by mutations in ATP13A2, encoding a lysosomal type 5 P-type ATPase.* Nature Genetics, 2006. **38**(10): p. 1184-1191.
50. Williams, D.R., et al., *Kufor Rakeb disease: Autosomal recessive, levodopa-responsive parkinsonism with pyramidal degeneration, supranuclear gaze palsy, and dementia.* Movement Disorders, 2005. **20**(10): p. 1264-1271.
51. Nagakubo, D., et al., *DJ-1, a novel oncogene which transforms mouse NIH3T3 cells in cooperation with ras.* Biochemical and Biophysical Research Communications, 1997. **231**(2): p. 509-513.
52. Taira, T., et al., *DJ-1 has a role in antioxidative stress to prevent cell death.* Embo Reports, 2004. **5**(2): p. 213-218.
53. Zhou, W.B., et al., *The oxidation state of DJ-1 regulates its chaperone activity toward alpha-synuclein.* Journal of Molecular Biology, 2006. **356**(4): p. 1036-1048.
54. Kim, R.H., et al., *Hypersensitivity of DJ-1-deficient mice to 1-methyl-4-phenyl-1,2,3,6-tetrahydropyrindine (MPTP) and oxidative stress.* Proc Natl Acad Sci U S A, 2005. **102**(14): p. 5215-20.
55. Lev, N., et al., *DJ-1 protects against dopamine toxicity.* J Neural Transm, 2009. **116**(2): p. 151-60.
56. Abou-Sleiman, P.M., et al., *The role of pathogenic DJ-1 mutations in Parkinson's disease.* Ann Neurol, 2003. **54**(3): p. 283-6.
57. Dekker, M., et al., *Clinical features and neuroimaging of PARK7-linked parkinsonism.* Mov Disord, 2003. **18**(7): p. 751-7.
58. Bonifati, V., et al., *Mutations in the DJ-1 gene associated with autosomal recessive early-onset parkinsonism.* Science, 2003. **299**(5604): p. 256-9.
59. Martinez-Vicente, M., G. Sovak, and A.M. Cuervo, *Protein degradation and aging.* Experimental Gerontology, 2005. **40**(8-9): p. 622-633.

60. McNaught, K.S., et al., *Failure of the ubiquitin-proteasome system in Parkinson's disease.* Nat Rev Neurosci, 2001. **2**(8): p. 589-94.
61. Vila, M. and S. Przedborski, *Genetic clues to the pathogenesis of Parkinson's disease.* Nat Med, 2004. **10 Suppl**: p. S58-62.
62. Cookson, M.R., *Parkinsonism due to mutations in PINK1, parkin, and DJ-1 and oxidative stress and mitochondrial pathways.* Cold Spring Harb Perspect Med, 2012. **2**(9): p. a009415.
63. Narendra, D.P., et al., *PINK1 Is Selectively Stabilized on Impaired Mitochondria to Activate Parkin.* Plos Biology, 2010. **8**(1).
64. Vives-Bauza, C., et al., *PINK1-dependent recruitment of Parkin to mitochondria in mitophagy.* Proceedings of the National Academy of Sciences of the United States of America, 2010. **107**(1): p. 378-383.
65. Thomas, K.J., et al., *DJ-1 acts in parallel to the PINK1/parkin pathway to control mitochondrial function and autophagy.* Hum Mol Genet, 2011. **20**(1): p. 40-50.
66. Schapira, A.H., *Mitochondrial disease.* Lancet, 2006. **368**(9529): p. 70-82.
67. Beal, M.F., *Mitochondria take center stage in aging and neurodegeneration.* Ann Neurol, 2005. **58**(4): p. 495-505.
68. Olanow, C.W. and W.G. Tatton, *Etiology and pathogenesis of Parkinson's disease.* Annu Rev Neurosci, 1999. **22**: p. 123-44.
69. Henchcliffe, C. and M.F. Beal, *Mitochondrial biology and oxidative stress in Parkinson disease pathogenesis.* Nat Clin Pract Neurol, 2008. **4**(11): p. 600-9.
70. Schapira, A.H., et al., *Mitochondrial complex I deficiency in Parkinson's disease.* J Neurochem, 1990. **54**(3): p. 823-7.
71. Parker, W.D., Jr., J.K. Parks, and R.H. Swerdlow, *Complex I deficiency in Parkinson's disease frontal cortex.* Brain Res, 2008. **1189**: p. 215-8.
72. Mann, V.M., et al., *Brain, skeletal muscle and platelet homogenate mitochondrial function in Parkinson's disease.* Brain, 1992. **115 (Pt 2)**: p. 333-42.
73. Vyas, I., R.E. Heikkila, and W.J. Nicklas, *Studies on the neurotoxicity of 1-methyl-4-phenyl-1,2,3,6-tetrahydropyridine: inhibition of NAD-linked substrate oxidation by its metabolite, 1-methyl-4-phenylpyridinium.* J Neurochem, 1986. **46**(5): p. 1501-7.
74. Greenamyre, J.T., R. Betarbet, and T.B. Sherer, *The rotenone model of Parkinson's disease: genes, environment and mitochondria.* Parkinsonism Relat Disord, 2003. **9 Suppl 2**: p. S59-64.
75. Hoglinger, G.U., et al., *Dysfunction of mitochondrial complex I and the proteasome: interactions between two biochemical deficits in a cellular model of Parkinson's disease.* J Neurochem, 2003. **86**(5): p. 1297-307.
76. Schapira, A.H. and M. Gegg, *Mitochondrial contribution to Parkinson's disease pathogenesis.* Parkinsons Dis, 2011. **2011**: p. 159160.
77. Esteves, A.R., et al., *Mitochondrial respiration and respiration-associated proteins in cell lines created through Parkinson's subject mitochondrial transfer.* Journal of Neurochemistry, 2010. **113**(3): p. 674-682.
78. Trimmer, P.A. and J.P. Bennett, Jr., *The cybrid model of sporadic Parkinson's disease.* Experimental Neurology, 2009. **218**(2): p. 320-5.

79. Gautier, C.A., T. Kitada, and J. Shen, *Loss of PINK1 causes mitochondrial functional defects and increased sensitivity to oxidative stress.* Proc Natl Acad Sci U S A, 2008. **105**(32): p. 11364-9.
80. Yang, Y.F., et al., *Pink1 regulates mitochondrial dynamics through interaction with the fission/fusion machinery.* Proceedings of the National Academy of Sciences of the United States of America, 2008. **105**(19): p. 7070-7075.
81. Pridgeon, J.W., et al., *PINK1 protects against oxidative stress by phosphorylating mitochondrial chaperone TRAP1.* PLoS Biol, 2007. **5**(7): p. e172.
82. Plun-Favreau, H., et al., *The mitochondrial protease HtrA2 is regulated by Parkinson's disease-associated kinase PINK1.* Nature Cell Biology, 2007. **9**(11): p. 1243-U63.
83. Deng, H., et al., *The Parkinson's disease genes pink1 and parkin promote mitochondrial fission and/or inhibit fusion in Drosophila.* Proc Natl Acad Sci U S A, 2008. **105**(38): p. 14503-8.
84. Poole, A.C., et al., *The PINK1/Parkin pathway regulates mitochondrial morphology.* Proc Natl Acad Sci U S A, 2008. **105**(5): p. 1638-43.
85. Hattori, N. and Y. Mizuno, *Pathogenetic mechanisms of parkin in Parkinson's disease.* Lancet, 2004. **364**(9435): p. 722-4.
86. Olzmann, J.A., et al., *Parkin-mediated K63-linked polyubiquitination targets misfolded DJ-1 to aggresomes via binding to HDAC6.* Journal of Cell Biology, 2007. **178**(6): p. 1025-1038.
87. Palacino, J.J., et al., *Mitochondrial dysfunction and oxidative damage in parkin-deficient mice.* J Biol Chem, 2004. **279**(18): p. 18614-22.
88. Itier, J.M., et al., *Parkin gene inactivation alters behaviour and dopamine neurotransmission in the mouse.* Hum Mol Genet, 2003. **12**(18): p. 2277-91.
89. Li, W.W., et al., *Localization of alpha-synuclein to mitochondria within midbrain of mice.* Neuroreport, 2007. **18**(15): p. 1543-1546.
90. Liu, G.W., et al., *alpha-Synuclein is differentially expressed in mitochondria from different rat brain regions and dose-dependently down-regulates complex I activity.* Neuroscience Letters, 2009. **454**(3): p. 187-192.
91. Martin, L.J., et al., *Parkinson's disease alpha-synuclein transgenic mice develop neuronal mitochondrial degeneration and cell death.* J Neurosci, 2006. **26**(1): p. 41-50.
92. Miller, D.W., et al., *L166P mutant DJ-1, causative for recessive Parkinson's disease, is degraded through the ubiquitin-proteasome system.* J Biol Chem, 2003. **278**(38): p. 36588-95.
93. Zhang, L., et al., *Mitochondrial localization of the Parkinson's disease related protein DJ-1: implications for pathogenesis.* Hum Mol Genet, 2005. **14**(14): p. 2063-73.
94. Usami, Y., et al., *DJ-1 associates with synaptic membranes.* Neurobiol Dis, 2011. **43**(3): p. 651-62.
95. Junn, E., et al., *Mitochondrial localization of DJ-1 leads to enhanced neuroprotection.* J Neurosci Res, 2009. **87**(1): p. 123-9.
96. Kim, S.J., et al., *Nuclear translocation of DJ-1 during oxidative stress-induced neuronal cell death.* Free Radic Biol Med, 2012. **53**(4): p. 936-50.

97. Hayashi, T., et al., *DJ-1 binds to mitochondrial complex I and maintains its activity.* Biochem Biophys Res Commun, 2009. **390**(3): p. 667-72.
98. Canet-Aviles, R.M., et al., *The Parkinson's disease protein DJ-1 is neuroprotective due to cysteine-sulfinic acid-driven mitochondrial localization.* Proc Natl Acad Sci U S A, 2004. **101**(24): p. 9103-8.
99. Kim, S.J., Y.J. Park, and Y.J. Oh, *Proteomic analysis reveals a protective role for DJ-1 during 6-hydroxydopamine-induced cell death.* Biochem Biophys Res Commun, 2012. **422**(1): p. 8-14.
100. Martinat, C., et al., *Sensitivity to oxidative stress in DJ-1-deficient dopamine neurons: An ES-derived cell model of primary Parkinsonism.* Plos Biology, 2004. **2**(11): p. 1754-1763.
101. Batelli, S., et al., *DJ-1 modulates alpha-synuclein aggregation state in a cellular model of oxidative stress: relevance for Parkinson's disease and involvement of HSP70.* PLoS One, 2008. **3**(4): p. e1884.
102. Shendelman, S., et al., *DJ-1 is a redox-dependent molecular chaperone that inhibits alpha-synuclein aggregate formation.* Plos Biology, 2004. **2**(11): p. 1764-1773.
103. Yang, Y., et al., *Inactivation of Drosophila DJ-1 leads to impairments of oxidative stress response and phosphatidylinositol 3-kinase/Akt signaling.* Proc Natl Acad Sci U S A, 2005. **102**(38): p. 13670-5.
104. Chen, L., et al., *Age-dependent motor deficits and dopaminergic dysfunction in DJ-1 null mice.* J Biol Chem, 2005. **280**(22): p. 21418-26.
105. Honbou, K., et al., *The crystal structure of DJ-1, a protein related to male fertility and Parkinson's disease.* J Biol Chem, 2003. **278**(33): p. 31380-4.
106. Baulac, S., et al., *Dimerization of Parkinson's disease-causing DJ-1 and formation of high molecular weight complexes in human brain.* Mol Cell Neurosci, 2004. **27**(3): p. 236-46.
107. Bonifati, V., B.A. Oostra, and P. Heutink, *Linking DJ-1 to neurodegeneration offers novel insights for understanding the pathogenesis of Parkinson's disease.* Journal of Molecular Medicine-Jmm, 2004. **82**(3): p. 163-174.
108. Moore, D.J., et al., *A missense mutation (L166P) in DJ-1, linked to familial Parkinson's disease, confers reduced protein stability and impairs homo-oligomerization.* J Neurochem, 2003. **87**(6): p. 1558-67.
109. Hague, S., et al., *Early-onset Parkinson's disease caused by a compound heterozygous DJ-1 mutation.* Ann Neurol, 2003. **54**(2): p. 271-4.
110. Okada, M., et al., *DJ-1, a target protein for an endocrine disrupter, participates in the fertilization in mice.* Biol Pharm Bull, 2002. **25**(7): p. 853-6.
111. Blackinton, J., et al., *Post-transcriptional regulation of mRNA associated with DJ-1 in sporadic Parkinson disease.* Neuroscience Letters, 2009. **452**(1): p. 8-11.
112. Lee, S.J., et al., *Crystal structures of human DJ-1 and Escherichia coli Hsp31, which share an evolutionarily conserved domain.* J Biol Chem, 2003. **278**(45): p. 44552-9.
113. Andres-Mateos, E., et al., *DJ-1 gene deletion reveals that DJ-1 is an atypical peroxiredoxin-like peroxidase.* Proceedings of the National Academy of Sciences of the United States of America, 2007. **104**(37): p. 14807-14812.

114. Gonzalez-Polo, R., et al., *DJ-1 as a Modulator of Autophagy: An Hypothesis.* TheScientificWorldJOURNAL, 2010. **10**: p. 1574-1579.
115. Irrcher, I., et al., *Loss of the Parkinson's disease-linked gene DJ-1 perturbs mitochondrial dynamics.* Hum Mol Genet, 2010. **19**(19): p. 3734-46.
116. Gonzalez-Polo, R., et al., *Silencing DJ-1 reveals its contribution in paraquat-induced autophagy.* J Neurochem, 2009. **109**(3): p. 889-98.
117. Gu, L., et al., *Involvement of ERK1/2 signaling pathway in DJ-1-induced neuroprotection against oxidative stress.* Biochem Biophys Res Commun, 2009. **383**(4): p. 469-74.
118. Kim, Y.C., et al., *Oxidation of DJ-1-dependent cell transformation through direct binding of DJ-1 to PTEN.* Int J Oncol, 2009. **35**(6): p. 1331-41.
119. Kim, R.H., et al., *DJ-1, a novel regulator of the tumor suppressor PTEN.* Cancer Cell, 2005. **7**(3): p. 263-73.
120. Aleyasin, H., et al., *DJ-1 protects the nigrostriatal axis from the neurotoxin MPTP by modulation of the AKT pathway.* Proc Natl Acad Sci U S A, 2010. **107**(7): p. 3186-91.
121. Junn, E., et al., *Interaction of DJ-1 with Daxx inhibits apoptosis signal-regulating kinase 1 activity and cell death.* Proc Natl Acad Sci U S A, 2005. **102**(27): p. 9691-6.
122. Im, J.Y., et al., *DJ-1 protects against oxidative damage by regulating the thioredoxin/ASK1 complex.* Neurosci Res, 2010. **67**(3): p. 203-8.
123. Waak, J., et al., *Oxidizable residues mediating protein stability and cytoprotective interaction of DJ-1 with apoptosis signal-regulating kinase 1.* J Biol Chem, 2009. **284**(21): p. 14245-57.
124. Bader, V., et al., *Expression of DJ-1 in the adult mouse CNS.* Brain Res, 2005. **1041**(1): p. 102-11.
125. Yokota, T., et al., *Down regulation of DJ-1 enhances cell death by oxidative stress, ER stress, and proteasome inhibition.* Biochem Biophys Res Commun, 2003. **312**(4): p. 1342-8.
126. Zhou, W. and C.R. Freed, *DJ-1 up-regulates glutathione synthesis during oxidative stress and inhibits A53T alpha-synuclein toxicity.* J Biol Chem, 2005. **280**(52): p. 43150-8.
127. Clements, C.M., et al., *DJ-1, a cancer- and Parkinson's disease-associated protein, stabilizes the antioxidant transcriptional master regulator Nrf2.* Proc Natl Acad Sci U S A, 2006. **103**(41): p. 15091-6.
128. Wilson, M.A., et al., *The 1.1-A resolution crystal structure of DJ-1, the protein mutated in autosomal recessive early onset Parkinson's disease.* Proc Natl Acad Sci U S A, 2003. **100**(16): p. 9256-61.
129. Tao, X. and L. Tong, *Crystal structure of human DJ-1, a protein associated with early onset Parkinson's disease.* J Biol Chem, 2003. **278**(33): p. 31372-9.
130. Spillantini, M.G., et al., *Alpha-synuclein in Lewy bodies.* Nature, 1997. **388**(6645): p. 839-40.
131. Schlossmacher, M.G., et al., *Parkin localizes to the Lewy bodies of Parkinson disease and dementia with Lewy bodies.* Am J Pathol, 2002. **160**(5): p. 1655-67.
132. Bandopadhyay, R., et al., *The expression of DJ-1 (PARK7) in normal human CNS and idiopathic Parkinson's disease.* Brain, 2004. **127**(Pt 2): p. 420-30.

133. Rizzu, P., et al., *DJ-1 colocalizes with tau inclusions: A link between parkinsonism and dementia.* Annals of Neurology, 2004. **55**(1): p. 113-118.
134. Meulener, M.C., et al., *DJ-1 is present in a large molecular complex in human brain tissue and interacts with alpha-synuclein.* Journal of Neurochemistry, 2005. **93**(6): p. 1524-1532.
135. Jin, J.H., et al., *Identification of novel proteins associated with both alpha-synuclein and DJ-1.* Molecular & Cellular Proteomics, 2007. **6**(5): p. 845-859.
136. Olzmann, J.A., et al., *Familial Parkinson's disease-associated L166P mutation disrupts DJ-1 protein folding and function.* J Biol Chem, 2004. **279**(9): p. 8506-15.
137. Gorner, K., et al., *Differential effects of Parkinson's disease-associated mutations on stability and folding of DJ-1.* J Biol Chem, 2004. **279**(8): p. 6943-51.
138. Tsuboi, Y., et al., *DJ-1, a causative gene product of a familial form of Parkinson's disease, is secreted through microdomains.* Febs Letters, 2008. **582**(17): p. 2643-2649.
139. Yanagida, T., et al., *Oxidative stress induction of DJ-1 protein in reactive astrocytes scavenges free radicals and reduces cell injury.* Oxid Med Cell Longev, 2009. **2**(1): p. 36-42.
140. Mullett, S.J. and D.A. Hinkle, *DJ-1 knock-down in astrocytes impairs astrocyte-mediated neuroprotection against rotenone.* Neurobiol Dis, 2009. **33**(1): p. 28-36.
141. Mullett, S.J., et al., *DJ-1 Expression Modulates Astrocyte-Mediated Protection Against Neuronal Oxidative Stress.* J Mol Neurosci, 2012.
142. Larsen, N.J., et al., *DJ-1 knock-down impairs astrocyte mitochondrial function.* Neuroscience, 2011. **196**: p. 251-64.
143. Inden, M., et al., *PARK7 DJ-1 protects against degeneration of nigral dopaminergic neurons in Parkinson's disease rat model.* Neurobiol Dis, 2006. **24**(1): p. 144-58.
144. Shinbo, Y., et al., *Proper SUMO-1 conjugation is essential to DJ-1 to exert its full activities.* Cell Death and Differentiation, 2006. **13**(1): p. 96-108.
145. Macedo, M.G., et al., *The DJ-1(L166P) mutant protein associated with early onset Parkinson's disease is unstable and forms higher-order protein complexes.* Human Molecular Genetics, 2003. **12**(21): p. 2807-2816.
146. Maita, C., et al., *Secretion of DJ-1 into the serum of patients with Parkinson's disease.* Neuroscience Letters, 2008. **431**(1): p. 86-89.
147. Waragai, M., et al., *Plasma levels of DJ-1 as a possible marker for progression of sporadic Parkinson's disease.* Neuroscience Letters, 2007. **425**(1): p. 18-22.
148. Waragai, M., et al., *Increased level of DJ-1 in the cerebrospinal fluids of sporadic Parkinson's disease.* Biochem Biophys Res Commun, 2006. **345**(3): p. 967-72.
149. Conner, S.D. and S.L. Schmid, *Regulated portals of entry into the cell.* Nature, 2003. **422**(6927): p. 37-44.
150. Anderson, R.G., *The caveolae membrane system.* Annu Rev Biochem, 1998. **67**: p. 199-225.
151. Pelkmans, L. and A. Helenius, *Endocytosis via caveolae.* Traffic, 2002. **3**(5): p. 311-20.

152. Edidin, M., *Shrinking patches and slippery rafts: scales of domains in the plasma membrane.* Trends Cell Biol, 2001. **11**(12): p. 492-6.
153. Pralle, A., et al., *Sphingolipid-cholesterol rafts diffuse as small entities in the plasma membrane of mammalian cells.* Journal of Cell Biology, 2000. **148**(5): p. 997-1007.
154. Sandvig, K., et al., *Endocytosis from coated pits of Shiga toxin: a glycolipid-binding protein from Shigella dysenteriae 1.* Journal of Cell Biology, 1989. **108**(4): p. 1331-43.
155. Lamaze, C., et al., *Interleukin 2 receptors and detergent-resistant membrane domains define a clathrin-independent endocytic pathway.* Mol Cell, 2001. **7**(3): p. 661-71.
156. Artalejo, C.R., A. Elhamdani, and H.C. Palfrey, *Sustained stimulation shifts the mechanism of endocytosis from dynamin-1-dependent rapid endocytosis to clathrin- and dynamin-2-mediated slow endocytosis in chromaffin cells.* Proc Natl Acad Sci U S A, 2002. **99**(9): p. 6358-63.
157. Seto, E.S., H.J. Bellen, and T.E. Lloyd, *When cell biology meets development: endocytic regulation of signaling pathways.* Genes & Development, 2002. **16**(11): p. 1314-1336.
158. Seto, E.S., H.J. Bellen, and T.E. Lloyd, *When cell biology meets development: endocytic regulation of signaling pathways.* Genes Dev, 2002. **16**(11): p. 1314-36.
159. Brodsky, F.M., et al., *Biological basket weaving: formation and function of clathrin-coated vesicles.* Annu Rev Cell Dev Biol, 2001. **17**: p. 517-68.
160. Gaidarov, I., et al., *Spatial control of coated-pit dynamics in living cells.* Nature Cell Biology, 1999. **1**(1): p. 1-7.
161. Fujimoto, L.M., et al., *Actin assembly plays a variable, but not obligatory role in receptor-mediated endocytosis in mammalian cells.* Traffic, 2000. **1**(2): p. 161-171.
162. Laburthe, M., B. Breant, and C. Rouyer-Fessard, *Molecular identification of receptors for vasoactive intestinal peptide in rat intestinal epithelium by covalent cross-linking. Evidence for two classes of binding sites with different structural and functional properties.* Eur J Biochem, 1984. **139**(1): p. 181-7.
163. Knoller, S., S. Shpungin, and E. Pick, *The Membrane-Associated Component of the Amphiphile-Activated, Cytosol-Dependent Superoxide-Forming Nadph Oxidase of Macrophages Is Identical to Cytochrome-B559.* Journal of Biological Chemistry, 1991. **266**(5): p. 2795-2804.
164. Gorner, K., et al., *Structural determinants of the C-terminal helix-kink-helix motif essential for protein stability and survival promoting activity of DJ-1.* J Biol Chem, 2007. **282**(18): p. 13680-91.
165. Hirel, P.H., et al., *Extent of N-Terminal Methionine Excision from Escherichia-Coli Proteins Is Governed by the Side-Chain Length of the Penultimate Amino-Acid.* Proceedings of the National Academy of Sciences of the United States of America, 1989. **86**(21): p. 8247-8251.
166. Xie, H.R., L.S. Hu, and G.Y. Li, *SH-SY5Y human neuroblastoma cell line: in vitro cell model of dopaminergic neurons in Parkinson's disease.* Chin Med J (Engl), 2010. **123**(8): p. 1086-92.

167. Yanagida, T., et al., *Protection against oxidative stress-induced neurodegeneration by a modulator for DJ-1, the wild-type of familial Parkinson's disease-linked PARK7.* J Pharmacol Sci, 2009. **109**(3): p. 463-8.
168. Kitamura, Y., et al., *Neuroprotective effect of a new DJ-1-binding compound against neurodegeneration in Parkinson's disease and stroke model rats.* Mol Neurodegener, 2011. **6**(1): p. 48.
169. Miyazaki, S., et al., *DJ-1-binding compounds prevent oxidative stress-induced cell death and movement defect in Parkinson's disease model rats.* J Neurochem, 2008. **105**(6): p. 2418-34.
170. Yanagisawa, D., et al., *DJ-1 protects against neurodegeneration caused by focal cerebral ischemia and reperfusion in rats.* J Cereb Blood Flow Metab, 2008. **28**(3): p. 563-78.
171. Ruffels, J., M. Griffin, and J.M. Dickenson, *Activation of ERK1/2, JNK and PKB by hydrogen peroxide in human SH-SY5Y neuroblastoma cells: role of ERK1/2 in H2O2-induced cell death.* Eur J Pharmacol, 2004. **483**(2-3): p. 163-73.
172. Cruz, C.D. and F. Cruz, *The ERK 1 and 2 pathway in the nervous system: from basic aspects to possible clinical applications in pain and visceral dysfunction.* Curr Neuropharmacol, 2007. **5**(4): p. 244-52.
173. Cavanaugh, J.E., et al., *Neuroprotective role of ERK1/2 and ERK5 in a dopaminergic cell line under basal conditions and in response to oxidative stress.* J Neurosci Res, 2006. **84**(6): p. 1367-75.
174. Brunet, A., S.R. Datta, and M.E. Greenberg, *Transcription-dependent and -independent control of neuronal survival by the PI3K-Akt signaling pathway.* Curr Opin Neurobiol, 2001. **11**(3): p. 297-305.
175. Gao, H., et al., *DJ-1 protects dopaminergic neurons against rotenone-induced apoptosis by enhancing ERK-dependent mitophagy.* Journal of Molecular Biology, 2012. **423**(2): p. 232-48.
176. Lu, L., et al., *DJ-1 upregulates tyrosine hydroxylase gene expression by activating its transcriptional factor Nurr1 via the ERK1/2 pathway.* Int J Biochem Cell Biol, 2012. **44**(1): p. 65-71.
177. Crossthwaite, A.J., S. Hasan, and R.J. Williams, *Hydrogen peroxide-mediated phosphorylation of ERK1/2, Akt/PKB and JNK in cortical neurones: dependence on Ca(2+) and PI3-kinase.* J Neurochem, 2002. **80**(1): p. 24-35.
178. Lokman, N.A., et al., *The role of annexin A2 in tumorigenesis and cancer progression.* Cancer Microenviron, 2011. **4**(2): p. 199-208.
179. Soldi, R., et al., *Role of alphavbeta3 integrin in the activation of vascular endothelial growth factor receptor-2.* EMBO J, 1999. **18**(4): p. 882-92.
180. Rogers, S.L., et al., *Neuron-specific interactions with two neurite-promoting fragments of fibronectin.* J Neurosci, 1985. **5**(2): p. 369-78.
181. Prange, C.K., et al., *Characterization of the human neurocan gene, CSPG3.* Gene, 1998. **221**(2): p. 199-205.
182. Hopf, M., et al., *Crystal structure and mutational analysis of a perlecan-binding fragment of nidogen-1.* Nat Struct Biol, 2001. **8**(7): p. 634-40.
183. Marr, H.S. and C.J. Edgell, *Testican-1 inhibits attachment of Neuro-2a cells.* Matrix Biol, 2003. **22**(3): p. 259-66.

184. Moreno-Flores, M.T., et al., *Semaphorin 3C preserves survival and induces neuritogenesis of cerebellar granule neurons in culture.* J Neurochem, 2003. **87**(4): p. 879-90.
185. Klintenberg, R. and P.E. Andren, *Altered extracellular striatal in vivo biotransformation of the opioid neuropeptide dynorphin A(1-17) in the unilateral 6-OHDA rat model of Parkinson's disease.* J Mass Spectrom, 2005. **40**(2): p. 261-70.
186. Billova, S., et al., *Immunohistochemical expression and colocalization of somatostatin, carboxypeptidase-E and prohormone convertases 1 and 2 in rat brain.* Neuroscience, 2007. **147**(2): p. 403-18.
187. Yamada, T., P.L. McGeer, and E.G. McGeer, *Lewy bodies in Parkinson's disease are recognized by antibodies to complement proteins.* Acta Neuropathol, 1992. **84**(1): p. 100-4.
188. van den Beld, A.W., et al., *Serum insulin-like growth factor binding protein-2 levels as an indicator of functional ability in elderly men.* European Journal of Endocrinology, 2003. **148**(6): p. 627-634.
189. Wang, J. and R. Milner, *Fibronectin promotes brain capillary endothelial cell survival and proliferation through alpha5beta1 and alphavbeta3 integrins via MAP kinase signalling.* J Neurochem, 2006. **96**(1): p. 148-59.
190. Boeve, B.F. and M. Hutton, *Refining frontotemporal dementia with parkinsonism linked to chromosome 17: introducing FTDP-17 (MAPT) and FTDP-17 (PGRN).* Arch Neurol, 2008. **65**(4): p. 460-4.
191. Akiyama, H., et al., *Expression of BRI, the normal precursor of the amyloid protein of familial British dementia, in human brain.* Acta Neuropathol, 2004. **107**(1): p. 53-8.
192. Rovelli, G., et al., *Specific Interaction of Vitronectin with the Cell-Secreted Protease Inhibitor Glia-Derived Nexin and Its Thrombin Complex.* European Journal of Biochemistry, 1990. **192**(3): p. 797-803.
193. Scotti, A.L., D. Monard, and C. Nitsch, *Re-expression of glia-derived nexin/protease nexin 1 depends on mode of lesion-induction or terminal degeneration: observations after excitotoxin or 6-hydroxydopamine lesions of rat substantia nigra.* J Neurosci Res, 1994. **37**(2): p. 155-68.
194. Bolkenius, F.N. and D. Monard, *Inactivation of protease nexin-1 by xanthine oxidase-derived free radicals.* Neurochem Int, 1995. **26**(6): p. 587-92.
195. Grand, R.J., A.S. Turnell, and P.W. Grabham, *Cellular consequences of thrombin-receptor activation.* Biochem J, 1996. **313 (Pt 2)**: p. 353-68.
196. Lee, D.Y., Y.J. Oh, and B.K. Jin, *Thrombin-activated microglia contribute to death of dopaminergic neurons in rat mesencephalic cultures: dual roles of mitogen-activated protein kinase signaling pathways.* Glia, 2005. **51**(2): p. 98-110.

7| SUPPLEMENTARY DATA

7.1. MOLECULAR SIZE EXCLUSION CHROMATOGRAPHY

In order to assess if the purified DJ-1 has a homodimer form, which is a functional important feature of the protein [112, 128-129], an HPLC-size exclusion chromatography was performed. Standards retention times were used to perform a calibration curve (Figure 7.1) and the molecular weight of purified DJ-1 was determined using the retention time of DJ-1 sample.

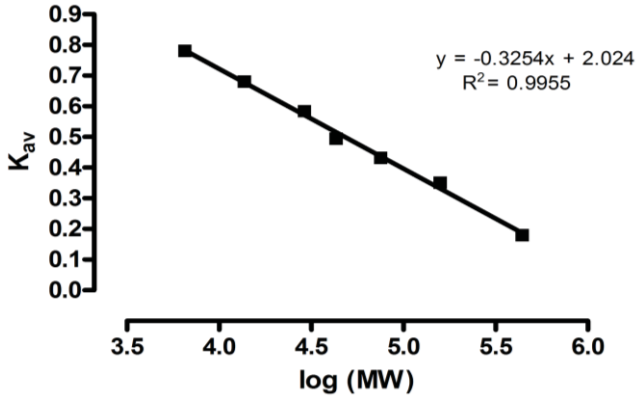

FIGURE 7.1| HPLC-SIZE EXCLUSION CHROMATOGRAPHY CALIBRATION CURVE. Standards from right to left: Blue Dextran (≈2,000 kDa); Ferritin (440 kDa); Aldolase (158 kDa); Conalbumin (75 kDa); Ovalbumin (43 kDa); Carbonic Anhydrase (29 kDa); Ribonuclease A (13.7 kDa); Aprotinin (6.5 kDa). The mobile phase was PBS with 10% of glycerol (purified recombinant DJ-1 buffer).

K_{av} is the partition coefficient, which is calculated from the measured elution volume (V_e) of each standard protein or protein of interest, using the formula: $K_{av} = \frac{V_e - V_0}{V_c - V_0}$, where the V_0 is the column void volume – elution volume for Blue Dextran 2000 –, and V_c is the geometric column volume.

After having the calibration curve of K_{av} versus log molecular weight either (Figure 7.1), the molecular weight of the protein of interest can be inferred, using its calculated K_{av}.

7.2. CELL VIABILITY ASSAYS

To assess the percentage of viable cells when they were treated different H_2O_2 concentrations, different tests can be used, such as the Cell Titer-Glo®Luminescent Cell Viability Assay (Promega) and the MTT assay (Life Technologies). The Cell Titer-Glo® assay "is a homogeneous method to determine the number of viable cells in culture based on quantitation of the ATP present, which signals the presence of metabolically active cells". "The MTT system is a simple, accurate, reproducible means of measuring the activity of living cells via mitochondrial dehydrogenase activity". As in the literature the MTT is the most used method, it is need to test if the Cell Titer-Glo® assay produces similar results.

Actually, by performing cell viability experiments, as described in the section 2.3., using different H_2O_2 concentrations, the luminescent and absorbance values obtained allowed the draw of similar dose-response curves, with similar LD50 values (366.6 µM using the MTT assay and 363.4 µM using the Cell Titer-Glo® asay) (Figure 7.2). Thus, the Cell Titer-Glo® assay was used in further experiments.

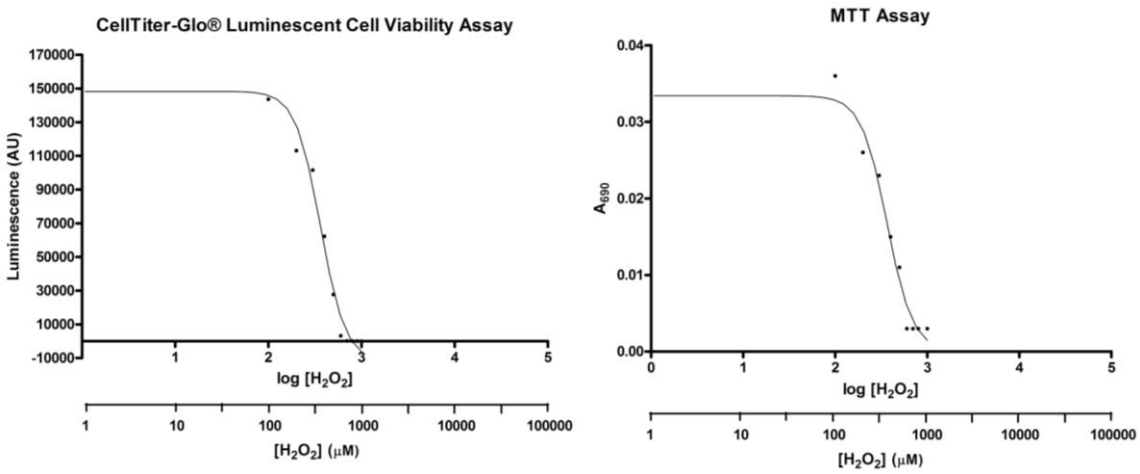

FIGURE 7.2| COMPARISON OF CELL TITER-GLO® ASSAY WITH MTT ASSAY. SH-SY5Y cells were plated and treated with various concentrations of hydrogen peroxide, 4 h after plating. After 24 h, cell viability was assessed by the by Cell Titer-Glo® or MTT assay.

As stated in the section 3.5 the inhibition of H_2O_2-induced cell death by the exogenous addition of a recombinant DJ-1 protein was assessed by using different H_2O_2 concentrations in the presence or absence of the purified DJ-1 (1 and 5 µM). The

results of the simultaneous treatment of cells with 5 µM of DJ-1 showed a significantly increase of the cell viability using 25, 50 and 100 µM of H_2O_2 (Figure 7.3).

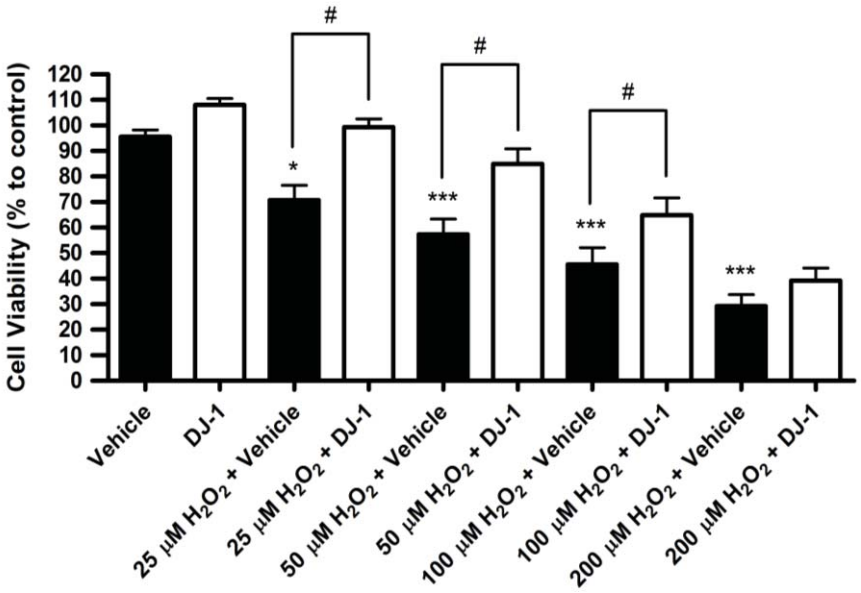

FIGURE 7.3| PROTECTIVE EFFECT OF RECOMBINANT DJ-1 AGAINST H_2O_2-INDUCED OXIDATIVE STRESS. SH-SY5Y cells were treated with H_2O_2 (25, 50, 100 and 200 µM) in the presence or absence of recombinant His-tagged human DJ-1 protein (5 µM) or vehicle, 4h after plating. After 24 h, cell viability was assessed by the Cell Titer-Glo® assay. Data are the mean±SEM of four determinations, based on untreated cultures as 100%. Significance (Tukey HSD post hoc comparisons after Two-way ANOVA): *$p < 0.05$, ***$p < 0.001$ treatment with H_2O_2 and vehicle vs. treatment with vehicle alone. #$p < 0.05$ treatment with H_2O_2 and DJ-1 vs. corresponding treatment with H_2O_2 and vehicle.

7.3. INTERNALIZATION OF DJ-1

One of the major goals of this project was to understand if DJ-1 released from astrocytes could be uptake by SH-SY5Y to exert its neuroprotective effect by activating intracellular signalling pathways or by a receptor-mediated activation of signalling pathways.

To observe the internalization of the produced recombinant DJ-1, that was already reported using a GST-DJ-1 [143], the methodology described in the referred paper was used.

In a first attempt, cells were treated with 100 µM H_2O_2 and 1 µM DJ-1 (simultaneously) or with 1 µM of DJ-1, during 4h. Cellular extracts were performed by scraping or shaving cells with trypsin, in order to try to eliminate the recombinant DJ-1 that could be bound to the cellular membrane, and the western-blot was performed

using the mouse Anti-His Tag TM0243 (1:5,000) (GenScript, USA), as described in section 2.6.3. (Figure 7.4).

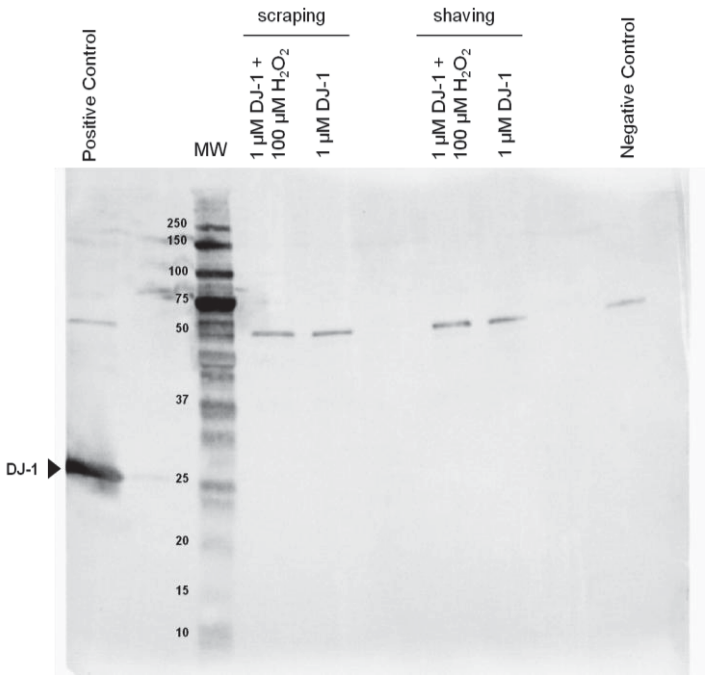

FIGURE 7.4| INTERNALIZATION OF 6-HIS-DJ-1. SH-SY5Y cells were treated with 100 µM H_2O_2 and 1 µM DJ-1 (simultaneously) or with µM of DJ-1, for 4h. Cellular extracts were performed by scraping or shaving cells with trypsin and the western-blot was performed using an anti-His antibody. The positive control is the purified DJ-1 and the negative control is a SH-SY5Y protein extract.

There is no evidence for a DJ-1 internalization by SH-SY5Y cells, as there is no band at approximately 25 kDa (except in the case of the positive control), corresponding to the recombinant protein. There are bands at ≈50 kDa, which could correspond to the dimeric form of the protein, but all samples were denatured with sample buffer with DTT, so all contained proteins must be unfolded and these bands appeared in all the conditions, including in the negative control. So, these are unspecific bands.

Another test was performed using 200 µM H_2O_2 and 1 µM DJ-1 (simultaneously) or 1 µM of DJ-1, and using DMEM with 0.1 or 10% FBS. The objective of this test was to understand if the oxidative stress stimulus wasn't enough (although an oxidative stress independent uptake was described [143]) and if the FBS was interfering with the test. Cellular extracts were performed by scraping and the western-blot was performed using the same anti-His antibody (Figure 7.5).

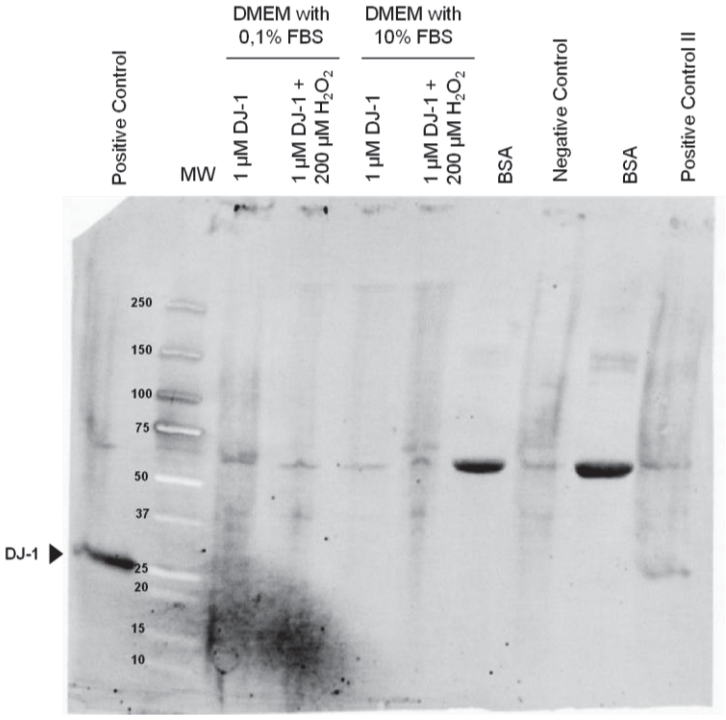

FIGURE 7.5| INTERNALIZATION OF 6-HIS-DJ-1. SH-SY5Y cells were treated with 200 µM H_2O_2 and 1 µM DJ-1 or 1 µM of DJ-1, and using DMEM with 0.1 or 10% FBS, for 4h. Cellular extracts were performed by scraping or shaving cells with trypsin and the western-blot was performed using an anti-His antibody. The positive control is the purified DJ-1, the positive control II is an SH-SY5Y protein extract with DJ-1, and the negative control is an SH-SY5Y protein extract.

Again, there is no evidence for a DJ-1 uptake by SH-SY5Y cells, because there is no band at approximately 25 kDa, corresponding to the recombinant protein (except in both positive controls). There are unspesific bands at ≈60 kDa in all the conditions, including control conditions.

One hypothesis for the absence of DJ-1 signal in the performed western-blots is the lower amount of internalized protein that enables its detection by this technique. Thus, an enrichment process was performed to try to concentrate the final sample with the possibly internalized protein (Figure 7.6). For this, an His-trap resin was used because the produced DJ-1 had an 6-His tag with affinity for this resin. The incubation of protein extracts with the His-trap resin and the further resin processing was performed as described on section 2.6.2.

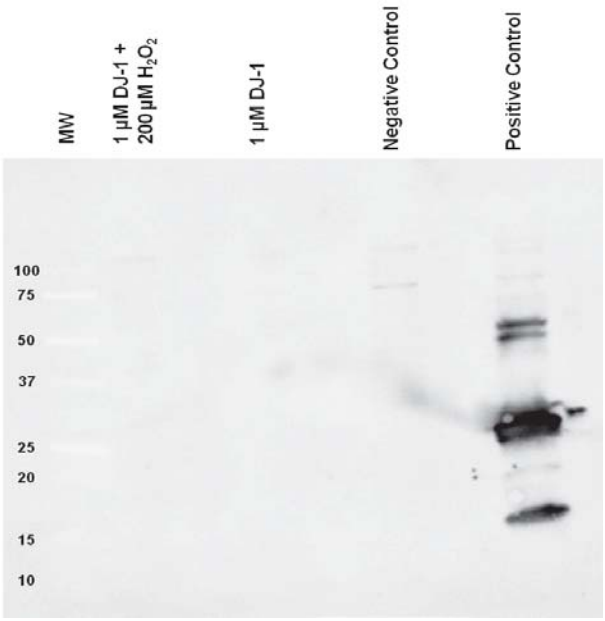

FIGURE 7.6| INTERNALIZATION OF 6-HIS-DJ-1. SH-SY5Y cells were treated with 200 µM H_2O_2 and 1 µM DJ-1 or with µM of DJ-1, for 4h and using DMEM with 0.1 % FBS. Cellular extracts were performed by shaving cells with trypsin and incubated with the His-trap resin. Western-blot was performed with the fraction of eluted proteins using an anti-DJ-1 antibody (KAM-SA100). The positive control is an SH-SY5Y protein extract with DJ-1, and the negative control is an SH-SY5Y protein extract.

Even using the enrichment strategy there is no evidence for a DJ-1 uptake by SH-SY5Y cells, because there is no band at approximately 25 kDa, corresponding to the recombinant protein (except in the positive control) (Figure 7.6). There are unspesific bands at ≈75 and ≈150 kDa in all the conditions, including control conditions.

A final experiment was performed to try to observe the internalization of exogenous DJ-1 in SH-SY5Y cells or its interaction with its membrane proteins (described in section 2.6.). This experiment involves an ultracentrifugation step to have two protein fractions: one enriched in membrane proteins and other enriched in cytosolic proteins. So, it is necessary to show the efficiency of this enrichment step. For that, membranes corresponding to proteins that did not bind to the His trap resin (Figure 3.13) were stripped and reprobed against a mouse Anti-GAPDH antibody (1:500) (sc-47724) (Santa Cruz) or a mouse Anti-Transferrin Receptor (1:500) (13-6800) (Invitrogen). The results showed a good enrichment of membrane proteins in the membrane enriched fraction and a good enrichment of cytosolic proteins in the cytosolic enriched fraction (Figure 7.7 and Figure 7.8), as there is a higher amount of

GAPDH (a cytosolic protein) in the cytosolic enriched fraction than in the membrane enriched fraction (Figure 7.7), and a higher amount of the transferring receptor (a membrane protein receptor) in the membrane enriched fraction than in the cytosolic enriched fraction (Figure 7.8).

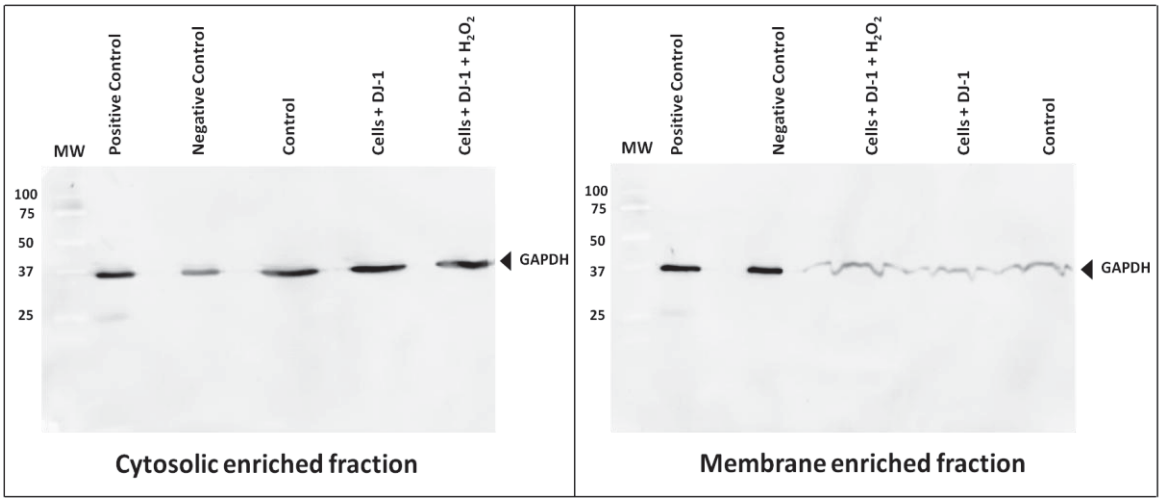

FIGURE 7.7| CYTOSOLIC PROTEINS ENRICHMENT. Control of the cytosolic proteins enrichment in the cytosolic enriched fraction. Western-blot performed with cytosolic and membrane enriched fractions using an anti-GAPDH antibody. The negative control is an SH-SY5Y total protein extract and the positive control is the same extract with the addition of 0.6 µg of the recombinant DJ-1.

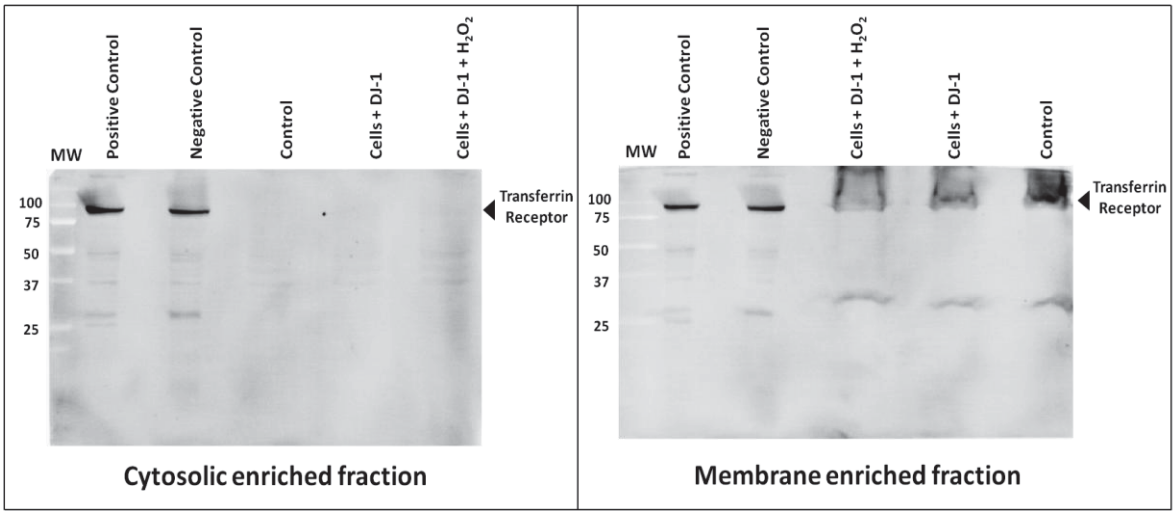

FIGURE 7.8| MEMBRANE PROTEINS ENRICHMENT. Control of the membrane proteins enrichment in the membrane enriched fraction. Western-blot performed with cytosolic and membrane enriched fractions using an anti-Transferrin Receptor antibody. The negative control is an SH-SY5Y total protein extract and the positive control is the same extract with the addition of 0.6 µg of the recombinant DJ-1.

7.4. EXTRACELLULAR AND MEMBRANE INTERACTORS

As no evidence for a DJ-1 uptake was found, strategies to find extracellular interactors were taken.

One of the strategies used was the use of a crosslinker (DTSSP) (Thermo Fisher Scientific) to try to crosslink extracellular proteins with the recombinant DJ-1 exogenously added. For that, cells cultured in 21 cm^2 plates (Corning) were incubated with 1 μM of recombinant DJ-1 in sodium medium (140 mM NaCl, 5 mM KCl, 1 mM $CaCl_2$, 1 mM $MgCl_2$, 10 mM glucose, 10 mM HEPES-Na^+, pH 7.4) for 1h at 37 °C. After this time period, the crosslinker was added (2 mM of DTSSP) and incubated for 30 min at the same temperature. The crosslinker reaction was quenched by adding 20 mM of Tris.

The culture medium was collected and concentrated by rotary evaporation, using the Concentrator Plus (Eppendorf) at 60 °C and then using concentrators with a cut-off of 5 kDa (500 μL) (Sartorius). To try to observe if DJ-1 was crosslinked with any membrane protein, cellular protein extracts were produced as described on section 2.5.2. with and without DTT (in RIPA buffer and sample buffer), because DTT cleaves the crosslinker, and both conditions are desired (cleaved and not cleaved). Culture mediums and protein extracts were incubated with the His-trap resin as described on section 2.6.2. The resin processing after the incubation is also described in the same section.

Samples were electrophoretically separated on pre-cast AnyKD™ SDS-polyacrylamide gels (Bio-Rad) and stained with silver. For western-blot samples were electrophoretically separated on pre-cast 12 % SDS-polyacrylamide gels (Bio-Rad) and western-bloted using the goat Anti-DJ-1 C-16 antibody (1:200) (Santa Cruz Biotechnology, Inc. (sc-27006) (Heidelberg, Germany), as described in section 2.6.3.

There are some evidence for a possible interaction of DJ-1 with extracellular proteins, as there are protein bands in the gel stained with silver, when the crossliker wasn't cleaved with DTT (Figure 7.9, A). Moreover, the western-blot shows the presence of DJ-1 at higher molecular weights (when the crosslinker wasn't cleaved), which can indicate the linkage between the interest protein and other proteins. When the crosslinker was cleaved, the bands corresponding to DJ-1 appeared at 50 or 25

kDa, which may be do the incomplete cleavage of the crosslinker in these samples (Figure 7.9, B).

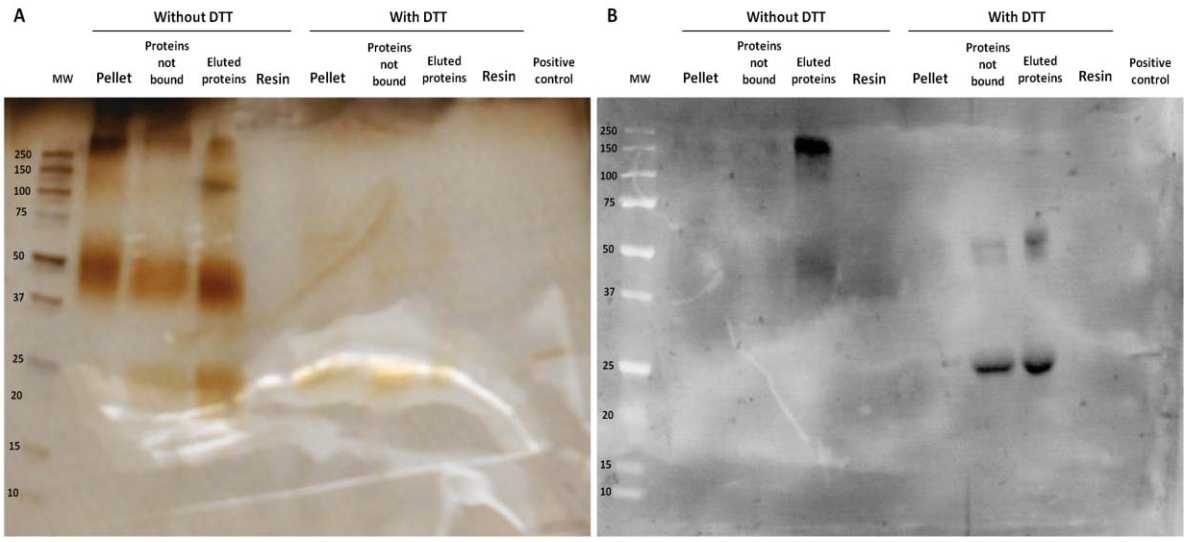

FIGURE 7.9| EXTRACELLULAR INTERACTORS – CULTURE MEDIUMS. A – Silverstained polyacrilamide gel. The positive control is the recombinant DJ-1. B – Western-blot. The positive control is the recombinant DJ-1.

On the other hand, there are no evidence for a DJ-1 interaction with any membrane protein, as there is no band corresponding to DJ-1 (Figure 7.10, B), except in the positive control.

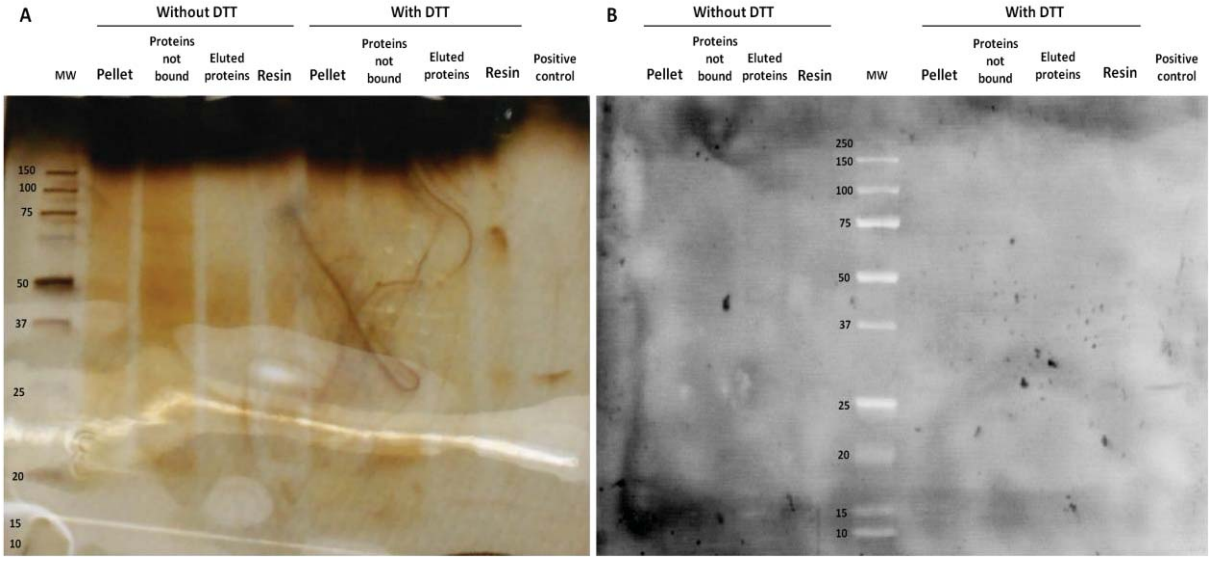

FIGURE 7.10| EXTRACELLULAR INTERACTORS – CELLULAR PROTEIN EXTRACTS. A – Silverstained polyacrilamide gel. The positive control is the recombinant DJ-1. **B** – Western-blot. The positive control is the recombinant DJ-1.

Although, by performing some controls of the experiment, it seems that the evidence for a DJ-1 interaction with extracellular proteins are only due to the interaction of DJ-1 with itself, or remaining serum proteins, as cells (or the plate without cells) were washed only once with sodium medium (Figure 7.11). The performed controls were:

1. With cells in culture: in the presence or absence of 1 µM of the recombinant DJ-1;
2. Without cells in culture: in the presence or absence of 1 µM of the recombinant DJ-1.

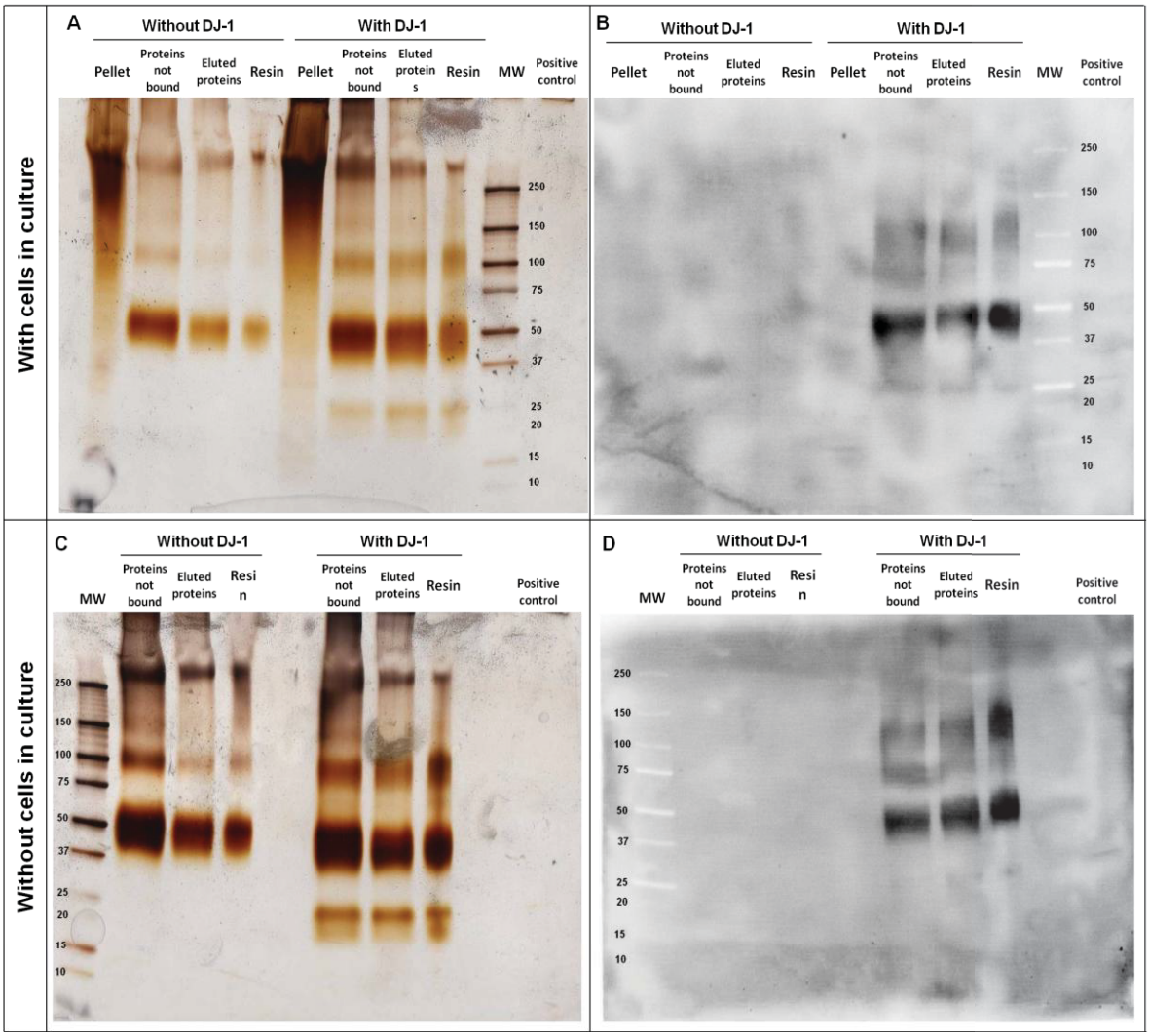

FIGURE 7.11| EXTRACELLULAR INTERACTORS – CELLULAR PROTEIN EXTRACTS. A and **C** – Silverstained polyacrilamide gel. The positive control is the recombinant DJ-1. **B** and **D** – Western-blot. The positive control is the recombinant DJ-1.

Another strategy was then taken, a pull-down assay (described on section 2.7). As previously stated, some proteins were found both in the pull-down assay performed using the recombinant protein bound to the His-trap resin, and using the His-trap resin without the addition of the recombinant protein. Furthermore, as one of these found proteins was the endogenous DJ-1 protein, maybe some of these identified proteins can be interacting not only with the His-trap resin, but also with the endogenous DJ-1. So, some of these proteins could also be DJ-1 interactors in the extracellular space Table 7.1. These results must be validated in the future by refining the experimental procedure. One of the possible improvements of the method is the increase of the number of washing steps.

TABLE 7.1| PROTEINS FROM THE CONDITIONED MEDIUM PULL-DOWNED AGAINST DJ-1 BOUND TO THE HIS-TRAP RESIN OR AGAINST THE HIS-TRAP RESIN WITHOUT DJ-1 (CONTROL).

Protein ID			**with DJ-1**	**without DJ-1**
Name	**Accessions**	**Specie**	**Unique Peptides**	**Unique Peptides**
Protein DJ-1	Q99497|PARK7_HUMAN	*Homo sapiens*	172	22
Secretogranin-1	P05060|SCG1_HUMAN	*Homo sapiens*	26	31
Peroxidasin homolog	Q92626|PXDN_HUMAN	*Homo sapiens*	31	29
Neurosecretory protein VGF	O15240|VGF_HUMAN	*Homo sapiens*	27	25
Agrin	O00468|AGRIN_HUMAN	*Homo sapiens*	25	24
EMILIN-1	Q9Y6C2|EMIL1_HUMAN	*Homo sapiens*	21	23
Sulfhydryl oxidase 1	O00391|QSOX1_HUMAN	*Homo sapiens*	16	18
Insulin-like growth factor-binding protein-like 1	Q8WX77|IBPL1_HUMAN	*Homo sapiens*	7	18
Chromogranin-A	P10645|CMGA_HUMAN	*Homo sapiens*	13	17
Plasma serine protease inhibitor	P05154|IPSP_HUMAN	*Homo sapiens*	16	15
Follistatin-related protein 5	Q8N475|FSTL5_HUMAN	*Homo sapiens*	10	13
Laminin subunit alpha-5	O15230|LAMA5_HUMAN	*Homo sapiens*	9	12
Tenascin	P24821|TENA_HUMAN	*Homo sapiens*	7	12
Tissue-type plasminogen activator	P00750|TPA_HUMAN	*Homo sapiens*	14	11
Laminin subunit beta-1	P07942|LAMB1_HUMAN	*Homo sapiens*	6	10
Lactotransferrin	P02788|TRFL_HUMAN	*Homo sapiens*	8	9
Phospholipid transfer protein	P55058|PLTP_HUMAN	*Homo sapiens*	7	8
A disintegrin and metalloproteinase with thrombospondin motifs 9	Q9P2N4|ATS9_HUMAN	*Homo sapiens*	8	8
Semaphorin-3A	Q14563|SEM3A_HUMAN	*Homo sapiens*	5	7

Peptidyl-prolyl cis-trans isomerase A	P62937|PPIA_HUMAN	*Homo sapiens*	7	6
Procollagen C-endopeptidase enhancer 1	Q15113|PCOC1_HUMAN	*Homo sapiens*	7	6
Protein kinase C-binding protein NELL2	Q99435|NELL2_HUMAN	*Homo sapiens*	5	6
Fibulin-1	P23142|FBLN1_HUMAN	*Homo sapiens*	5	5
Thrombospondin type-1 domain-containing protein 7A	Q9UPZ6|THS7A_HUMAN	*Homo sapiens*	4	5
A disintegrin and metalloproteinase with thrombospondin motifs 19	Q8TE59|ATS19_HUMAN	*Homo sapiens*	6	4
Laminin subunit gamma-1	P11047|LAMC1_HUMAN	*Homo sapiens*	6	4
Lumican	P51884|LUM_HUMAN	*Homo sapiens*	3	4
Clusterin	P10909|CLUS_HUMAN	*Homo sapiens*	6	3
Dickkopf-related protein 1	O94907|DKK1_HUMAN	*Homo sapiens*	3	3
Galectin-3-binding protein	Q08380|LG3BP_HUMAN	*Homo sapiens*	5	3
Galectin-1	P09382|LEG1_HUMAN	*Homo sapiens*	2	3
Secreted frizzled-related protein 3	Q92765|SFRP3_HUMAN	*Homo sapiens*	2	3
Collagen alpha-1(VI) chain	P12109|CO6A1_HUMAN	*Homo sapiens*	2	2
Complement C1q tumor necrosis factor-related protein 3	Q9BXJ4|C1QT3_HUMAN	*Homo sapiens*	1	1

Non-secreted proteins that putatively interacts with the exogenous DJ-1 in the extracellular space of cells (only identified in the pull-down assay against the recombinant DJ-1 bound to the His-trap Resin) are presented in the table below. To the aim of the work these proteins weren't relevant, but it is possible that due to the death of some cells, some intracellular proteins were found. Among these proteins can be some interesting ones, so these results must be analysed in the future and approaches using total proteins extracts can also be performed to try to identify DJ-1 intracellular interactors.

TABLE 7.2| NON-SECRETED PROTEINS FROM THE CONDITIONED MEDIUM PULL-DOWNED WITH DJ-1.

Name	Accessions	Specie	Unique Peptides
Tubulin alpha-1B chain	P68363|TBA1B_HUMAN	*Homo sapiens*	16
78 kDa glucose-regulated protein	P11021|GRP78_HUMAN	*Homo sapiens*	16
ATP synthase subunit beta, mitochondrial	P06576|ATPB_HUMAN	*Homo sapiens*	15
Transketolase	P29401|TKT_HUMAN	*Homo sapiens*	15
ATP-citrate synthase	P53396|ACLY_HUMAN	*Homo sapiens*	12

Vimentin	P08670|VIME_HUMAN	*Homo sapiens*	10
T-complex protein 1 subunit gamma	P49368|TCPG_HUMAN	*Homo sapiens*	10
Heat shock 70 kDa protein 1	P08107|HSP71_HUMAN	*Homo sapiens*	8
Tryptophan--tRNA ligase, cytoplasmic	P23381|SYWC_HUMAN	*Homo sapiens*	8
Stress-70 protein, mitochondrial	P38646|GRP75_HUMAN	*Homo sapiens*	7
Nucleoside diphosphate kinase B	P22392|NDKB_HUMAN	*Homo sapiens*	7
Histone H4	P62805|H4_HUMAN	*Homo sapiens*	6
Calsyntenin-3	Q9BQT9|CSTN3_HUMAN	*Homo sapiens*	6
Pleiotropic regulator 1	O43660|PLRG1_HUMAN	*Homo sapiens*	6
Puromycin-sensitive aminopeptidase	P55786|PSA_HUMAN	*Homo sapiens*	6
Plastin-3	P13797|PLST_HUMAN	*Homo sapiens*	6
Tubulin beta-3 chain	Q13509|TBB3_HUMAN	*Homo sapiens*	6
Histone H2A.x	P16104|H2AX_HUMAN	*Homo sapiens*	5
T-complex protein 1 subunit delta	P50991|TCPD_HUMAN	*Homo sapiens*	5
Hypoxia up-regulated protein 1	Q9Y4L1|HYOU1_HUMAN	*Homo sapiens*	5
Spectrin beta chain, brain 1	Q01082|SPTB2_HUMAN	*Homo sapiens*	3
Cytosolic non-specific dipeptidase	Q96KP4|CNDP2_HUMAN	*Homo sapiens*	5
Histidine triad nucleotide-binding protein 1	P49773|HINT1_HUMAN	*Homo sapiens*	5
Septin-7	Q16181|SEPT7_HUMAN	*Homo sapiens*	5
Peroxiredoxin-5, mitochondrial	P30044|PRDX5_HUMAN	*Homo sapiens*	4
Septin-2	Q15019|SEPT2_HUMAN	*Homo sapiens*	4
Cadherin-2	P19022|CADH2_HUMAN	*Homo sapiens*	4
Tubulin alpha-1A chain	Q71U36|TBA1A_HUMAN	*Homo sapiens*	4
Immunity-related GTPase family Q protein	Q8WZA9|IRGQ_HUMAN	*Homo sapiens*	4
DNA-(apurinic or apyrimidinic site) lyase	P27695|APEX1_HUMAN	*Homo sapiens*	4
RuvB-like 2	Q9Y230|RUVB2_HUMAN	*Homo sapiens*	4
Enhancer of rudimentary homolog	P84090|ERH_HUMAN	*Homo sapiens*	4
Protein transport protein Sec23A	Q15436|SC23A_HUMAN	*Homo sapiens*	4
Heterogeneous nuclear ribonucleoproteins C1/C2	P07910|HNRPC_HUMAN	*Homo sapiens*	3
Splicing factor 3B subunit 3	Q15393|SF3B3_HUMAN	*Homo sapiens*	3
14-3-3 protein theta	P27348|1433T_HUMAN	*Homo sapiens*	3
Neutral alpha-glucosidase AB	Q14697|GANAB_HUMAN	*Homo sapiens*	3
Glycine--tRNA ligase	P41250|SYG_HUMAN	*Homo sapiens*	3
Actin, muscle-type A2	P68032|ACTC_HUMAN	*Homo sapiens*	3
Tubulin beta-4 chain	Q3ZCM7|TBB8_HUMAN	*Homo sapiens*	3
Splicing factor 1	Q15637|SF01_HUMAN	*Homo sapiens*	3
Retinol-binding protein 1	P09455|RET1_HUMAN	*Homo sapiens*	3
Profilin-2	P35080|PROF2_HUMAN	*Homo sapiens*	3
Actin-related protein 3	P61158|ARP3_HUMAN	*Homo sapiens*	3
Glucose-6-phosphate 1-dehydrogenase	P11413|G6PD_HUMAN	*Homo sapiens*	3
Poly [ADP-ribose] polymerase 1	P09874|PARP1_HUMAN	*Homo sapiens*	3

SUMO-activating enzyme subunit 2	Q9UBT2|SAE2_HUMAN	*Homo sapiens*	3
Proteasome activator complex subunit 1	Q06323|PSME1_HUMAN	*Homo sapiens*	3
40S ribosomal protein S10	P46783|RS10_HUMAN	*Homo sapiens*	3
60S acidic ribosomal protein P0	P05388|RLA0_HUMAN	*Homo sapiens*	3
Bone morphogenetic protein 1	P13497|BMP1_HUMAN	*Homo sapiens*	3
Nucleobindin-1	Q02818|NUCB1_HUMAN	*Homo sapiens*	3
40S ribosomal protein S20	P60866|RS20_HUMAN	*Homo sapiens*	3
GTP-binding nuclear protein Ran	P62826|RAN_HUMAN	*Homo sapiens*	3
Isocitrate dehydrogenase [NADP] cytoplasmic	O75874|IDHC_HUMAN	*Homo sapiens*	3
Paraspeckle component 1	Q8WXF1|PSPC1_HUMAN	*Homo sapiens*	3
Mannosyl-oligosaccharide 1,2-alpha-mannosidase IA	P33908|MA1A1_HUMAN	*Homo sapiens*	3
Small nuclear ribonucleoprotein Sm D3	P62318|SMD3_HUMAN	*Homo sapiens*	3
Serine/threonine-protein phosphatase 2A 65 kDa regulatory subunit A alpha isoform	P30153|2AAA_HUMAN	*Homo sapiens*	2
26S proteasome non-ATPase regulatory subunit 1	Q99460|PSMD1_HUMAN	*Homo sapiens*	2
Cellular retinoic acid-binding protein 1	P29762|RABP1_HUMAN	*Homo sapiens*	2
Trifunctional purine biosynthetic protein adenosine-3	P22102|PUR2_HUMAN	*Homo sapiens*	2
Biliverdin reductase A	P53004|BIEA_HUMAN	*Homo sapiens*	2
Acetyl-CoA acetyltransferase, mitochondrial	P24752|THIL_HUMAN	*Homo sapiens*	2
Coronin-1B	Q9BR76|COR1B_HUMAN	*Homo sapiens*	2
Kinesin-1 heavy chain	P33176|KINH_HUMAN	*Homo sapiens*	2
Fermitin family homolog 2	Q96AC1|FERM2_HUMAN	*Homo sapiens*	2
Serine hydroxymethyltransferase, mitochondrial	P34897|GLYM_HUMAN	*Homo sapiens*	2
Septin-9	Q9UHD8|SEPT9_HUMAN	*Homo sapiens*	2
Nuclear autoantigenic sperm protein	P49321|NASP_HUMAN	*Homo sapiens*	2
Aldose reductase	P15121|ALDR_HUMAN	*Homo sapiens*	2
Gamma-enolase	P09104|ENOG_HUMAN	*Homo sapiens*	2
Beta-1,4-galactosyltransferase 5	O43286|B4GT5_HUMAN	*Homo sapiens*	2
ALK tyrosine kinase receptor	Q9UM73|ALK_HUMAN	*Homo sapiens*	2
PDZ and LIM domain protein 5	Q96HC4|PDLI5_HUMAN	*Homo sapiens*	2
DNA replication licensing factor MCM2	P49736|MCM2_HUMAN	*Homo sapiens*	2
60S ribosomal protein L27	P61353|RL27_HUMAN	*Homo sapiens*	2
Protein mago nashi homolog	P61326|MGN_HUMAN	*Homo sapiens*	2
Polyadenylate-binding protein 1	P11940|PABP1_HUMAN	*Homo sapiens*	2
N-acetyl-D-glucosamine kinase	Q9UJ70|NAGK_HUMAN	*Homo sapiens*	2
Histone H2A.V	Q71UI9|H2AV_HUMAN	*Homo sapiens*	1
Nuclear mitotic apparatus protein 1	Q14980|NUMA1_HUMAN	*Homo sapiens*	1
Succinate dehydrogenase [ubiquinone] flavoprotein subunit,	P31040|DHSA_HUMAN	*Homo sapiens*	1

mitochondrial			
Probable ATP-dependent RNA helicase DDX17	Q92841|DDX17_HUMAN	*Homo sapiens*	1
DNA replication licensing factor mcm4	P33991|MCM4_HUMAN	*Homo sapiens*	1
40S ribosomal protein S13	P62277|RS13_HUMAN	*Homo sapiens*	1
AP-2 complex subunit beta	P63010|AP2B1_HUMAN	*Homo sapiens*	1
Glucosylceramidase	P04062|GLCM_HUMAN	*Homo sapiens*	1
Alpha-centractin	P61163|ACTZ_HUMAN	*Homo sapiens*	1
Polyubiquitin	P62987|RL40_HUMAN	*Homo sapiens*	1
Barrier-to-autointegration factor	O75531|BAF_HUMAN	*Homo sapiens*	1
BolA-like protein 2	Q9H3K6|BOLA2_HUMAN	*Homo sapiens*	1
Myosin light polypeptide 6	P60660|MYL6_HUMAN	*Homo sapiens*	1
Platelet-activating factor acetylhydrolase IB subunit gamma	P68402|PA1B2_HUMAN	*Homo sapiens*	1
Alcohol dehydrogenase class-3	P11766|ADHX_HUMAN	*Homo sapiens*	1
Peptidyl-glycine alpha-amidating monooxygenase	P19021|AMD_HUMAN	*Homo sapiens*	1
Melanoma-associated antigen 10	P43363|MAGAA_HUMAN	*Homo sapiens*	1
Porphobilinogen deaminase	P08397|HEM3_HUMAN	*Homo sapiens*	1
Acetyl-CoA acetyltransferase, cytosolic	Q9BWD1|THIC_HUMAN	*Homo sapiens*	1
Mitochondrial fission 1 protein	Q9Y3D6|FIS1_HUMAN	*Homo sapiens*	1
Stomatin-like protein 2	Q9UJZ1|STML2_HUMAN	*Homo sapiens*	1
Small nuclear ribonucleoprotein-associated protein B'	Q92611|EDEM1_HUMAN	*Homo sapiens*	1
26S protease regulatory subunit 6A	P17980|PRS6A_HUMAN	*Homo sapiens*	1
Polymerase delta-interacting protein 2	Q9Y2S7|PDIP2_HUMAN	*Homo sapiens*	1

Moreover, as in the case of secreted proteins, there are also non-secreted proteins identified in both pull-down fractions, using the recombinant DJ-1 bound to the His-trap resin, and using the His-trap resin without the addition of the recombinant protein (Table 7.3). Again, these proteins weren't relevant to the aim of the work, but among these proteins can be some interesting ones, so these results must be analysed in the future and the technical procedure must be improved to avoid the possible effect of the binding of the endogenous DJ-1 to the His-trap resin.

TABLE 7.3| NON-SECRETED PROTEINS FROM THE CONDITIONED MEDIUM PULL-DOWNED AGAINST DJ-1 BOUND TO THE HIS-TRAP RESIN OR AGAINST THE HIS-TRAP RESIN WITHOUT DJ-1 (CONTROL).

Protein ID			with DJ-1	without DJ-1
Name	**Accessions**	**Specie**	**Unique Peptides**	**Unique Peptides**
Prelamin-A/C	P02545|LMNA_HUMAN	*Homo sapiens*	32	37
Heat shock cognate 71 kDa protein	P11142|HSP7C_HUMAN	*Homo sapiens*	26	27
60 kDa heat shock protein, mitochondrial	P10809|CH60_HUMAN	*Homo sapiens*	23	27
Calsyntenin-1	O94985|CSTN1_HUMAN	*Homo sapiens*	20	27
Elongation factor 2	P13639|EF2_HUMAN	*Homo sapiens*	31	26
Pyruvate kinase isozymes M1/M2	P14618|KPYM_HUMAN	*Homo sapiens*	26	23
Protein DJ-1	Q99497|PARK7_HUMAN	*Homo sapiens*	172	22
Alpha-enolase	P06733|ENOA_HUMAN	*Homo sapiens*	18	21
Splicing factor, proline- and glutamine-rich	P23246|SFPQ_HUMAN	*Homo sapiens*	16	18
Non-POU domain-containing octamer-binding protein	Q15233|NONO_HUMAN	*Homo sapiens*	16	17
T-complex protein 1 subunit theta	P50990|TCPQ_HUMAN	*Homo sapiens*	12	16
T-complex protein 1 subunit zeta	P40227|TCPZ_HUMAN	*Homo sapiens*	17	14
Dopamine beta-hydroxylase	P09172|DOPO_HUMAN	*Homo sapiens*	8	14
Filamin-A	P21333|FLNA_HUMAN	*Homo sapiens*	23	13
Heat shock protein HSP 90-beta	P08238|HS90B_HUMAN	*Homo sapiens*	17	13
Fascin	Q16658|FSCN1_HUMAN	*Homo sapiens*	12	13
Calsyntenin-2	Q9H4D0|CSTN2_HUMAN	*Homo sapiens*	13	13
Glyceraldehyde-3-phosphate dehydrogenase	P04406|G3P_HUMAN	*Homo sapiens*	14	12
Heterogeneous nuclear ribonucleoprotein K	P61978|HNRPK_HUMAN	*Homo sapiens*	13	12
T-complex protein 1 subunit beta	P78371|TCPB_HUMAN	*Homo sapiens*	10	12
Peroxiredoxin-6	P30041|PRDX6_HUMAN	*Homo sapiens*	3	12
Spliceosome RNA helicase Ddx39b	Q13838|DX39B_HUMAN	*Homo sapiens*	11	11
Alpha-actinin-4	O43707|ACTN4_HUMAN	*Homo sapiens*	12	11
Isochorismatase domain-containing protein 1	Q96CN7|ISOC1_HUMAN	*Homo sapiens*	7	11
Clathrin heavy chain 1	Q00610|CLH1_HUMAN	*Homo sapiens*	22	10
Alpha-1,6-mannosylglycoprotein 6-beta-N-acetylglucosaminyltransferase A	Q09328|MGT5A_HUMAN	*Homo sapiens*	10	10
Glutathione S-transferase P	P09211|GSTP1_HUMAN	*Homo sapiens*	6	10
Phosphoglycerate kinase 1	P00558|PGK1_HUMAN	*Homo sapiens*	6	10
Protein disulfide-isomerase A6	Q15084|PDIA6_HUMAN	*Homo sapiens*	10	9
Fructose-bisphosphate aldolase A	P04075|ALDOA_HUMAN	*Homo sapiens*	9	9
Lissencephaly-1 homolog	P43034|LIS1_HUMAN	*Homo sapiens*	9	9
Heterogeneous nuclear ribonucleoproteins A2/B1	P22626|ROA2_HUMAN	*Homo sapiens*	8	9
Dihydropyrimidinase-related protein 2	Q16555|DPYL2_HUMAN	*Homo sapiens*	11	8

6-phosphogluconate dehydrogenase, decarboxylating	P52209|6PGD_HUMAN	*Homo sapiens*	12	8
Interleukin enhancer-binding factor 2	Q12905|ILF2_HUMAN	*Homo sapiens*	8	8
Creatine kinase B-type	P12277|KCRB_HUMAN	*Homo sapiens*	8	8
L-lactate dehydrogenase B chain	P07195|LDHB_HUMAN	*Homo sapiens*	7	8
Rab GDP dissociation inhibitor beta	P50395|GDIB_HUMAN	*Homo sapiens*	8	8
Multifunctional protein ADE2	P22234|PUR6_HUMAN	*Homo sapiens*	7	8
Peroxiredoxin-1	Q06830|PRDX1_HUMAN	*Homo sapiens*	4	8
Fatty acid synthase	P49327|FAS_HUMAN	*Homo sapiens*	19	7
Splicing factor 3B subunit 4	Q15427|SF3B4_HUMAN	*Homo sapiens*	9	7
Spectrin alpha chain, brain	Q13813|SPTA2_HUMAN	*Homo sapiens*	14	7
Heterogeneous nuclear ribonucleoprotein L	P14866|HNRPL_HUMAN	*Homo sapiens*	8	7
DNA damage-binding protein 1	Q16531|DDB1_HUMAN	*Homo sapiens*	10	7
Interleukin enhancer-binding factor 3	Q12906|ILF3_HUMAN	*Homo sapiens*	6	7
T-complex protein 1 subunit epsilon	P48643|TCPE_HUMAN	*Homo sapiens*	9	7
Polypyrimidine tract-binding protein 1	P26599|PTBP1_HUMAN	*Homo sapiens*	6	7
Peroxiredoxin-2	P32119|PRDX2_HUMAN	*Homo sapiens*	6	7
Amyloid-like protein 1	P51693|APLP1_HUMAN	*Homo sapiens*	6	7
Heterogeneous nuclear ribonucleoprotein A1	P09651|ROA1_HUMAN	*Homo sapiens*	3	7
Putative pre-mRNA-splicing factor ATP-dependent RNA helicase DHX15	O43143|DHX15_HUMAN	*Homo sapiens*	3	7
Noelin	Q99784|NOE1_HUMAN	*Homo sapiens*	4	7
Adenylyl cyclase-associated protein 1	Q01518|CAP1_HUMAN	*Homo sapiens*	9	7
Creatine kinase U-type, mitochondrial	P12532|KCRU_HUMAN	*Homo sapiens*	8	6
Profilin-1	P07737|PROF1_HUMAN	*Homo sapiens*	7	6
Ubiquitin-like modifier-activating enzyme 1	P22314|UBA1_HUMAN	*Homo sapiens*	11	6
T-complex protein 1 subunit alpha	P17987|TCPA_HUMAN	*Homo sapiens*	10	6
Cytosolic acyl coenzyme A thioester hydrolase	O00154|BACH_HUMAN	*Homo sapiens*	6	6
Malate dehydrogenase, mitochondrial	P40926|MDHM_HUMAN	*Homo sapiens*	5	6
Transitional endoplasmic reticulum ATPase	P55072|TERA_HUMAN	*Homo sapiens*	9	5
Cofilin-1	P23528|COF1_HUMAN	*Homo sapiens*	6	5
Eukaryotic translation initiation factor 5A-1	P63241|IF5A1_HUMAN	*Homo sapiens*	5	5
Vinculin	P18206|VINC_HUMAN	*Homo sapiens*	7	5
Eukaryotic initiation factor 4A-I	P60842|IF4A1_HUMAN	*Homo sapiens*	5	5
T-complex protein 1 subunit eta	Q99832|TCPH_HUMAN	*Homo sapiens*	4	5
X-ray repair cross-complementing protein 6	P12956|XRCC6_HUMAN	*Homo sapiens*	6	5

Heterogeneous nuclear ribonucleoprotein D0	Q14103|HNRPD_HUMAN	*Homo sapiens*	4	5
Heterogeneous nuclear ribonucleoprotein Q	O60506|HNRPQ_HUMAN	*Homo sapiens*	3	5
Talin-1	Q9Y490|TLN1_HUMAN	*Homo sapiens*	4	5
Aldehyde dehydrogenase family 16 member A1	Q8IZ83|A16A1_HUMAN	*Homo sapiens*	3	5
Sia-alpha-2,3-Gal-beta-1,4-GlcNAc-R:alpha 2,8-sialyltransferase	O43173|SIA8C_HUMAN	*Homo sapiens*	4	5
Far upstream element-binding protein 1	Q96AE4|FUBP1_HUMAN	*Homo sapiens*	2	5
ATP synthase subunit alpha, mitochondrial	P25705|ATPA_HUMAN	*Homo sapiens*	12	4
Dihydropyrimidinase-related protein 3	Q14195|DPYL3_HUMAN	*Homo sapiens*	11	4
Ubiquitin-conjugating enzyme E2 N	P61088|UBE2N_HUMAN	*Homo sapiens*	6	4
Endoplasmin	P14625|ENPL_HUMAN	*Homo sapiens*	7	4
Protein disulfide-isomerase A3	P30101|PDIA3_HUMAN	*Homo sapiens*	3	4
Thrombospondin-3	P49746|TSP3_HUMAN	*Homo sapiens*	3	4
Plasminogen activator inhibitor 1 RNA-binding protein	Q8NC51|PAIRB_HUMAN	*Homo sapiens*	7	4
Cysteine-rich protein 2	P52943|CRIP2_HUMAN	*Homo sapiens*	2	4
Heat shock 70 kDa protein 4	P34932|HSP74_HUMAN	*Homo sapiens*	3	4
Actin-related protein 2/3 complex subunit 1B	O15143|ARC1B_HUMAN	*Homo sapiens*	2	4
Protein FAM49B	Q9NUQ9|FA49B_HUMAN	*Homo sapiens*	1	4
Elongation factor 1-alpha 2	Q05639|EF1A2_HUMAN	*Homo sapiens*	12	3
Importin subunit beta-1	Q14974|IMB1_HUMAN	*Homo sapiens*	8	3
Adenosylhomocysteinase	P23526|SAHH_HUMAN	*Homo sapiens*	5	3
Microtubule-associated protein 1B	P46821|MAP1B_HUMAN	*Homo sapiens*	8	3
Serpin H1	P50454|SERPH_HUMAN	*Homo sapiens*	4	3
Elongation factor Tu, mitochondrial	P49411|EFTU_HUMAN	*Homo sapiens*	3	3
Peptidyl-prolyl cis-trans isomerase FKBP4	Q02790|FKBP4_HUMAN	*Homo sapiens*	6	3
Ubiquitin-conjugating enzyme E2 variant 1	Q13404|UB2V1_HUMAN	*Homo sapiens*	3	3
Histone H2B type 1-L	Q99880|H2B1L_HUMAN	*Homo sapiens*	2	3
ATP-dependent RNA helicase DDX1	Q92499|DDX1_HUMAN	*Homo sapiens*	3	3
RuvB-like 1	Q9Y265|RUVB1_HUMAN	*Homo sapiens*	6	2
40S ribosomal protein SA	P08865|RSSA_HUMAN	*Homo sapiens*	7	2
Protein arginine N-methyltransferase 1	Q99873|ANM1_HUMAN	*Homo sapiens*	5	2
X-ray repair cross-complementing protein 5	P13010|XRCC5_HUMAN	*Homo sapiens*	4	2
Heat shock protein HSP 90-alpha	P07900|HS90A_HUMAN	*Homo sapiens*	3	2
Heterogeneous nuclear ribonucleoprotein H	P31943|HNRH1_HUMAN	*Homo sapiens*	5	2

Obg-like ATPase 1	Q9NTK5|OLA1_HUMAN	*Homo sapiens*	4	2
Signal recognition particle 14 kDa protein	P37108|SRP14_HUMAN	*Homo sapiens*	3	2
Coronin-1C	Q9ULV4|COR1C_HUMAN	*Homo sapiens*	3	2
Hemoglobin subunit alpha-3	P01935|HBA3_PANTR	*Pan troglodytes*	3	2
Platelet-activating factor acetylhydrolase IB subunit beta	P68402|PA1B2_HUMAN	*Homo sapiens*	2	2
Heat shock protein beta-1	P04792|HSPB1_HUMAN	*Homo sapiens*	1	2
Echinoderm microtubule-associated protein-like 4	Q9HC35|EMAL4_HUMAN	*Homo sapiens*	4	1
40S ribosomal protein S28	P62857|RS28_HUMAN	*Homo sapiens*	1	1

7.5. ACTIVATION OF AKT AND ERK1/2 SIGNALLING PATHWAYS

The next figure allows the definition of the time-points of the experiment of the activation of Akt and ERK1/2 signalling pathways (Figure 7.12). These results were obtained by Sandra Anjo during her master thesis project (unpublished data) using a commercially available recombinant DJ-1.

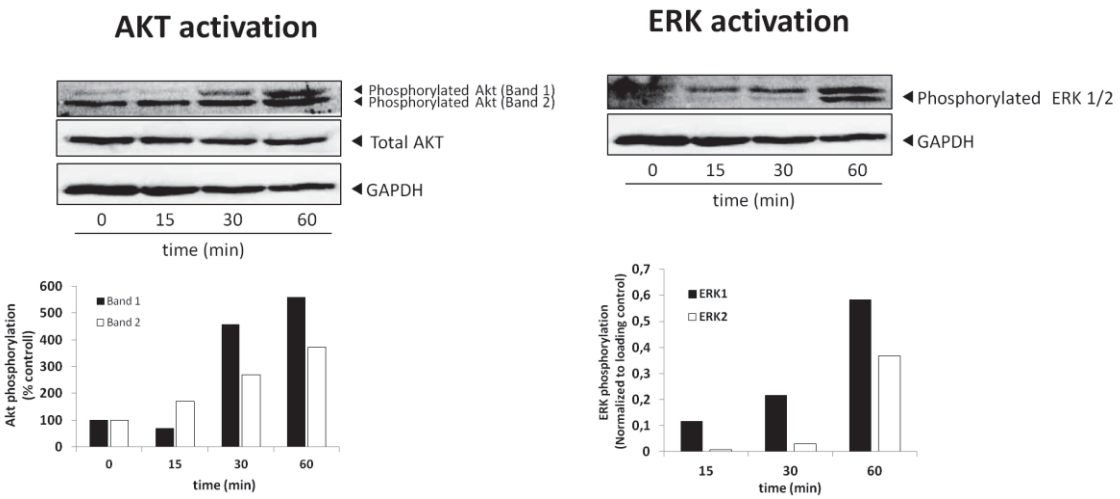

FIGURE 7.12| TIME-COURSE PROFILE FOR THE PURCHASED RECOMBINANT DJ-1-INDUCED AKT AND ERK1/2 ACTIVATION IN SH-SY5Y CELLS.